Optimal Design and Operation of Polygeneration Systems Incorporating Renewable Energy Sources and Chemical Production

by

Tuhin Kanti Poddar

A thesis

presented to the University of Waterloo

in fulfilment of the

thesis requirement for the degree of

Doctor of Philosophy

in

Chemical Engineering

Waterloo, Ontario, Canada, 2022

Examining Committee Membership

The following served on the Examining Committee for this thesis. The decision of the Examining Committee is by majority vote.

External Examiner	HOSSAM GABER Professor
Supervisor(s)	ALI ELKAMEL Professor
	PETER L. DOUGLAS Professor
Internal Member	ERIC CROISET Professor
Internal Member	TIZAZU MEKONNEN Assistant Professor
Internal-external Member	FATIH SAFA ERENAY Associate Professor

Author's Declaration

This thesis consists of material that has been authored or co-authored by me: see Statement of Contributions section below. This is a true copy of the thesis, including any required final revisions, as accepted by the examiners.

I understand that my thesis may be made electronically available to the public.

Statement of Contributions

The unit commitment model presented in Chapter 3 and extended in subsequent chapters was developed in collaboration with Prof. Jalal Kazempour of the Technical University of Denmark. Certain components of the planning of the models presented in Chapter 5, 6 and 7 were aided by Mohammed Adel Alkatheri, a fellow PhD student in my research group. The remainder of the content presented within this thesis, including the literature review, model development in optimization software and generation of results were done solely by me. The overall direction of the thesis and guidance along the way was provided by my supervisors Prof. Elkamel and Prof. Douglas.

Abstract

With the energy transition underway, there is a consensus effort from both worldwide governments and industry, to facilitate the integration of more renewable energy into power grids. However, the main challenge with integrating renewables like wind and solar, is the intermittent nature of these sources that result in inefficiencies and a lack of reliability. One possible energy system that can allow for an effective integration with intermittent sources is a polygeneration energy system (PES). The concept of a PES has been proposed in academic literature in recent times, where a typical pathway is the use of excess power from a fossil power plant being directed towards the production of valuable liquid fuels, in addition to electricity to the grid. In this study, the concept of a polygeneration system has been modified and extended to include renewable energy generation from wind, and a chemical production pathway of methanol to act as a form of long duration storage for times when the wind generation is much higher for any load demand and therefore increasing the flexibility. The model takes advantage of both a deterministic and stochastic approach to better reflect the real-world phenomena of wind power that is intermittent.

The approach taken in this model development departs from past polygeneration modelling studies, by using a network constrained Unit Commitment (UC) model that is well established in the domain of power systems engineering, to optimally schedule the power planning and power flow. First, the design and operation of a power generation planning model is developed to showcase how the power system responds to the intermittency of wind in the form of wind scenarios. This model was extended to show a storage mechanism in the form of a typical hydrogen electrolysis system and fuel cell. Mixed-Integer Linear Programming (MILP) models are then developed for the chemical production of methanol and integrated with the power planning model

as a multi-scale (design and operation) model of a renewable polygeneration energy system (RPES) with chemical storage. To showcase the design and operation of the proposed RPES, the model is first solved in a deterministic manner. Following this, the uncertainty of wind generation is incorporated through the development of a stochastic programming approach with recourse, which would mimic the real world impact of having such an energy system in play. The total RPES system cost, based on real world wind power data and load demand data, was found to be USD 2317.93 million. The chemical production block had a cost of USD 138.51 million when integrated as a part of the RPES and the power generation planning block had a cost of USD 2179.42 million. The integrated model resulted in costs for the chemical production block that were much lower than the stand-alone plant while the RPES model also showed how excess intermittent wind power could be used for driving the chemical production. A key contribution to this work is also the implementation of machine learning methods, like K-Means clustering to help with the model's solution tractability and representation of a full year's hourly wind data and load demand. The MILP models have been developed using the General Algebraic Modelling System (GAMS) software and solved using state of the art optimization solvers BARON and CPLEX.

Acknowledgements

I would like to express my deep gratitude to my supervisor, Prof. Ali Elkamel for his unwavering support, empathy and encouragement during my time as a PhD student. I am also grateful for the guidance provided by my co-supervisor Prof. Peter Douglas and the many discussions that paved the way for this thesis project. I would like to thank my examining committee members, Prof. Eric Croiset, Prof. Tizazu Mekonnen, Prof. Fatih Safa Erenay and Prof. Hossam Gaber for reviewing this thesis document and providing valuable feedback.

I am grateful to Prof. Jalal Kazempour and the entire ELMA (Electricity and Markets Analysis) group at the Technical University of Denmark for graciously hosting me as a visiting PhD student in the fall of 2019. For this visit, I would like to thank Mitacs for the financial assistance provided.

I would like to thank the Department of Chemical Engineering at the University of Waterloo for the continuous support and assistance during my PhD and also to the Graduate Students and Postdoctoral Affairs (GSPA) for their financial assistance in past terms. I would like to thank my parents, the rest of my family and my UWaterloo friends for their help and support.

Last and most importantly, I thank my fiancé, Parul, for her patience, for being my tireless and loudest cheerleader, for the many sacrifices and endless support and for being the best partner I could ask for throughout my PhD journey.

Dedication

To my Family

Table of Contents

List of Figures

List of Tables

List of Abbreviations

ASU	Air Separation Unit
CAES	Compressed Air Energy Storage
CC	Carbon Capture
CCS	Carbon Capture and Storage/Sequestration
DME	Dimethyl Ether
DSM	Demand Side Management
ESS	Energy Storage System
FT	Fischer-Tropsch
GAMS	General Algebraic Modelling System
GBD	Generalized Benders Decomposition
GHG	Greenhouse Gas
HRSG	Heat Recovery Steam Generator
MIP	Mixed Integer Programming
MILP	Mixed Integer Linear Programming
MINLP	Mixed Integer Non-Linear Programming
NLP	Non-linear Programming
NPV	Net Present Value
OA	Outer Approximation
PES	Polygeneration Energy System
PHES	Pumped Hydro Energy Storage
PV	Photovoltaic
RPS	Renewable Portfolio Standard
RPES	Renewable Polygeneration Energy System
VRE	Variable Renewable Energy

List of Symbols

List of symbols for the power generation planning model:

Indices

g index for conventional generation units

k index for wind farm

h index for hours

s index for wind power scenarios

l index for demand loads

(n, m) indices for system nodes

First-stage Continuous Variables

$c^{SU}_{g,h}$ start-up cost of conventional unit g in hour h ($)

$c^{SD}_{g,h}$ shut-down cost of conventional unit g in hour h ($)

$p^{DA}_{g,h}$ power scheduled for conventional unit g in hour h in day-ahead stage (MW)

$w^{DA}_{k,h}$ power scheduled for wind farm k in hour h in day-ahead stage (MW)

$\Theta^{DA}_{n,h}$ voltage angle at node n in hour h at day-ahead stage (radian)

Second-stage Continuous Variables

$p^{SH}_{l,h,s}$ involuntary active load shedding of load l in hour h under scenario s (MW)

$r_{g,h,s}$ power adjustment of conventional unit g in hour h under scenario s (MW)

$w^{SP}_{k,h,s}$ wind power spillage of farm k in hour h under scenario s (MW)

$\Theta^{RT}_{n,h,s}$ voltage angle at node n in hour h under scenario s at the real-time stage (radian)

Binary Variables (First-stage)

$u_{g,h}$ 0/1 variable that is equal to 1 if conventional unit g is scheduled to be committed in hour h

Parameters

ρ_s probability of wind scenario s

λ^{SU}_g start-up cost of conventional unit g ($)

λ^{SD}_g shut-down cost of conventional unit g ($)

C_g marginal cost of conventional unit g ($)

P^{max}_g capacity of existing conventional unit g (MW)

P^{min}_g minimum power output of existing conventional unit g (MW)

P^{ini}_g initial active power output of conventional unit g (MW)

R^{+}_g ramp-up limit of existing conventional unit g (MW/h)

R^{-}_g ramp-down limit of existing conventional unit g (MW/h)

U^{ini}_g initial commitment status of conventional unit g (0/1)

$DL_{l,h}$ power consumption of load l in hour h (MW)

X^{cap}_k capacity of existing wind farm k (MW)

V^{SH}_l value of lost load for load l ($/MW)

$W_{k,h,s}$ wind power realization of farm k in hour h under scenario s

$W^{DAmax}_{k,h}$ maximum wind power factor (in per unit) of farm k in hour h scheduled at day-ahead

$B_{n,n}$ imaginary part of the admittance of lines

$F_{n,m}$ capacity of transmission line (n, m) (MW)

Chapter 1 Introduction

1.1 Background

In this project, a systems engineering approach that is interdisciplinary in nature will be taken into consideration to work towards the design and operation of energy systems that are flexible and be able to also satisfy the key characteristics that have come to describe an energy system as advanced or future-driven. One solution that has the potential to address this, is the operational flexibility of these energy systems, which needs to be increased [1]. The present work has taken advantage of effective solution techniques using various modelling and optimization tools that fall within the domain of process systems engineering.

Over the past decade or so, there has been industry-wide push to revamp and upgrade the existing power generation sector, which primary relies on conventional fossil fuel inputs to meet the world's energy demands. This is especially true in developing economies with high populations such as India, China and nations in Africa and South-east Asia, where utilization of naturally occurring resources such as coal to generate power has supported the increased electrification, even in the most rural areas, thus improving the standards of living of these regions. In contrast, with increased knowledge of the negative effects of carbon emissions and other greenhouse gases (GHG), especially high levels of carbon emissions that arise from burning coal, have inspired developed countries to embrace increased penetration of renewable energy sources such as wind, solar and hydro [2]. Several countries would also rely on clean nuclear power for its generation, but the 2011 Fukushima Disaster has prompted nations to rethink if nuclear power would be the safest option to power their base-load demand. While some countries like Germany have made it clear that renewables are the future and nuclear power has to be gradually reduced down to zero,

other developed countries have looked into carbon capture (CC) technologies to be retrofitted into existing infrastructures to help curb emissions [3]. While CC technology has been proven to be effective, the costs associated with retrofitting and operating CC in tandem with conventional power plants have been high and are therefore roadblocks in the face of widespread adoption. Emerging literature surrounding conventional power generation plants has pointed towards the need for upgrading current plants, not only by installing CC capabilities but also hybrid input systems that would allow for greater power generation from renewable or cleaner energy sources. While many nations have increased the share of the power mix that comes from renewable energy sources, a number of challenges continue to exist with their utilization. Among the leading renewable energy sources currently being tapped into are solar and wind power due to their widespread abundance in large swaths of the geographical locations worldwide, along with the continual reduction in costs associated with their power generation. However, a key feature of solar and wind, is that these sources are intermittent, with a significant variation in their availability even during a 24-hour period, let alone the natural seasonal variation [1]. This intermittency from variable renewable energy (VRE) sources puts a significant amount of stress on the electrical grid, with the grid being unable to handle the excess power during increased generation periods from solar and wind. At the same time, when their availability is low, ramping up conventional generators to fulfil the demand, incurs higher operating costs [4]. With these challenges in mind, there is a need to design future energy systems that are both economically attractive for the operator as well as environmentally benign so as to not exacerbate the problems arising from greenhouse gas (GHG) emissions.

Polygeneration energy systems (PES) have been proposed as a stepping-stone towards a future energy system since it can integrate electric power generation with value added product synthesis

[5]. This integrated approach has been proven to not only reduce operational costs in comparison to stand-alone plants, but also as a solution to curb GHG emissions as the world scrambles to prevent the catastrophic impact of climate change. However, as of this moment, significant deficiencies are present in the general polygeneration process operation which have impeded their widespread adoption. These include the intermittency of renewable energy sources, high costs associated with flexible operation between the power generation and product synthesis units as well as high operational costs due to uncertainties related to fuel and product prices and their corresponding supply. This project aims to address these challenges and develop a framework that allows for the design and the flexible operation of the polygeneration energy system which comprises of power generation planning, chemical product synthesis while also utilizing renewable energy sources like wind. Also included in the framework will be an investigation into energy storage as a solution to the intermittency problem of renewable fuel sources. The project will focus on modelling and optimization techniques to obtain design decision solutions as well as operational schedules that minimize costs and energy while ensuring that power load demand is always being met. Multiple case studies will be investigated to validate and observe the behaviour of the models developed.

1.2 Research Objectives and Steps

The main objective of this thesis, is to develop generic process systems engineering based models that represent polygeneration systems which are able to integrate renewable energy sources and produce chemicals and power. Another outcome of this study will be to show how the chemical production can act as an innovative energy storage pathway and maximise the use of renewables regardless of their intermittency.

In accordance with objectives above, the following are the steps that will be taken in this study:

- Conduct a thorough literature review on the topics of polygeneration energy system design and operation to identify ways mathematical modelling methods can be used to integrate renewable energy into polygeneration.
- Develop a general power planning model that incorporates unit commitment characteristics and linearized power flow constraints with the objective of minimizing the overall cost. A recourse real-time correction for day-ahead decisions are used to account for the realization of wind uncertainties. This model can be used as a base to be integrated with the chemical production planning model to form the polygeneration model.
- Develop a first principles chemical production planning model (i.e., design and operation) that can act as a chemical production block integrated with the power generation block. A methanol-based production block that converts hydrocarbon based fuels to methanol is selected as the chemical production node. The process starts by gasifying the coal (any type of hydrocarbon fuel can be used), where syngas is produced followed, by subsequent conversion of syngas to methanol based on catalyst-driven chemical reactions.
- Develop a deterministic polygeneration design and operation model that is based on the integration of the aforementioned power and chemical production planning models. This model can showcase the benefit of simultaneously planning both power generation that includes renewable resources and chemical production in which both power and chemical (e.g., methanol) demands can be effectively satisfied.
- A polygeneration design and operation model under wind uncertainty is modelled using stochastic approach. The impact of the wind power variability on the overall operation of the

polygeneration system can be investigated and the proposed polygeneration system flexibility can be evaluated.

- Reduce the polygeneration model's computational tractability by applying machine learning tools, specifically data clustering that reduces the number of yearly operational days to the representative typical days of the full year's hourly wind power and load demand This aids the model in obtaining solutions in shorter computational times.

1.3 Research Methodology

For the power system planning block, the general model will be an extension of established unit commitment based models that are commonplace in electric power systems theory. The power planning models will not only provide results that describe the schedule of the various generators over a period of 24 hours' operation but also provide a design decision values which let the stakeholders know how much wind and power capacity needs to be designed.

Similarly, for the methanol production block, the model will be fairly detailed at the preliminary stages and will require non-linear mixed integer programming to account for equations representing the capital cost calculations which are non-linear. However, in chapter 5, the models will be converted to linearized forms using linear regression which allow for the model solution to be provided within shorter computation times without sacrificing a significant amount of accuracy in the results. Also to be showcased in this chapter is a novel shortcut method that extracts key variable results from a single hour's operation, and proceeds to input them as parameters for subsequent runs until the full 24 hours of operation has been completed. This allows for the reduction in the computational tractability as well. Further explanations of this method will be illustrated in chapter 5.

The main outcome of this research work will be the development of general models that can be used for the optimal design and operation of a polygeneration energy system that can be integrated with renewable energy. The models developed can be simultaneously applied to the process and energy industry infrastructure to optimally integrate renewable energy with the aim of maximizing the use of renewables under infrastructure operational and policy constraints, for instance unit commitment constraints and renewable portfolio standards (RPS), respectively. By implementing the models developed there will be a component by component build-up of the renewable energy based polygeneration energy system beginning with power generation planning, and integrating it with methanol chemical production. Additional constraints, aside from the RPS and natural intermittent variation in the wind power, may also be defined, for instance on the dynamics associated with the chemical production block, capacity limits of the methanol reactor and gasifier units, as well as maximum and minimum operational limits on the power production generator units. In all the various cases that will be investigated, the underlying objective is to showcase the manner in which an integrated renewable-based polygeneration energy system can be designed and operated in a flexible manner, allowing for increased utilization of wind energy and maximizing the production of value added chemicals during periods of high intermittency, all while meeting the necessary load demand which is non-negotiable for an energy system's functioning.

1.4 Dissertation Outline

Chapter 2 of this dissertation comprises of a comprehensive literature review of polygeneration energy systems, unit commitment, renewable energy driven production of alternate fuels and chemicals. Chapter 3 shows the development of the power generation planning model which is built around the stochastic unit commitment model. Chapter 4 extends the power generation

planning model to showcase the impact of an energy storage system integrated with the power generation planning model. Chapter 5 details the model development of the methanol production from syngas, first as a nonlinear non-convex model and then modified for convenience for integration to a linearized and convex model. Chapter 6 outlines the integration of the power generation planning and methanol production in a deterministic manner and lays the foundation for the renewable polygeneration energy system. Chapter 7 shows how the integrated renewable polygeneration energy system can be made to design and operate in a stochastic manner. Finally, Chapter 8 draws conclusions from this research work, stating the significant findings from different studies presented in this work. Recommendations are presented for researchers with interest to conduct any further work in this area.

Chapter 2 Literature Review

In this chapter, a literature review has been conducted on the broader topics of polygeneration energy systems, renewable energy sources and energy storage methodologies to understand the existing landscape of modern energy systems and how they may be incorporated for future implementations. In addition to the subjects mentioned, an overview has also been included on the mathematical modelling tools that will be utilized to develop the various models in this dissertation, in particular mixed-integer programming, stochastic programming and the machine learning method of data clustering.

2.1 Features of Energy Systems of the Future:

As energy systems are being investigated for the future, the following characteristics or requirements will have to be met for an energy system to be considered advanced.

- The upgraded energy system should comprise of technology that is already in operation at present or is close to units that are in conventional power sectors to allow for greater ease in the up-gradation process.
- Energy efficiency of future systems should be higher than conventional technologies so as to reduce the overall energy consumption levels.
- Allow for effective utilization of renewable energy sources. Basically work as a transitional technology, which facilitates a decrease in dependency on fossil fuel, based energy to increasing use of renewable energy. Higher utilization of renewable energy is key to lower emissions, which as a future energy system, is an objective that needs to be achieved compared to existing conventional technologies.

- Future energy systems need to be able to operate with greater flexibility. Depending on market scenarios, fuel prices and demand variability, the energy system should be able to adapt in a low-cost and efficient manner to respond to changes while still providing the required amount of energy output.

2.2 Challenges in the Way for Future Energy Systems Adoption

In this section, the challenges faced as a result of increased renewable energy integration will be elaborated upon. Based on the challenges, the section goes on to lay out the key features that will need to be present in energy systems in order to distinguish them as future-driven energy systems.

Renewable Energy Penetration

Figure 2.1 shows the growth in global renewable energy consumption from 2004 to 2014, with modern renewables growing at more than twice the rate of demand. The average 10-year growth rate has been 4.7% for renewable energy sources.

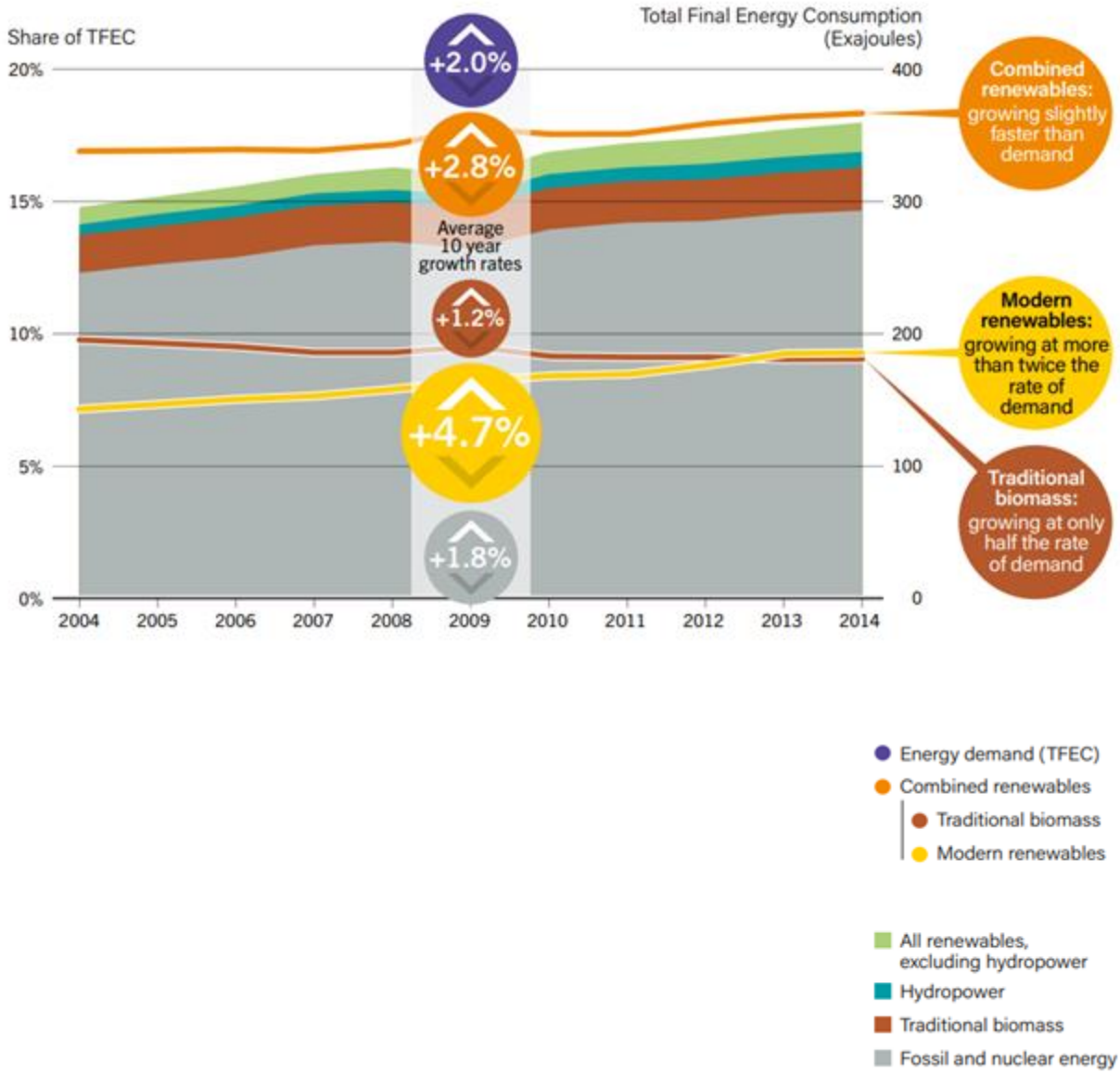

Figure 2.1 Growth in Global Renewable Energy Compared to Total Final Energy Consumption, 2004-2014 [9]

Among renewable sources, like wind and solar, the variability, uncertainty, and a-synchronism of these resources present implications for reliable power system operation and utilities.

In most scenarios, variable generation is connected to the grid, benefitting from its electrical support, and reliability but not integrated with the operation of the grid. As a result, the full value of variable generation is not realized with respect to providing support for grid reliability.

The following section will further explain the impact of intermittent renewable energy sources in more detail.

2.3 Impact of Variable Renewable Energy

The cost of harnessing solar power and wind has in recent years decreased substantially due to innovations in their associated technology (wind turbines, solar panels, etc.) and more broadly due to economies of scale, directly influenced by government policy in many western developed nations such as Germany and France [3,7]. The share of power supply in the global mix attributed to solar PV and wind is only expected to increase in the coming years. Despite these upward trends in utilization, there remain significant barriers to integrating high amounts of solar and wind. Both solar and wind can be described as renewable energy that is variable, a direct result of not being in constant supply for power utilization. These variable renewable energies (VRE) introduce into the power system an increased level of intermittency and uncertainty, which make operation of power systems more challenging. Some of the key challenges are listed below:

- Disturbances in the system marginal prices of electricity that are brought about by expensive generation units coming online to balance the variability of demand.
- An increase in the operating costs of conventional generating units arising from being forced to operate far from the optimal levels. Also expected is an increase in capital costs from additional ancillary services that will be needed to deal with the high level of uncertainty associated with VRE.

In response to these unprecedented challenges, a number of technical solutions have been proposed to mitigate the effects of increased VRE in the power system. These include establishing distributed sources for renewable power in terms of geographic location in an attempt to reduce the net load variability and uncertainty. Another approach is to take advantage of locations where both solar and wind power can be harnessed in a synergistic manner, this would lead to efficient implementation of Demand Side Management (DSM) technologies and methods [8]. Increasing the flexibility of the grid itself is one of the options to integrate large scale VRE into an energy system. An early idea of possibly achieving grid flexibility is by investing in more gas fired power plants which have greater flexible generation capacity, along with greater investments in transmission networks which would serve to interconnect different grid to allow for a larger balance zone. A more recent solution strategy has been the implementation of energy storage, which will be looked at closely in this project. The potential energy storage technology (such as compressed air energy storage, power-to-gas etc.) will depend on the nature of each power system along with the time scale of operation that will be considered for the energy system in question.

2.4 Polygeneration Energy Systems

A polygeneration process, as shown below as an example from [10] in Figure 2.2 is a multi-in in multi-out energy system that co-produces electricity and chemical fuels, where the chemical fuels can be used as substitutes of conventional oil based transportation fuels. Depending on the type of chemical synthesis, its chemical products could be methanol, ethanol, dimethyl ether (DME), Fischer-Tropsch (FT) oil, and hydrogen. It has a large range of available feedstock, typical instances of which are coal, petroleum coke, refinery tars, fuel oil, and biomass.

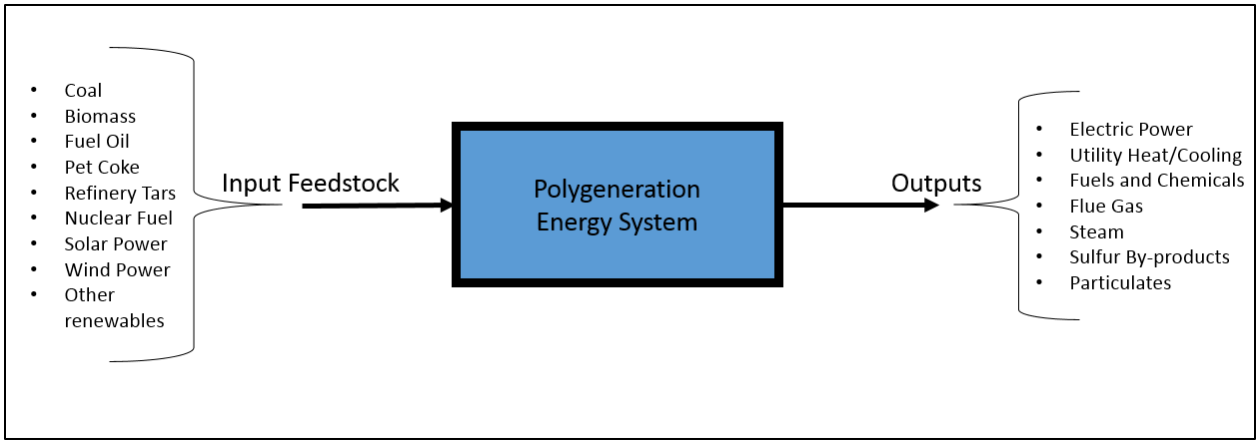

Figure 2.2 System Based Representation of a Generic Polygeneration Energy System.

A coal or biomass based polygeneration process starts with the production of syngas via gasification of feedstock in a gasifier as shown in Figure 2.3. Besides syngas, the gasifier also produces slag and ash, which can be used as construction materials or as fertilizer. The gasifier is usually oxygen-blown and requires an air separation unit (ASU). Upon exiting the gasifier, the syngas goes through a series of clean-up procedures to remove fine particles and sulphur compounds. The syngas is then split into two streams, one going to a chemical synthesis block to produce fuel, whilst the other goes to a power generation block. The power generation block usually comprises a gas turbine, a steam turbine, and a heat recovery steam generator (HRSG). A detailed overview of the key blocks that comprise a standard polygeneration process has been provided in a later section 2.3.1.

Polygeneration has many advantages over conventional power generation and chemical synthesis technologies. Firstly, polygeneration is of great interest to both the power and transportation sectors, which are the top two conventional sectors in terms of energy consumption and emissions, because of the ability of simultaneous production of electricity and transportation fuels and other chemicals. Secondly, the energy efficiency of a polygeneration process is higher than that of

traditional stand-alone power plants and chemical production plants due to the tight integration between the power generation and chemical synthesis blocks. Third, and perhaps most important in terms of requirement for future energy system application, is that polygeneration provides options for low to zero GHG emissions.

A modified energy polygeneration process could potentially be the answer to the most plausible future energy system that can be deployed in the near future as a solution to the most pressing problems associated with the energy generation sector [11].

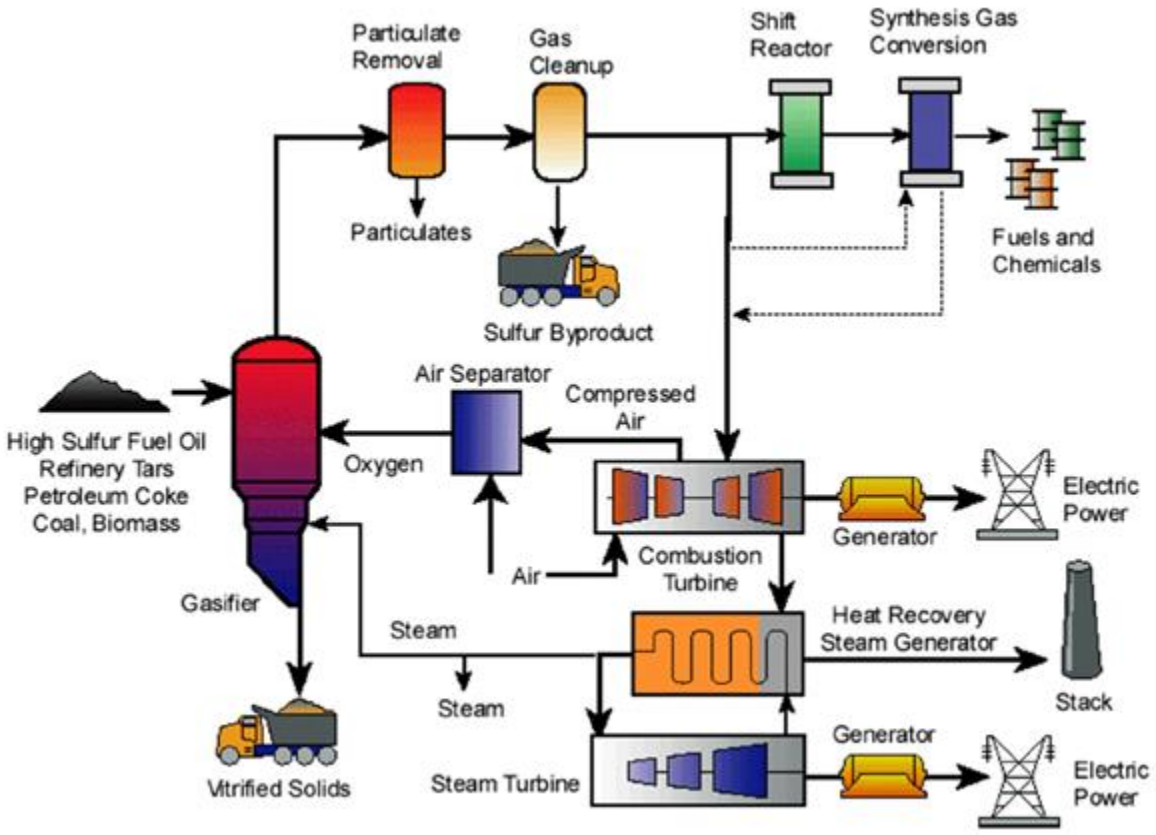

Figure 2.3 Layout of a Conventional Fossil-Fuel Driven Polygeneration Process [10].

Based on the layout shown in Figure 2.3, a systems representation of the polygeneration process is shown below in Figure 2.4. Later in this thesis, the manner in which this energy system is

modified and upgraded will be shown in a similar systems based diagram. The proposed energy system will have to be designed based on increasing operational flexibility for better economic attractiveness as well as for greater environmental benefits.

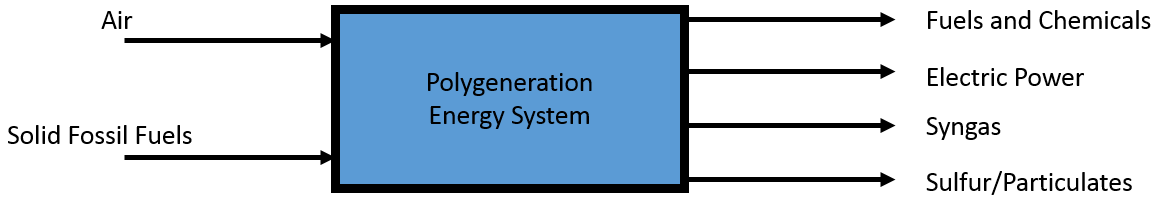

Figure 2.4 Systems Based Representation of a Fossil-Fuel Driven Polygeneration Energy System.

General description of traditional PES components:

A number of functional blocks can comprise the general form of the polygeneration process as reported by the previous studies in the literature. Each of these functional blocks can have a single or multiple technologies that govern their operation. For a typical polygeneration process that co-produces electricity and an additional chemical, the functional blocks are as follows [12]:

- Air separation unit or ASU. This block is used for preparing the oxygen that is fed into an oxygen-blown gasifier unit.
- Gasification block. Raw feedstock is gasified in this block to produce crude syngas. Sensible heat from the syngas could be recovered, depending on the equipment.
- Syngas clean-up unit. Hazardous components such as particulates, sulphur and chloride compounds are removed from this block.
- Water gas shift block. In this block, the composition of the syngas is altered via the water gas shift reaction to meet the necessary requirements for downstream chemical synthesis.

- Pre-combustion carbon capture/Post-combustion carbon capture. In this block, either the concentrated carbon dioxide in syngas after the WGS reaction can be separated out (pre-combustion carbon capture), or the block will separate the carbon capture present in flue gas emanating from the power generation block (post combustion carbon capture).
- Chemical synthesis. Either a split stream or a full stream of the syngas goes into this block for the purpose of producing methanol via a catalyzed reaction, for this specific system. The synthesis could either be gas phase or liquid phase.
- Gas turbine block. Unconverted syngas from the methanol synthesis block, together with any bypassed fresh syngas, combusts in this block that produces high pressure and temperature gas that drives a turbine to produce power.
- HRSG and steam turbine block. A HRSG recovers heat from the flue gas emerging from the gas turbine block, which produces steam, which in turn drives a set of steam turbines to produce more power.

Using specific functional blocks, a polygeneration energy system design that will be used for this project has been described later in Chapter 4. The difference in this proposed polygeneration flow diagram is the addition of blocks representing energy storage, which is a key technology to increase the flexibility of the system.

Table 2.1 Summary of Previous Studies On Polygeneration

Authors	Inputs	Outputs	Study Objective
Bose et al. [13]	Coal	Power, Urea, Heat	Process simulation
Buonomano et al. [14]	Solar only	Heat, Cooling, Electricity	Design, simulation, optimization
Chen et al. [15]	Coal, Biomass	Power, Liquid Fuels, Chemicals	Design optimization
De Kam et al. [16]	Biomass	Ethanol, Power, Heat	Process simulation
Farhat and Reichelstein [17]	Coal	Hydrogen, Power, Urea	Economic Modelling
Gao et al. [18]	Natural Gas	Power, Methanol	System Design
Guo et al. [19]	Lignite	Electricity, Tar	Simulation, optimization
Ilic et al. [20]	Biomass	Ethanol, Biogas, Electricity	Process optimization
Jana and De [21]	Agriculture waste	Power, Heat, Ethanol	Process simulation
Kyriakarakos et al. [22]	Wind and Solar	Electricity, Water	Simulation and optimization
Li et al. [23]	Coal, coke oven gas	Methanol, DME, Electricity	Simulation and optimization
Liu et al. [24]	Coal, Natural Gas, Biomass	Methanol, DME, Electricity	Optimal design, planning
Lythcke-Jorgensen et al.[25]	Biomass	Power, Heat, Ethanol	Exergy Analysis
Narvaez et al. [26]	Syngas	Power, Methanol	Process design
Pellegrini and Oliveira Jr. [27]	Sugarcane	Electricity, Sugar, Ethanol	Exergy optimization
Rubio-Maya et al. [28]	Natural Gas , solar	Electricity, Heating	Optimal design
Salkuyeh and Adams II [29]	Coal	Methanol, DME, Electricity	Chemical looping
Song et al. [30]	Biomass	Ethanol, Power, Heat	Drying process
Yu and Chien [31]	Coal	SNG, Ammonia, Electricity	Design, economic evaluation
Zhu et al. [32]	Coal	Electricity, Hydrogen	Modelling using chemical loop
Adams II and Barton [33]	Methanol, Electricity	Pre-combustion	NG reforming, methanol
Bose et al. [13]	Urea, Electricity	Pre-combustion	Hydrogen production
Fan and Zhu [34]	Hydrogen, Electricity	Pre-combustion	Hydrogen production
Farhat and Reichelstein [17]	Hydrogen, Electricity, Ammonia	Pre-combustion	Hydrogen separation
Guo et al. [19]	Tar, Electricity	Post-combustion	CCS
Hu et al. [35]	Methanol, Electricity	Pre-combustion	CO2 recovery, methanol
Jana and De [36]	Ethanol, Electricity, Heat		Hydrogen and CO ratio
Li et al. [37]	Methanol, Electricity	Pre-combustion	CO2 recovery, methanol
Li et al. [38]	Methanol, Electricity	Pre-combustion	Methanol
Li et al. [23]	Synthetic NG, Electricity	Post-combustion	Life-cycle GHG emission
Ng et al. [39]	Methanol, Electricity	Pre-combustion	CCU for methanol synthesis
Yu and Chien [31]	Synthetic NG, Electricity	Pre-combustion	Hydrogen
Zhu et al. [32]	Hydrogen, Electricity	Oxy-fuel combustion	CCS

In this work, the model will take advantage of the polygeneration system being multi-input and consider wind power and coal to demonstrate integration of renewable energy with conventional power production and generation planning

2.5 Research Gaps in Polygeneration Modelling Studies

From the literature review of previous polygeneration studies, the following research gaps can be identified and will be addressed in this project:

- While some studies have considered renewable energy inputs like solar power, the integration of feedstock with both conventional sources and renewable sources has not been taken into account. This integration will be a focal point in the present work.
- Many polygeneration system models have included carbon capture as key functional block, but have not studied the role energy storage plays in the overall operation. This project will look at energy storage blocks and their impact on a polygeneration energy system.
- Lastly, the concept of flexibility has not been explored to any significant extent by previous studies. In this project, mathematical optimization methods will be utilized to further analyze how a PES can have increased flexibility in its operation, in particular in response to situations with increased renewable energy availability and surges in load demand.

2.6 Renewable Energy Sources and their penetration

By the end of 2016, it was estimated that a total of 24.5% of the global electricity share came from renewable sources. Among the renewable sources, hydroelectric power had the maximum share with 16.6% followed by wind at 4.0% and solar at 1.5% [9].

Wind Power

Approximately 24 countries worldwide met 5% or more of their annual electricity demand by harnessing wind power of which 13 countries met more than 10% of their annual demand. In 2016 alone, almost 55 GW of wind power capacity was added bringing the total global capacity to nearly 487 GW. Wind power accounted for roughly one-fourth of newly installed power generating capacity in the US, ranking third after solar PV and natural gas for gross capacity additions. By the start of 2017, an additional 10.4 GW of wind power capacity was under construction. In Canada, 0.7 GW of capacity was added in 2016. Wind energy represents Canada's largest source

of new electricity generation for 11 years running. The province of Ontario has the highest wind power capacity among all Canadian provinces with a total capacity of 4.8 GW [6].

There are two methods of wind generation, which are broadly classified based on location – onshore wind and offshore wind. Onshore wind power has seen a steady increase in installed capacity in recent years. Offshore wind power in comparison has greater capital costs associated and thus has been adopted in a limited manner worldwide, with only European economies such as UK and Germany investing heavily on offshore wind.

Wind energy, while considered to be environmentally friendly, is not free of emissions primarily due to the production of equipment, transportation, installation and construction of wind farms. These activities require a high amount of energy and the required energy is generally tapped into from conventional fossil fuels.

Solar Power

Solar photovoltaic power (PV) use semiconductor materials to convert sunlight into electricity. It has applications in a variety of areas, including lighting, communication and signals and consumer products. Solar PV has emerged in the last two decades as the renewable energy sector with the fastest growth worldwide [9].

The fast growth can be attributed to a rapid decline in production costs of PV cells and therefore a drop in the price of PV generated electricity. Concurrently, there have been significant improvements in the efficiency of solar PV thanks to increased focus in worldwide research and development.

2.7 Energy Storage Technologies

Implementing energy storage can increase energy system efficiency both in terms of economic efficiency and energy utilization efficiency. In this section an overview of energy storage benefits as reported in the literature is discussed followed by brief descriptions of the existing storage technologies that have been studied as possible applications to further improve the overall flexibility of an energy system [80]

When the energy demand during a time period is low, storing the energy allows the baseload power production to continue operating at high efficiency. When the energy demand is high, the stored energy can be tapped into without forcing the use of peak power generation with high marginal costs.

Wind power and solar power are variable and non-dispatchable and cannot be considered for baseload power production. Additionally, if fossil fuel based power generation at higher amounts is needed to compensate for this variability then the effectiveness of utilizing renewable energy in the first place is rendered pointless. The negative effects of variability of renewables like wind and solar can be significantly reduced by using energy storage technologies. In this thesis, the extent to which energy storage can serve as a solution to the intermittency of renewable generation is studied [40].

In literature studies so far, two approaches to integrating energy storage systems with variable renewable energy generation have been studied [76-79]. The first method is to consider the location of the energy storage node as along the point of generation and link the generation operation to this individual facility. This method implies that the storage is associated with just one power plant. In order to maximize the operational flexibility, it would mean considering the second approach to incorporating storage, as a system-level flexibility resource. The following

sections outline different storage technologies with a description of their characteristics and prior studies done in integrating with renewable generation. The most widespread energy storage technologies in place are pumped hydro, compressed air and lead-acid batteries. In recent years, alternative technologies have also emerged to serve as energy storage methods including hydrogen-based storage. Pumped hydro energy storage (PHES) is by far the largest energy storage technology and accounts for roughly 99% of the world's total storage capacity [41].

The following are the leading energy storage technologies that have been deployed worldwide in an attempt to increase the operational flexibility from power generation systems, either from renewable sources of conventional ones.

Pumped-Hydroelectric Energy Storage

In pumped hydro energy storage systems (PHES), electricity that has been produced by variable renewable generation is stored by pumping water to a higher gravitational potential for instance to the top of a hill. The pumped water is then released to a lower situated reservoir via a hydro turbine and this recovers the electricity that was originally stored. Worldwide there are more than 300 PHES setups that are operational. PHES is a mature storage technology and has an energy storage efficiency of 65-85% [41]. However, as a potential storage technology application, it is severely limited by geography [72-75].

Compressed Air Energy Storage

Compressed air energy storage (CAES) is the second largest form of energy storage currently in use worldwide. The principle behind it's working is the compression of air to a higher pressure. When the energy needs to be recovered, the stored compressed air is mixed with fuel leading to a combustion that expands through a turbine or a series of turbines. CAES can be summed up as a

gas turbine with the compressor and the expander operating independently and at different times [42].

Battery Storage

A rechargeable electrochemical battery is a chemical energy storage mechanism based on two electrodes with different electron affinities. There is a range of available battery technologies, based on their chemical properties. Each battery type has its own advantages and disadvantages in terms of energy density, efficiency and cost. Across the board, batteries have self-discharge losses associated with operation and therefore can be considered only for relatively short-term storage. Another demerit of batteries is that their performance reduces with an increasing number of cycles. While maintenance and operation costs of batteries are low, the capital costs associated with replacing batteries frequently is high [43].

Hydrogen as Energy Storage

Hydrogen can be used as a chemical storage form for electrical energy. A hydrogen-based electricity storage system comprises of three main components – an electrolyser that produces hydrogen from water with electricity, and electricity producing fuel cell that does the reverse, producing electricity from hydrogen, and a separate hydrogen container [42]. Hydrogen can also be stored as compressed gas, cryogenic liquid and in liquid carriers, though large-scale hydrogen storage is expensive as an option. The attractiveness of hydrogen as a storage solution is the lack of emissions surrounding its use, provided it is produced from renewable energy sources. The hydrogen to electricity conversion fuel cell only produces water vapour as a side product thereby making the technology clean and when used with clean energy sources, the entire storage cycle can be considered environmentally friendly [42]. Recently the concept of Power-to-Gas has been gaining traction and has emerged as an effective way of integrating renewables by converting

surplus power to hydrogen gas. The hydrogen produced can be injected into the natural gas system to displace natural gas and thus reducing GHG emissions. Power-to-Gas allows for the storage of significant amounts of energy and the provision of carbon neutral fuels [80-84].

2.8 Energy System Flexibility

Within the domain of process systems engineering, Grossman and Pistikopoulos [45] have formulated the concept of flexibility as an index that can be increased by modifications to design parameters as a response to uncertainties that may arise in any process technology. The following section briefly describes the methodology proposed to increase the flexibility index of a process.

A linear model of an existing flowsheet with fixed equipment sizes and fixed structure is given. Nominal values together with positive and negative expected deviations are also given for a set of uncertain parameters. The issue is to determine the minimum cost modifications for redesigning the flowsheet so as to increase the flexibility index. This index provides a scalar measure of the largest rectangle that can be inscribed within the feasible region of operation. This hyper-rectangle is centered at the nominal parameter point and its sides are proportional to the expected deviations. This index also accounts for the fact that the process can be adjusted during operation through control variables.

Flexibility in Power Systems

The power system operation is predicated on it being in balance, which means that the power supply and demand in the grid has to always match at any given instant. Electrical systems are designed in a manner that it has a limit up to which it can handle levels of uncertainty and variability on both demand and supply sides. An example of exhibiting flexibility on the supply side would be the operation of different power plants having different response times with some

having significantly shorter response times to make up for quick increases in demand at a given time.

The introduction of renewable energy sources which are high in variability such as solar and wind, will increase the amount of flexibility within the energy system. This could be achieved be modifications to the supply/demand side. From the point of view of electricity systems, flexibility is seen as closely related to grid frequency and voltage control, power delivery uncertainty and ramping rates of power generation systems. Huber et al [46] used the above characterizations to define three metrics to describe system flexibility which are ramp magnitude, ramp frequency and response time, especially for the net load which results when the VRE generation has been removed from the total gross load.

In contrast, Denholm et al. [44] defined flexibility in terms of the mix of power plants with each type of plant accounting for the base load, intermediate load and peak load. Their study of the state of Texas in USA concluded that reducing the share of rigid base-load power plants would increase the flexibility of the system to allow for increased penetration of variable power generation.

Since there exist variations in the definition of flexibility, calls for a multidisciplinary approach to account for the benefits that it may bring to an energy system. Different aspects of the energy system have its own description of flexibility and therefore using a single indicator to measure it is not applicable. For a given system that is in consideration, its own custom defined flexibility will have to be explained and measured.

Flexible Operation of a Polygeneration Energy System

With respect to a polygeneration process, according to [15], a flexible polygeneration process is one which allows variable product output mixed during the lifetime of the project according to market prices and demands. In such a process, the plant can vary the production rates of individual

products as a direct response to changing market conditions by typically oversizing equipment. In the flexible polygeneration process assessed in [15] the flexible plant maintains power generation levels during peak times when the price of electricity as well as the demand is high, and switches to production of chemicals/liquids during off-peak times when the price of electricity and demand is significantly lower. Under this operating framework, the liquids produced can be stored for a short-term period and then sold to the market.

2.9 Mathematical Modeling Methods

Mixed-Integer Programming

An optimization model with both integer and continuous variables is denoted as a mixed-integer programming problem (MIP). Integer variables in MIP problems usually refer to 0-1 variables, also known as binary variables. MIP is widely used in process systems engineering. Typical applications include superstructure modelling, allocation problems, scheduling problems, and so on.

$$\begin{aligned} min\ C &= f(x,y) \\ s.t.\quad g(x,y) &\leq 0 \\ k(x,y) &= 0 \\ y &\in \{0,1\}^m \end{aligned} \tag{2.1}$$

Where the objective function C = f (x, y) in general, represents a desired economic measure, for instance the net present value (NPV) of a plant, while the equality and inequality constraints k (x,

y) and g (x, y) can be made to represent the mass and energy balances, design equations, physical constraints, design specifications or logical conditions that will need to be satisfied.

Continuous variables, x can be attributed to flow-rates, equipment sizes, pressures and temperatures, whereas 0-1 binary variables, y can be attributed to the existence of units based on whether they are operating or not.

MIP problems can be classified into two categories: mixed-integer linear programming problems (MILP) where the objective function and all constraints are linear, and mixed integer nonlinear programming problems (MINLP), where either the objective function or some constraints are nonlinear. MINLP problems can be further classified as convex MINLP problems, where the objective function is a convex function and the feasible region is a convex region, and non-convex MINLP problems, where either the objective function is non-convex or the feasible region is a non-convex region [47].

Optimization under Uncertainty

Uncertainty is inevitable in the planning and design of systems over a long time horizon. Due to the nature of uncertainty, many parameters obtained at the design phase are subject to considerable variability and therefore impossible to predict with a high level of accuracy. One clear instance of high variability present in this project is the availability of wind and solar power over a given time period, which due to its very natural occurrence has a high intermittency associated with it. The approach of optimization under uncertainty takes into consideration the uncertain parameters at the design stage thus improving the design of the system in question both in terms of operability and feasibility.

Optimization under uncertainty has been widely used in production planning and scheduling as well as in other sectors of modelling. In these types of problems, uncertainty usually arises from a wide variety of sources. According to their nature, sources of uncertainties have been classified by Pistikopoulos (1995) [48] in the following ways:

- Model-inherent uncertainty: these are uncertainties related to the physical characteristics of the system such as heat transfer coefficients, which can be described as either ranges of possible values or as probability distribution functions that can be modelled from experimental data.

- Process-inherent uncertainty: these are fluctuations in flowrates, temperatures etc. that can also be described as probability distribution functions derived from on-line measurements.

- External uncertainty: these are uncertainties external and not related to the process in question; these include product demands, price fluctuations and environmental conditions. These can be generally input into the model as approximate ranges of uncertainty or even as probability distribution functions that can be obtained from forecasting techniques or historical data.

- Discrete uncertainty: these are uncertainties arising from random discrete events that typically cannot be foreseen or predicted such as failure of equipment or even availability of certain nodes/equipment.

One possible solution approach for optimization under uncertainty comprises the use of stochastic programming, stochastic dynamic programming and fuzzy programming. In most chemical engineering applications, stochastic programming has been considered as the preferred modelling framework [49]. Depending on the type of uncertainty that appears within the mathematical model

as described above, stochastic programming can range from probabilistic programming, recourse or corrective programming and dynamic programming [48].

In the general form, stochastic programming is presented as a two stage programming problem. At the first stage, certain decisions are required to be made in the presence of uncertainty, whilst corrective actions can be taken at the second stage when more information is available after uncertainties are revealed. The second-stage variables are treated as corrective measures to avoid infeasibility when random events have presented themselves. These variables can also be representing operational level decisions that need to be made when facing uncertainty realizations.

$$max_y\, f^{(1)}(y) + \sum_{h=1}^{s} Occu_h M_h(y)$$

$$s.t. \quad g^{(1)}(y) \leq 0$$

$$k^{(1)}(y) = 0$$

$$\forall h \begin{cases} M_h(y) \equiv max_{x_h}\, f^{(2)}(y, x_h) \\ s.t. \quad g^{(2)}(y, x_h) \leq 0 \\ k^{(2)}(y, x_h) = 0 \\ x_h \in X_h \end{cases}$$

$$y \in Y$$

(2.2)

Where y are design decision variables, x_h are operational decision variables in scenario h; Y are bounds on the design decision variables, X_h are bounds on the operational decision variables in scenario h; $g^{(1)}$ and $k^{(1)}$ are design inequality and equality constraints, respectively such as cost calculations for equipment sizes; $g^{(2)}$ and $k^{(2)}$ are operational inequality and equality constraints,

respectively, such as energy and mass balances, feedstock characteristics and emission regulations. $f^{(1)}$ is the part of the objective function that is only dependent on design decision variables, e.g., a function of capital costs; $f^{(2)}$ is the part of the objective function that is dependent on both design and operational variables such functions related to product revenues, cost of feedstock etc.; $Occu_h$ is the probability of occurrence of scenario h over the lifetime of the system. M_h is the optimal solution of the h^{th} second stage (or operational stage) program. The problem size will depend on the number of scenarios to be considered s. When s is large, the problem can become a large-scale MINLP problem even if the M_h second stage problem is small.

Based on the form of the objective function and constraints and the nature of variables in both stages of the stochastic problem, the two stage stochastic programming can be further classified as stochastic linear programming, stochastic integer programming, and stochastic nonlinear programming.

General Algebraic Modeling System

For this thesis, the models for the future energy systems will be developed using the General Algebraic Modeling System (GAMS). GAMS is one of the leading commercial modeling system for mathematical programming and optimization. It is comprised of a language compiler and a wide range of integrated solvers that can be called based on the nature of programming being performed. GAMS has a reputation for being tailored for complex, large scale modeling applications and allows users to build large models that can be adapted quickly to different situations [50].

In previous studies on the optimal design and operation of polygeneration energy systems, some of the models developed turned out to be nonconvex NLP models. The objective was to maximize

the net present value (NPV) of the system subject to design and operational constraints such as mass and energy balances, consumption rates of feedstock. The models were formulated in GAMS and solved to global optimality by the BARON solver with SNOPT as the NLP solver and CPLEX as the LP solver [15].

The success of previous model formulations for complex energy system modeling in GAMS is persuasive in adopting the same modeling platform for the studies to be done in this project as well.

Potential Approaches to Solve Models with High Complexity

The evaluation of the expectation term in the objective function of the first stage problem is the key challenge in solving a two-stage stochastic programming problem. It requires integration over the entire uncertainty space where the integrand is the optimal solution of the second stage problem. In order to facilitate this, approximations via numerical approaches have been outlined in [48], which are: (i) multi-period approach, where the uncertain space is approximated via scenario analysis. (ii) probabilistic approach, where the probability distribution functions of the uncertain parameters are used directly and (iii) sensitivity analysis theory. These approached require generation of a large numbers of scenarios, or a large number of sampling points, thus increasing the problem size to an extent that obtaining a solution become computationally difficult.

Stochastic programming problems thus require sampling and decomposition techniques in order to make them solvable within a reasonable time frame. Sampling techniques help to reduce the size of the problem by reducing the number of sample points while still maintaining a degree of accuracy. Decomposition techniques split a large-scale problem into several sub-problems of a

smaller size, which significantly improve the computational performance of the solution procedure, especially when applied together with parallel computational techniques [51].

Two commonly used algorithms for solving MINLP problems are Generalized Benders Decomposition (GBD) and Outer Approximation (OA), both of which have a large number of varieties. Both algorithms solve an MINLP problem by creating a primal problem and a master problem, solving them to obtain lower and upper bounds of the original problem, and keeping an updating these bounds until they converge within an acceptable criterion in a finite number of iterations. The two algorithms differ primarily in the way to obtain lower bounds and updating constraints. GBD algorithms obtain lower bounds based on duality theory, whilst OA algorithms depend on solving a primal problem. However, both types of algorithms are local algorithms, i.e. they can only guarantee a global optimum for convex MINLP problems. These algorithms have also been widely implemented in commercial solvers.

Algorithms for solving non-convex MINLP problems, however, are not yet fully developed as compared with those for convex MINLP problems. There are primarily two groups of approaches to obtain a global optimum of a non-convex MINLP problem so far. One group of approaches is to perform global optimization techniques to a non-convex MINLP problem via constructing a convex relaxation, solving the relaxed problem to obtain a lower bound, solving the original problem using a local solver to obtain an upper bound, and keeping on this procedure until it converges. One approach for convex relaxation is to use a commercial global solver, which solves a MINLP problem directly and gives the global optimum. A typical global solver is BARON, which applies a branch-and-reduce algorithm to a MINLP problem and finds the global optimum. Compared with local solvers, global solvers are computationally more expensive and may encounter computational difficulties in solving large-scale MINLP problems [52].

2.10 Machine Learning – Clustering

Renewable energy companies have benefited greatly from the power of machine learning over the years. ML can lower costs, make better predictions and increase the portfolio's rate of return and this trend is expected to continue at a more rapid pace.

Some of the ways ML is changing the energy landscape:

Better grid management. AI and ML can help with better predictions of various VRE's electricity production capacities, typically wind and solar. The challenge with the modern grid is that power generation and power demand must match at all times or the alternative is issues like blackouts and system failures.

Another way is the demand response issues. By better forecasting how much wind and solar is expected at any given time, which allows operators to make up for excess electricity demand by using non-renewable energy whenever necessary. One such method is the training of ML algorithms with the use of large historical data sets in order to accurately match the supply and demand.

Another avenue where ML can help in the energy industry is by assuring the reliability and robustness of power grids. This can be done through predictive maintenance, where ML algorithms can predict from data collected from equipment and machinery, when that piece of equipment is expected to fail. So these algorithms efficiently predict machine failure, avoid blackouts and optimize maintenance activities and periodicity thus cutting down on maintenance costs and costs incurred from unexpected events.

K Means Clustering Algorithm

This algorithm is an iterative clustering algorithm which attempts to assign data points to exactly one cluster of the K number of clusters that have been pre-defined.

Typical with the concept of clustering, this algorithm works to make the items inside a cluster as similar as possible while also making the clusters vary from each other. It does this by making sure that the sum of the squared distance between the data points in a cluster and the centroid of that cluster is minimum. The centroid of the cluster is the mean value of all the values in the cluster.

In a more technical term, the desired outcome is to have data in one cluster as homogeneous as possible while making the clusters as heterogeneous as possible. The number K which represents the number of clusters can be varied by the user until a satisfactory result is obtained.

<u>The algorithm -</u>

1. Initialize cluster centroids randomly
2. Repeat until convergence

The above can be further simplified to a few simple steps -

1. Assign the K number of clusters
2. Shuffle the data and randomly assign each data point to one of the K cluster and assign initial random centroids
3. Calculate the squared sum between each data point and all the centroids
4. Reassign each data point to the closest centroid based on the computation outlined in step 3

5. Reassign the centroid by calculating the mean value for every cluster

6. Repeat steps 3,4 and 5 until we no longer have to change anything in the clusters

The duration needed to run the K-means clustering algorithm depends on the size of the dataset, the K-number defined and the patterns inherent within the data. The final outcome of clustering a dataset is that two items from the same group are similar to each other, while two items from different groups are as different as possible.

Basic Idea of K-means -

This is an algorithm that can help organize data without any labels. In machine learning, labels are an essential ingredient to a supervised algorithm like Support Vector Machines, which learns a hypothesis function to predict labels given features. In this work, the data being used is without any feature labels since they are load data and wind generation data. One of the most straightforward tasks that can be performed on a data set without labels is to find groups of data within the dataset which are similar to one another - which are called clusters. Among the many ways to cluster in the machine learning mathematical tools, is K-means. The K-means stored "k" centroids that it uses to define clusters. A point is considered to be in a particular cluster to that cluster's centroid than any other centroid. K-means finds the best centroids by alternating between (1) assigning data points to clusters based on the current centroids (2) choosing centroids (points which are the center of a cluster) based on the current assignment of data points to clusters.

Machine Learning

Unsupervised machine learning is a type of machine learning algorithm that seeks to infer patterns in the data without any prior knowledge or labels within the data. The opposite of this is supervised

machine learning, where there is a training set and the algorithm works to find the patterns in the data by matching inputs to predefined outputs.

Clustering by itself is a tool for unsupervised machine learning. When applying a clustering algorithm, it is not possible to know the categories beforehand. It is expected that the categories will emerge after the algorithm has finished analyzing the data and therefore clustering is referred to as an exploratory machine learning task.

2.11 Summary of Literature Review

In this chapter, the background literature surrounding energy systems and their relevant components has been presented. Previous research projects that have looked at polygeneration energy systems with and without carbon capture have also been summarized. The key concepts of future energy systems have also been described, in particular, potential energy storage technologies and how these can enhance the energy system flexibility. Also discussed in this chapter are modeling approaches that have been undertaken, including mixed integer programming and stochastic programming as well as the applicability of using GAMS as the main software for the development and solutions for the models.

Chapter 3 Power Generation Planning

This chapter discusses the development of a unit commitment based model to represent the power systems component of the renewable-based polygeneration energy system. It describes the integration of wind power to a network constrained Direct Current Unit Commitment (DCUC) model using a stochastic DCUC model.

3.1 The Unit Commitment Model to Represent Power Systems

The unit commitment (UC) problem addresses a fundamental decision in the operation of a power system, namely determining the schedule of power production for each generating unit in the system so that that the demand for electricity is met at minimum cost. The schedule must also ensure that each unit operates within this technical limits; these typically include ramping constraints and also the minimum uptime/downtime constraints. Units that are scheduled to produce electricity during a given time period are said to be committed for that period.

The UC problem can be formulated as a mixed-integer nonlinear optimization problem and it is generally large-scale and non-convex. It is NP-hard in general, but its practical importance has motivated a tremendous amount of research dedicated to techniques for computing global optimal solutions [63-65]. This is both because of the significance of the operational costs and because in competitive market environments, the non-convexity of the UC problem allows the existence of multiple local optimal solutions that may lead to considerably different pricing and market settlements outcomes [66]. Indeed, a mixed-integer linear (or nonlinear but convex) optimization model of the UC problem is among the few techniques that can provide provably global optimal solutions for the commitment decisions and corresponding financial settlements. At the same time,

the time available to solve the problem is a hard constraint in practice. Hence, UC is an optimization problem that is both important and challenging.

With the increasing penetration of stochastic sources of electricity in modern power systems, most notably wind and solar generation, techniques for handling uncertainty are acquiring greater importance in UC modeling.

3.2 Stochastic Unit Commitment with Uncertainty

A stochastic optimization formulation is relevant if the UC is affected by important uncertainty in the data. Handling the stochastic behaviour is currently of great importance because of the uncertainty arising from the variability in generation from stochastic production facilities such as wind and solar-based generating units. These types of generating units often benefit from priority in dispatch by virtue of their low marginal cost or regulatory policies. They are therefore not scheduled per se but rather their production is subtracted from the demand, and other units are then scheduled to meet the resulting net demand which is the actual demand minus the stochastic production.

When formulating a stochastic UC, two stages are generally considered:

- The first stage pertains to the optimal scheduling of the generation capacity which is the decisions about which units to commit in advance of the actual operation.
- The second stage constitutes a representation of a number of plausible operating conditions that may arise in the future as a result of the uncertainty realization. These possible operating conditions are called scenarios and for each scenario, and optimal dispatch can be computed based on the commitment decisions made in the first stage [67-69].

Reserves are scheduled in the first stage so that the system will be able to accommodate any uncertainty realization/scenario.

The philosophy of this two-stage formulation is that in the first stage, scheduling decisions are made using only the information that is available hours or days in advance of real time operations. The uncertainty is then realized is the second stage, and the dispatch adjusts the amount scheduled in the first stage up or down, as required according to the scenario.

The scenarios take into account the possible wind realizations over the planning period. Each scenario is assigned a probability, and the optimization objective is to minimize the sum of the deterministic cost of the first stage decisions and the expected cost of the second stage decisions.

There are several limitations of the stochastic optimization approach, one of them is the quality of the solutions obtained critically depends on the choice of the scenarios, in the sense that having a broader range of scenarios usually leads to a more accurate model. However, increasing the number of scenarios increases the computational cost of the optimization. Another issue is that this approach assumes explicit knowledge of the probability distribution of the uncertain wind realization. In practice, this distribution is estimated empirically based on past data and experience and/or using simulation models and the limitations of the probability estimation may impact the quality of the results [70-71].

3.3 Model Formulation

This section describes the power generation planning model and its various components followed by the main equations, variables and constraints that comprise the optimization model.

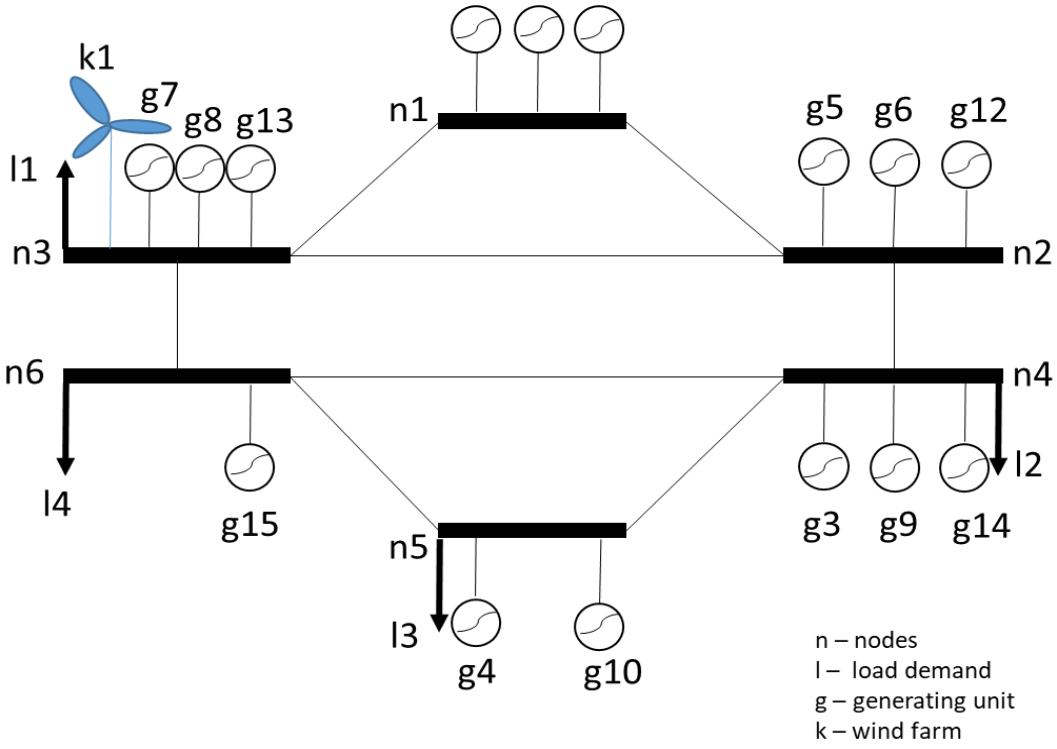

Figure 3.1 Topology of the 7-node power system with storage mechanism [72]

In figure 3.1 above, the topology is the representation of the power system and an additional the storage mechanism, where every generator, power loads and a single wind farm are inter-connected by a network of nodes. Power flows are made possible via networks adhering to the DC optimal power flow. Therefore, the unit commitment model considered is that of a stochastic DCUC model. There are a total of 6 nodes, 15 conventional generators, 4 load demand nodes and 1 wind farm situated at node 3.

The objective function of this stochastic DCUC model consists of the system cost in the day-ahead stage and the expected imbalance costs that are incurred in real-time operation. The objective function variable *AnnualCost* represents the summation of the operating and capital cost

components of the power planning model and the objective function equation is shown below in equation 3.1:

$$AnnualCost = Annualized\ Capital\ Cost + \sum_{1\ year} OF_{DA}^{Oper} + OF_{RT}^{Oper} \quad (3.1)$$

The variable *z* represents the constituent terms in the annual operating cost of the system as shown in equation (3.2) [72].

Operating Cost Components:

$$z = \sum_{g,h} (c_{g,h}^{SU} + c_{g,h}^{SD} + C_g p_{g,h}^{DA}) + \sum_{s} \rho_s * (\sum_{g,h} C_g * r_{g,h,s} + \sum_{l,h} V_l^{SH} p_{l,h,s}^{SH}) \quad (3.2)$$

Where $c_{g,h}^{SU}$, $c_{g,h}^{SD}$ and $C_g p_{g,h}^{DA}$ are the terms making up the day-ahead stage costs, representing the cost of start-up and shutdown of each conventional generator g at every hour h while the third term is the product of the marginal cost of each generator g in USD/MWh and the power scheduled in the day ahead stage at every hour h by each generator g, respectively.

The stochastic components are the remaining terms in the equation. The probability of occurrence of each scenarios is represented by ρ_s . The power adjustment of each conventional generator unit in hour h under scenario s is given by $r_{g,h,s}$. The value of the lost load for each load l is a parameter input into the model and is denoted as V_l^{SH} with a unit of USD/MWh and the $p_{l,h,s}^{SH}$ is the involuntary active load shedding of load l in hour h under scenario s in MW.

Day-Ahead Constraints:

The following equations in this section make up the day-ahead stage constraints.

The maximum and minimum power generation capacity constraints on the generator applies in the day-ahead stage:

$$p_g^{min} * u_{g,h} \leq p_{g,h}^{DA} \leq p_g^{max} * u_{g,h} \qquad \forall g, \forall h \tag{3.3}$$

Where p_g^{min} and p_g^{max} is the minimum power output and maximum capacity respectively, of the conventional generator, g and $u_{g,h}$ is the binary variable that is equal to 1 if the conventional generator unit is scheduled to be committed at any hour h. $p_{g,h}^{DA}$ is the power scheduled in the day-ahead stage by conventional generator g, at hour h.

Maximum and minimum ramp up and ramp down limits in day-ahead:

$$-R_g^- \leq \left(p_{g,(h=1)}^{DA} - p_g^{ini}\right) \leq R_g^+ \qquad \forall g \tag{3.4}$$

$$-R_g^- \leq \left(p_{g,h}^{DA} - p_{g,(h-1)}^{DA}\right) \leq R_g^+ \qquad \forall g, \forall h > 1 \tag{3.5}$$

Equations (3.4). and (3.5) limit the ramp rates for conventional generator units which is to say the change in the hourly power production may not exceed the maximum ramp-up and ramp-down rate of each generator at every hour., R_g^- and R_g^+ is the ramp-down limit and ramp-up limit of the conventional generators g in MW/h while p_g^{ini} is the initial active power output of conventional unit g.in MW.

Transmission capacity in day-ahead stage:

$$B_{(n.m)}\left(\theta_{n,h}^{DA} - \theta_{m,h}^{DA}\right) \leq F_{n,m} \qquad \forall n, \forall m, \forall h \tag{3.6}$$

Equation (3.6) is the constraint that enforces the capacity limits between the transmission lines. $F_{n,m}$ is the capacity of the transmission line between nodes m and n in MW. $B_{(n.m)}$ is the inverse

of the reactance of the transmission line between nodes m and n and $\theta_{n,h}^{DA}$ is the voltage angle at node n in hour h in radians.

Start-up cost for generators in day-ahead:

$$c_{g,(h=1)}^{SU} \geq \lambda_g^{SU}\left(u_{g,(h=1)} - U_g^{ini}\right) \quad \forall g \tag{3.7}$$

$$c_{g,h}^{SU} \geq \lambda_g^{SU}\left(u_{g,h} - u_{g,(h-1)}\right) \quad \forall g, \forall h > 1 \tag{3.8}$$

$$c_{g,h}^{SU} \geq 0 \quad \forall g, \forall h \tag{3.9}$$

Shut-down cost for generators in day-ahead:

$$c_{g,(h=1)}^{SD} \geq \lambda_g^{SD}\left(U_g^{ini} - u_{g,(h=1)}\right) \quad \forall g \tag{3.10}$$

$$c_{g,h}^{SD} \geq \lambda_g^{SD}\left(u_{g,(h-1)} - u_{g,h}\right) \quad \forall g, \forall h > 1 \tag{3.11}$$

$$c_{g,h}^{SD} \geq 0 \quad \forall g, \forall h \tag{3.12}$$

Equations (3.7) – (3.12) represent the constraints that calculate the start up and shut down costs of the conventional generator units, respectively.

Power balance of system in day-ahead:

$$\sum_g p_{g,h}^{DA} + \sum_k w_{k,h}^{DA} - \sum_l DL_{l,h} = \sum_m B_{(n.m)}\left(\theta_{n,h}^{DA} - \theta_{m,h}^{DA}\right) \quad \forall n, \forall h \tag{3.13}$$

Equation (3.12) is the power balance equation for the day ahead stage at each node. The left hand side of the equation are the variables for the power scheduled by conventional generators, g at every hour, the wind power scheduled by wind farm k at every hour and the power consumption

of load l at every hour h, respectively. The right hand side of the equation is the transmission capacity constraint set earlier in equation (3.6).

Real Time Constraints:

The following equations in this section represent the real time or second stage constraints of the stochastic DCUC model:

Power balance in real time stage:

$$\sum_{g}(p_{g,h}^{DA} + r_{g,h,s}) + \sum_{k}(W_{k,h,s} - w_{k,h,s}^{SP}) - \sum_{l}(DL_{l,h} - p_{l,h,s}^{SH}) = \sum_{m} B_{(n.m)}\left(\theta_{n,h,s}^{RT} - \theta_{m,h,s}^{RT}\right) \qquad \forall n, \forall h, \forall s \tag{3.14}$$

Constraint equation (3.14) enforces the power balance in the real-time operation at each node at every hour under each scenario s, by resolving the adjustments brought about by the actual wind production with regulating power provision by conventional units, and/or wind power curtailment, and/or load shedding. $W_{k,h,s}$ characterizes the wind power uncertainty.

Maximum and minimum power generation capacity in real time:

$$p_g^{min} * u_{g,h} \leq (p_{g,h}^{DA} + r_{g,h,s}) \leq p_g^{max} * u_{g,h} \qquad \forall g, \forall h, \forall s \tag{3.15}$$

Constraint (3.14) enforces the lower and upper bounds for the actual power production which represents the tentative production schedule at the first stage together with the adjustment brought about by the regulating power provided in the real time stage.

Maximum and minimum ramp-up and ramp-down limits in real time:

$$-R_g^- \leq [(p_{g,(h=1)}^{DA} + r_{g,(h=1),s}) - p_g^{ini}] \leq R_g^+ \qquad \forall g, \forall s \qquad (3.16)$$

$$-R_g^- \leq \left[\left(p_{g,h}^{DA} + r_{g,h,s}\right) - \left(p_{g,(h-1)}^{DA} + r_{g,(h-1),s}\right)\right] \leq R_g^+ \qquad \forall g, \forall h > 1, \forall s \ldots. \quad (3.17)$$

Constraint equations (3.16) and (3.17) enforce the ramping limits for the actual power production of the conventional generator units g, at every hour h under scenario s.

Power transmission capacity limit in real time:

$$B_{(n.m)}\left(\theta_{n,h,s}^{RT} - \theta_{m,h,s}^{RT}\right) \leq F_{n,m} \qquad \forall n, \forall m, \forall h, \forall s \qquad (3.18)$$

Constraint equation (3.18) limits the capacity of each transmission line in the system in the real time stage under all scenarios s.

Given that the network constrained stochastic DCUC model has two stages, day-ahead (first) and real-time (second), there is a requirement of ensuring that there are equations that act as linking constraints between the first and second stages. These linking constraints are equations (3.15) - (3.17).

3.4 Results and Discussion from the Stochastic DCUC Model

In this section, the power generation planning model developed in the previous section will be subjected to certain case studies to further study the model's validity and applicability to represent the power system that has been integrated with wind.

3.4.1 Base Case – DCUC Stochastic Power Generation Planning Model

Model Inputs:

For the base case model, the total number of wind probability scenarios considered is 50 with each scenario having its own unique probability of occurrence. The power generation planning model is subjected to a life time of 25 years with a discount rate of 7% which is used to calculate the capital return factor (CRF) of the power system. For this study, there is a need to use a hydrocarbon source for the greater polygeneration energy system, the reason being that the hydrocarbon to syngas pathway is crucial for the basis of chemical production. While coal is in the process of being phased out in many countries, including Canada, this study uses coal to act as the main fuel source for the conventional power generator as well as the source for the feed stream to the gasifier. As such, the model that will be developed in later chapters will be generic enough, for any other hydrocarbon fuel source to replace coal. In this study, the price of coal is assumed to be constant and not subject to variation at a price of USD 61 per ton [35]. The system according to the topology figure 3.1 has 4 loads and the value of load shed for each of the loads is set at USD 1000. The capital cost for each of the conventional generators is assumed to be USD 750,000 [72] and the higher heating value for the coal that is used for this system as feedstock for the conventional generators is assumed to be 8.39 kWh/kg [40].

The input data for the wind factors used to represent the actual wind realizations that are brought about by the uncertainty realization and their corresponding probability scenarios, is sourced from the open-source website managed by the Elia Group [91]. The data selected was the hourly wind factor for a full year's operation for the aggregate wind farms in Belgium for the year 2018. The motivation behind using this source for the wind power generation, was to showcase the typical European power system behavior and their characteristics (as shown in the topology figure 3.1).

The input data for the load demand sourced from open-source load data from the PJM electricity markets website. The PJM is a regional transmission organization that coordinates the transactions of wholesale electricity in all or parts of 13 states in the US and the District of Columbia. The hourly load demand for a specific jurisdiction (reflecting the typical urban block within a standard EU nation) was chosen for the year 2018 [92].

To aid in the system modeling and calculation of associated costs, an assumption was made that the cost of operating the wind power farm is negligible compared to the capital cost, so it has been assumed to be zero.

The model was solved using the typical linear programming solver CPLEX 11.1.1 and was modeled within the GAMS modeling software environment. The model consisted of 15,331 single equations, 6,168 single variables and 375 discrete variables. The total CPU time used to arrive at the optimal solution was 41.76 seconds. The main results of the model are presented below:

Table 3.1 Design Decision Variable Results of Base Case Power Generation Planning Model

Design Decisions	
X_{cap_k} (MW)	2686.6
Xgen (MW)	976

Table 3.2 Schedule of Conventional Generators in the Base Case Power Generation Planning Model

Generator	On/Off
g1	1
g2	0
g3	1
g4	0
g5	1
g6	0
g7	0
g8	1

Generator	On/Off
g9	0
g10	0
g11	0
g12	0
g13	0
g14	0
g15	0

In table 3.1, the reported value of the total wind power that is installed *Xcapk* is shown, which is 2686.6 MW and the total conventional power generation, *Xgen*, designed via generator scheduling is 976 MW. This implies that for a full year's operation, a higher amount of wind power capabilities is installed than conventional power for the above system. In table 3.2, the schedule of which conventional generators are switched on during the operation of the base case model is shown. Only 4 generators (g1, g3, g5 and g8) out of possible 15 total generators are designed, indicating that the wind capabilities are high and the actual wind power profiles are providing a significant portion of the load demand.

Table 3.3 Cost Results of the Base Case Power Generation Planning Model

Costs	USD (millions)
Total Cost (per year)	521.82
Operating Cost (per year)	90.15
Annualized Capital Cost	431.68

The main costs associated with the base case power generation planning model are shown in table 3.3 above. The total system cost is USD 521.82 million per year, which is comprised of the capital costs of installing the conventional generators and the wind farm based on the total wind power installed, which comes to a total of 431.68 USD million. The operating cost per year is USD 90.15

million/year, which is mainly the operating costs of running and maintaining the conventional generators, as the wind farm operating cost is assumed to be zero.

A key impact of integrating wind into power systems is the reduction in the overall greenhouse gas emissions. While this has been mentioned in the background section of the present work, the emphasis is on showcasing the use of excess wind in the overall polygeneration system by helping to drive the production of value added chemicals. For this reason, the emissions and its variation from this chapter and subsequent chapters will not be considered as a focal point of the design and operation modeling studies.

3.4.2 Impact of Clustering the Wind Probability Scenarios

In accordance with the base case model results shown in section 3.4.1, the model has 50 probability scenarios of wind power. However, the solution time for arriving at the solution is considerably longer. The general consensus from the mathematical optimization community is that the higher the number of scenarios, the longer and more computationally intensive it is to arrive at the solution.

For the purpose of reducing the solution time, the total number of probability scenarios for the wind is clustered based on the k-means clustering algorithm. As discussed in section 2.10, the k-means algorithm works to identify centroids and group similarly distanced data points close together until the scenario size is significantly lower but still able to represent the full scale data.

For the wind factors model inputs used in the previous section, the k-means clustering algorithm was able to reduce the number of scenarios from 50 to 6. The results of the clustering mechanism are shown in figure 3.2 below.

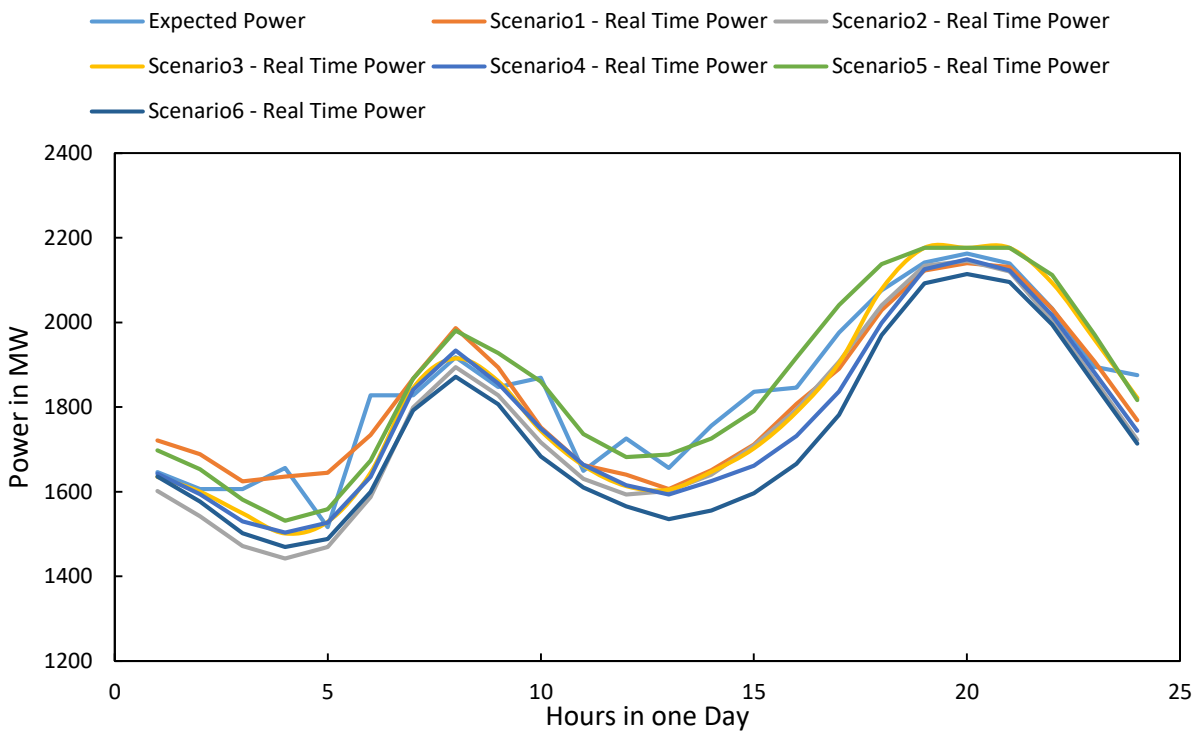

Figure 3.2 The results of the clustering algorithm on the expected wind power data, represented as the base case and 6 additional clusters.

The newly formed 6 wind probability scenarios are input into the model to replace the original 50 scenarios. The model is solved once again using CPLEX 11.1.1 using the GAMS 24.5 environment. The number of equations and variables is the same, however the model solved in 15.83 CPU time seconds. This solution time is significantly lower than the base case model with 50 scenarios, which solved in 41.76 seconds.

Table 3.4 Cost Results of the Power Generation Planning Model with Clustered Wind Scenarios

Cost Results	**USD (millions)**
Total Cost (per year)	541.78
Operating Cost (per year)	91.27
Annualized Capital Cost	450.51

The main cost results from the model with 6 wind probability scenarios is shown in table 3.4. It can be seen that the total cost per year has increased to USD 541.78 million largely due to the increased amount of wind installed at the day ahead stage, which adds to the overall capital cost of the system. The total wind power installed increased from 2686 MW to 2823 MW, once the clustered wind data was used as an input. So while the cost results of the model are higher by a sizable percentage, the solution time decreases from 41.76 seconds to 15.83 seconds which aids in the overall computational tractability of the model, in particular, when the above model is extended to include other components like storage systems etc. Moving forward in this chapter and the next chapter 4, all power generation planning models will be using the 6 wind probability scenarios.

3.4.3 Impact of a Surge in the Hourly Load Demand

The main purpose of this section is to showcase the benefit of modeling the power generation planning model under the conditions of uncertainty. The hourly load demand data used in this chapter has been increased by a surging amount of 20% in a manner to replicate what an extreme case may require the power system to respond to in order to satisfy the load.

The new load demand data is input into the model and solved under two different conditions.

1) The first condition is that the model is allowed to solve as per normal with the solution determining the new installed amounts of the wind power and the conventional generation power.
2) The second condition is that the model will be solved under the values of the fixed design decision variables of installed power for wind and conventional generators that were calculated in the base case model from the previous section. Which implies that in order to meet any load that the system falls short of providing, the operator can purchase from an external grid.

The following equations consider a new variable which is the amount of power purchased from the grid during the day ahead stage and real time stage. The price of electricity purchased from the grid is assumed to be USD 150 per MW.

The equation (3.18) below calculates the total cost of the power that is purchased from the grid to meet the surging load demand based on a unit electricity price of USD 150/MW:

$$P_{purchased} = 150 * \sum_{n,h} Pgrid_{n,h}^{DA} - \sum_{s} \rho_s * \left(Pgrid_{n,h}^{DA} - Pgrid_{n,h,s}^{RT}\right) \qquad \forall n, h, s$$

(3.18)

Where $P_{purchased}$ is the total power purchased from the grid, $Pgrid_{n,h}^{DA}$ is the power purchased from the grid in the day-ahead stage and $Pgrid_{n,h,s}^{RT}$ is the power purchased from the grid in real-time stage.

With this new cost variable calculated, the overall objective function of the power generation planning model needs to be updated:

$$minimize \qquad totalC$$
$$= Annualized\ Capital\ Cost + 365 * (OF_{DA}^{Oper} + OF_{RT}^{Oper} + P_{purchased})$$

(3.19)

All other parameters and inputs and assumptions are the same as the previous iterations of the model. The models in both conditions are solved again using CPLEX in GAMS software environment, and the results are reported below.

Results of Condition 1 (Design variables not fixed):

Table 3.5 Main Costs of Power Planning Model under Condition 1

Cost Results	**USD (millions)**
Total Cost (per year)	651.39
Operating Cost (per year)	117.66
Annualized Capital Cost	533.73

Table 3.6 Design Decision Variables of Power Planning Model under Condition 1

Design Decisions	
Xcapk (MW)	3312.7
Xgen (MW)	1226

From tables 3.5 and 3.6, it can be seen that with a surging load demand, both the design decision variable values and the main costs of the system increase across the board. The total cost increases from the base case of USD 541 million per year to USD 651.39 million per year, which correlates with the increase in the amount of wind power and conventional generator power installed.

Results of Condition 2 (Design variables fixed):

Under this condition, the system operator is permitted to purchase power from the grid and model incorporates equations (3.18) and (3.19).

Table 3.7 Main Costs of Power Planning Model under Condition 2

Cost Results	**USD (millions)**
Total Cost (per year)	659.07
Operating Cost (per year)	164.65
Annualized Capital Cost	450.51
Cost of Power Purchased (per year)	43.91

From table 3.7, it can be seen that the capital cost of 450.51 USD million per year is the same as that of the base case model, on account of the design decision variables are fixed prior to the model being solved. With the operator permitted to purchase power from the grid, the total cost of power that was purchased was 43.91 USD Million per year. Interestingly, the total cost of the system per year which is 659.07 USD Million per year is not that much greater than the total cost from the first condition which allowed the model to design the wind and conventional power capabilities from scratch. Additionally, it shows that the model from the base case design, is flexible in responding to any surges in power load by purchasing any additional power and still meeting the load demand.

The above two models, showcase the benefit of stochastic formulation as opposed to allowing the model to design under worst case scenarios. An example of designing under worst case would be using load demand data that is several orders of magnitude higher than the base load used (as opposed to the surged data used) or under a situation where the wind power available is zero. In reality, these types of worst case scenarios are extremely rare and only result in the model deciding to over-design the power system. By performing the above analysis, it can be said that the stochastic formulation provides optimal results in response to a situation that has a higher probability of occurrence with respect to uncertainty in load demand.

3.5 Concluding Remarks

In this chapter, a power generation planning model was developed based on a network-constrained DCUC model. The model developed was stochastic in nature with wind probability scenarios being utilized to showcase the uncertainty associated with intermittent wind power. The model aided in providing design decision variables for the system, and proceeded to provide results for

the operation of the power system in the day-ahead stage and followed by the real time stage. One aspect that was investigated was the impact of clustering the number of wind probability scenarios. It was found that despite some increases in the total cost of the system, when the total number of scenarios was reduced from 50 to 6, the total time taken to arrive at the solution of the model was reduced from 41 seconds to 15 seconds, which aids greatly in maintaining computational tractability, especially when the model is extended to become larger in scale. Another case that was investigated was how the model would respond to a surge in load demand and proceed under two conditions, one where the model's design is made from scratch to account for the higher loads, and the second where the system's design was fixed based on the base case results and the system was able to purchase power from an external grid. In both conditions, the total cost was comparable and only reinforced that modelling this power system under uncertainty is the right approach as opposed to extreme worst case scenarios which would only lead to an over-designed power generation planning model. Under all cases, the model was able to meet the load demand while also utilizing the available wind power hence successfully being able to simulate a power generation planning model which is able to integrate renewable energy.

Chapter 4 Power Generation Planning Model with Energy Storage System

This chapter discusses the extension of the previous stochastic DCUC model to include an energy storage mechanism. In this model, the storage mechanism will be represented by an electrolyser driven conversion from electricity to hydrogen. The chapter showcases how excess power from hourly time periods with high wind power realizations can be stored in the form of hydrogen. Additionally, this chapter will highlight the benefit of clustering the scenarios in the stochastic model and its applicability in building large-scale energy system models.

4.1 Energy Storage System with Stochastic DCUC Model

A response to the intermittency challenge posed by renewable energy sources like wind, has been the use of various energy storage methods. Among these, the ones with the most traction in recent years (outside of long-duration storage methods) has been the use the battery technology and chemical storage in the form of hydrogen. The mechanism works by first converting the excess power from renewable wind profiles to hydrogen with the use of an electrolyser. This hydrogen that is produced is stored in a tank or in larger scale projects, can be stored in caverns that are natural rock formations under the ground. The storage mechanism is completed when during periods of high demand, the stored hydrogen is extracted and converted to power once again by a fuel cell.

In the stochastic DCUC model developed in chapter 3, for hourly periods where the amount of wind available is not correlated with the load demand, the excess wind is spilled and there is a penalty that is paid by the operator as the wind power could have alternatively been used for storing to be used at a later time, or used in alternative means to extract value from that energy.

The level of wind spillage in the base case of the power system planning model from the previous chapter, was considerable in this chapter, the model will be extended to show the design and operation of a hydrogen electrolyser and fuel cell based energy storage system (ESS). The chapter will first focus on the model formulation of the ESS system, how it integrates with the original base case stochastic DCUC model and finally display and discuss the results and impact of having the ESS block.

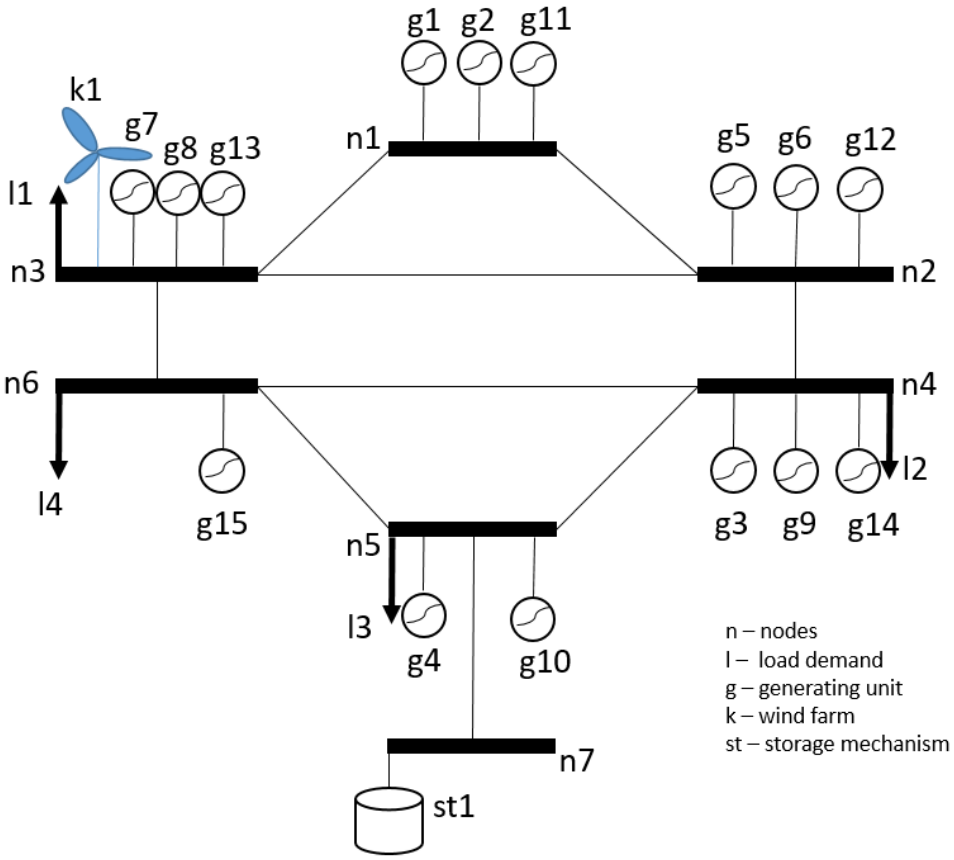

Figure 4.1 Topology of the 7-node power system with a storage mechanism node.

Figure 4.1 shows the amended node-based power system mechanism, which now includes an additional node that has the storage set, *st1* included. The *st* represents the ESS block comprising the hydrogen electrolyser and fuel cell components. The remainder of the figure is the same power system nodes set up earlier in chapter 3 of the thesis.

4.2 Model Formulation for the Energy Storage System

In this section, the modified equations from chapter 3 as well as the additional constraints and equations representing the ESS block are presented.

The approach taken in modelling the ESS block, is that the ESS and its associated variables and constraints will come into effect and respond only when the wind probability scenarios are realized, which is to say when the actual power is realized from the wind farm and the conventional generators. The capacities of the ESS components are first stage variables while the scheduled dispatched charging and discharging power (power to hydrogen and the hydrogen back to power) are second stage variables (function of uncertainty scenarios).

Equation (4.1) is the objective function of the model with ESS, with the objective function variable being the total cost of the system that is comprised of the capital and operating costs (day ahead and real time):

$$minimize\ \ totalC = Annualized\ Capital\ Cost + \sum_{1year}(OF_{DA}^{Oper} + OF_{RT}^{Oper}) \qquad (4.1)$$

Where *totalC* is the total cost of the power generation planning system, *cap* is the total capital cost of the power generation planning system and $OF_{DA}^{Oper}\ and\ OF_{RT}^{Oper}$ is the total operational cost in day-ahead and real-time respectively.

Equation (4.2) below represents the operating cost of the power generation system at the day ahead stage of the model.

$$OF_{DA}^{Oper} = \sum_{g,h}(c_{g,h}^{SU} + c_{g,h}^{SD} + C_g p_{g,h}^{DA}) + fuel_{DA} * pr_{coal} + \sum_{k} w_{k,h}^{DA} * OperW \qquad (4.2)$$

Where OF_{DA}^{Oper} is the operating cost of the power generation planning system model in day-ahead, $fuel_{DA}$ is the amount of fuel (coal) used by the power system in day ahead, pr_{coal} is the price of coal in USD and *OperW* is the operational cost of the wind farm.

Equation (4.3) below represents the operating cost of the power generation system at real-time stage of the model.

$$OF_{RT}^{Oper} = \sum_{h}\sum_{s} \rho_s * [\ (fuel_{RT} * pr_{coal}) + \sum_{g} C_g r_{g,h,s} + \sum_{l} (V_l^{SH} p_{l,h,s}^{SH}) + \sum_{k} (Xcap_k * W_{k,h,s} * OperW\ - w_{k,h}^{DA} * OperW) + \sum_{st} (ESS_{oper} *\ r_{st,h,s}^{EL} + ESS_{oper} *\ r_{st,h,s}^{FC})\ ] \quad (4.3)$$

Where OF_{RT}^{Oper} is the operating cost of the power generation planning system model in real-time, $fuel_{RT}$ is the amount of fuel used by the power system in the real-time stage. ESS_{oper} is the operating cost of the energy storage system block and $r_{st,h,s}^{EL}$ and $r_{st,h,s}^{FC}$ is the power converted to hydrogen in the electrolyser, and the power discharged from the fuel cell respectively, at every hour under each scenario s.

The equation (4.4) below is used to calculate the capacity of the electrolyser within the energy storage block.

$$cap_{EL} = \sum_{st} r_{st,h,s}^{EL} \qquad \forall st, h, s \quad (4.4)$$

Where cap_{EL} is the capacity in MW of the electrolyser in the storage system and one of the design decision variables to describe the installed capacity of the electrolyser.

The equation (4.5) below is used to calculate the capacity of the fuel cell within the energy storage block.

$$cap_{FC} = \sum_{st} r_{st,h,s}^{FC} \qquad \forall st, h, s \tag{4.5}$$

Where cap_{FC} is the capacity in MW of the fuel cell within the storage system.

The equation (4.6) is used to calculate the level of hydrogen in the hydrogen storage tank at every hour of the operation of the storage system but not inclusive of the first hour.

$$Hlevel_h^{RT} = EL_{Eff} * \sum_{s} \left(\rho_s * r_{st,h,s}^{EL}\right) + Hlevel_{h-1}^{RT} - \frac{\sum_s \left(\rho_s * r_{st,h,s}^{FC}\right)}{FC_{Eff}} \qquad \forall h > 1 \tag{4.6}$$

Where EL_{Eff} and FC_{Eff} are the efficiency ratings of the electrolyzer and the fuel cell respectively and $Hlevel_{h-1}^{RT}$ is the hydrogen level in the storage tank in the previous hour of operation.

Following the previous equation, equation (4.7) below is for calculating the level of hydrogen in the storage tank for the first hour (h = 1) of operation of the storage system.

$$Hlevel_h^{RT} = EL_{Eff} * \sum_{s} \left(\rho_s * r_{st,h,s}^{EL}\right) + initialHlevel - \frac{\sum_s \left(\rho_s * r_{st,h,s}^{FC}\right)}{FC_{Eff}} \qquad h = 1 \tag{4.7}$$

Where $initialHlevel$ is the initial storage tank level prior to the start of the operation of the storage system.

The equation (4.8) below is a charging constraint

$$r_{st,h,s}^{EL} \leq Ch_{st,h} * BigM \qquad \forall st, h \tag{4.8}$$

Where $Ch_{st,h}$ is a binary variable that holds a value 1 when the electrolyser is operating and 0 when it is off.

The equation (4.9) below is constraint that ensures that the power produced

$$r_{st,h,s}^{FC} \quad \leq \quad Dsch_{st,h} * BigM \qquad \forall st, h \tag{4.9}$$

Where $Dsch_{st,h}$ is a binary variable that holds a value 1 when the fuel cell is operating and 0 when it is off.

Equation (4.10) is to ensure that only one operation is performed by the entire storage system block at any given hour, so it is either converting the excess power via the electrolyser to hydrogen to store or it is converting hydrogen to power to meet load demand.

$$Ch_{st,h} \; + \; Dsch_{st,h} \; \leq \; 1 \quad \forall st, h \tag{4.10}$$

The following constraint is imposed to enforce a minimum amount of the total wind power available to storage and activate the energy storage system which comprises the operation of the electrolyser and the fuel cell.

$$cap_{FC} \quad \geq \quad RPS_{ESS} \; * \; \sum_{k} Xcap_{k} \qquad \forall k \tag{4.11}$$

Where, RPS_{ESS} is the storage portfolio standard that may be imposed at a policy level to ensure the renewable wind energy is stored for future regeneration.

To incorporate the impact of the ESS block effectively, the power balance equation in the real time mode needs to be updated accordingly as well. This equation (4.12) shows the updated power balance equation:

$$\sum_{g}(p_{g,h}^{DA} + r_{g,h,s}) + \sum_{k}(W_{k,h,s} - w_{k,h,s}^{SP}) - \sum_{l}(DL_{l,h} - p_{l,h,s}^{SH}) + \sum_{st} r_{st,h,s}^{EL} + \sum_{st} r_{st,h,s}^{FC} = \sum_{m} B_{(n.m)}\left(\theta_{n,h,s}^{RT} - \theta_{m,h,s}^{RT}\right) \quad \forall n, \forall h, \forall s \tag{4.12}$$

4.3 Results of the Power Planning Model with ESS

In order to model the power planning model with energy storage system, the following assumptions and input parameters were utilized. The portfolio constraint on the energy storage system block (shown in Equation (4.11)) is to ensure that some percentage of the wind power delivered to the system is redirected to the energy storage block for conversion to hydrogen. For this model , the RPS_{ESS} parameter has been set at 10%, implying at least 10% of the total wind power harnessed must be directed to the ESS block. The initial hydrogen tank level is assumed to be empty. The other input parameters are the same as the values input to the model in chapter 3. The power generation planning model is assumed to operate for 365 days to calculate the yearly cost of the entire system which includes the operational cost on a yearly basis as well. The operation cost of the wind farm is assumed to be zero and the capital costs of the electrolyser and the fuel cell are set as USD 500,000 and USD 1,500,000 which are approximate prices as mentioned in the following reference [72]. The model results are in accordance to the same wind power factor probability scenarios (based on 6 scenarios)

The model was solved using CPLEX 11.1.1 solver on GAMS 24.5 software environment. The model comprised of 15,956 equations, 6240 single variables and 423 discrete variables. The total CPU time in order to arrive at the solution was 36.26 seconds. The following section details the main results of the model accompanied by general discussions.

Table 4.1 Design Decision Variable Results of Power Generation Planning Model with ESS.

Design Decisions	
Xcapk (MW)	2697.31
Xgen (MW)	976
Electrolyser Capacity (MW)	20.84
Fuel Cell Capacity (MW)	269.73

Table 4.2 Conventional Generator Design Decision of the ESS Power Generation Planning Model.

Generator	g1	g2	g3	g4	g5	g6	g7	g8	g9	g10	g11	g12	g13	g14	g15
Design Yes/No	1	0	1	0	1	0	0	1	0	0	0	0	0	0	0

The main design decision variable results are displayed in table 4.1. The value of *Xcapk* is found to be 2697.31 MW installed wind power and the *Xgen*,value of 976 MW is the total power installed from convention power generators. Table 4.2 is the schedule of the available conventional generators in the system. From the table it can be seen that generators g1, g3, g5 and g8 are scheduled to be ON throughout the operation of the power planning model. For the ESS block, the capacities of the electrolyser and fuel cell are reported in Table 4.1 as well. The capacity of each of the equipment is the maximum power rating utilized for its operation, in the case of the electrolyser it is 20.84 MW and for the fuel cell it is 269.73 MW.

Table 4.3 Hourly Schedule of the Electrolyser in the ESS Block

Hour	Average Power(MW)
1	20.839
2	20.839
3	9.949
4	7.532
5	10.138
6	7.309
7	19.399
8	20.839
9	20.839
10	14.587
11	10.002
12	11.670
13	15.408
14	15.837
15	15.837
16	0
17	0
18	0
19	0
20	0
21	0
22	0
23	0
24	0

In table 4.3 above, the hourly schedule of the electrolyser operation is shown. The electrolyser is on and operational (converting excess power to hydrogen) from hours 1 to 15 and the corresponding power rating in MW is highlighted for each hour that it is on.

Table 4.4 Hourly Schedule of Fuel Cell in the ESS block

Hour	Average Power(MW)	Load Demand (MW)
1	0	1921.17
2	0	1903.32
3	0	1867.62
4	0	1855.89
5	0	1888.02
6	0	2002.26
7	0	2206.26
8	0	2287.35
9	0	2219.52
10	0	2114.97
11	0	2037.96
12	0	1994.1
13	0	1970.13
14	0	1989
15	0	2031.33
16	19.481	2107.32
17	21.578	2247.06
18	9.928	2420.46
19	8.671	2552.55
20	7.562	2571.42
21	9.363	2530.62
22	0	2424.54
23	0	2277.15
24	0	2127.21

In table 4.4 above, the hourly schedule of the fuel cell operation is shown. The fuel cell is on and operational (converting hydrogen stored in the tank back to power) from hours 16 to 21 and the corresponding power rating in MW is highlighted for each hour that it is on. The hours that the fuel cell is on corresponds to when the electrolyser is switched off which is in accordance with the constraint set up in equation (4.10).

An additional column showing the load demand at each hour is also included in table 4.4 to highlight that during hours 16 to 21, the load demand is higher than average for that particular day.

Hence, it would make sense that when the load is higher, more power can be obtained from the ESS by converting stored hydrogen to power via the fuel cell.

Table 4.5 Cost Results of the Power Planning Model with ESS

Cost Results	USD (millions)
Total Cost (per year)	576.24
Operating Cost (per year)	107.48
Annualized Capital Cost	468.76

Table 4.5 above reports the main costs of the power planning model with ESS block. The total cost of the system is found to be USD 576.24 million per year and this comprises the operating cost per year which is at USD 107.4 million and the total capital cost from installation at USD 468.76 million. The total cost of USD 576.24 million is higher in contrast to the power planning model base case using 6 probability scenarios for wind, which was USD 541.78 million per year. This difference in cost is directly linked to the addition of the ESS block equipment and their associated capital and operating cost.

4.3.1 ESS Impact on Wind Spill

Wind spill as a phenomenon occurs due to the non-correlation between the load and the wind power profile, which is to say that when the load demand at any given hour is lower than the amount of wind available at that same hour, the wind power that is not utilized is spilled and no benefit is gained from it, unless the operator is able to sell it to nearby grids in short notice. The concept of energy storage is directly borne of the need to avoid or minimize the amount of wind that is spilled as a result of this mismatch between the load the wind power profile. Wind spill is also an outcome from poor error-laden forecasting that is significantly different from the actual

wind power on that day. This phenomenon directly shows the need to not only model with the presence of uncertainty (probability based wind realizations in real time) but also taking advantage of and ESS.

The models presented in this chapter as well as the previous chapter have considered the amount of wind that is spilled by allowing the model to calculate the variable $w_{k,h,s}^{sp}$ which is the wind power spilled at every hour h under scenario s. To further show the difference in the level of wind spill between the base case power planning model and the power planning model incorporated with ESS, the average $w_{k,h,s}^{sp}$ over the 6 scenarios considered is calculated and their variation on an hourly basis is shown in figure below:

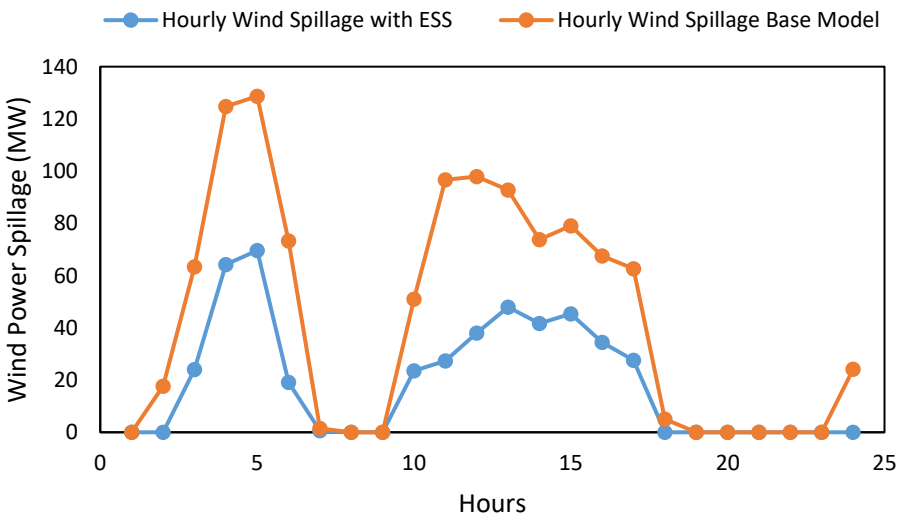

Figure 4.2 Comparison in Wind Spill levels between base case power planning model and power planning model with ESS.

In figure 4.2 above, it can be seen that the average wind spill levels in the case of the power planning model without ESS is higher than that of the case with ESS. Between hours 3 and 5 as well as between hours 10 and 17, the amount of wind spilled is consistently higher with a peak spillage of 128 MW at hour 5 in the base case model without ESS. In comparison, the peak wind

spilled in the model with ESS is 69.6 MW. The figure above further reinforces the benefit of using ESS as a potential solution to counter the intermittency of wind power and the mismatch that may arise from the load not aligning with the available wind power profile.

So while the overall system cost with ESS is higher than the base case model, the economic benefit gained from applying ESS and using the stored power compensates adequately for the higher capital and operating costs. Not to mention the benefits that may also be gained by directly selling the converted hydrogen to the economy as a clean energy source by itself, a concept that has recently gained much popularity [80].

4.3.2 ESS Model Results with 50 Wind Probability Scenarios

In chapter 3, the benefit of using clustered wind probability scenarios (from 50 to 6) was discussed and found to bring about significant reduction in solution time and without impacting the accuracy of the model results by a wide margin.

In this section, the model was solved using the initial 50 scenarios to compare the results with the ESS model with 6 scenarios. The model was solved in GAMS 24.5 using the CPLEX 11.1.1 solver. The model with 50 scenarios had 111,788 single equations, 38,976 single variables and 423 discrete variables and the total solution time was 5941.97 seconds of CPU time which amounted to approximately 99.03 minutes. The other key results with regards to design decisions and main costs are presented in tabular form below.

Table 4.6 Design Decision Variable Results of Power Generation Planning Model with ESS with 50 Wind Probability Scenarios.

Design Decisions	
X_{capk} (MW)	2657.22
Xgen (MW)	1076
Electrolyser Capacity (MW)	35.18
Fuel Cell Capacity (MW)	265.86

Table 4.7 Conventional Generator Schedule of the ESS Power Generation Planning Model with 50 Wind Probability Scenarios.

Generator	Design Yes/No
g1	1
g2	1
g3	1
g4	0
g5	1
g6	0
g7	0
g8	1
g9	0
g10	0
g11	0
g12	0
g13	1
g14	0
g15	0

Table 4.8 Cost Results of the Power Planning Model with ESS with 50 Wind Probability Scenarios.

Cost Results	USD (millions)
Total Cost (per year)	581.86
Operating Cost (per year)	112.07
Annualized Capital Cost	469.79

From the results obtained from the model with 50 probability scenarios, the total power installed from the conventional generators is higher at 1076 MW while a lower amount of wind power is designed in the wind farm at 2657.22 MW as shown in table 4.6. This increase in power installed is due to a higher number of conventional generators being switched on during the operation of the system. From table 4.7, it can be seen that generators g1, g2, g3, g5, g8 and g13 is scheduled to be on, which is an additional 2 generators designed when compared to the model with 6 scenarios. The overall cost of the system increases from USD 576.24 million per year to USD

581.86 million which is also owing to the higher number of generators and their associated capital and operating costs.

Seeing as how the difference in costs and design decision variable values do not vary by a significant amount, the main benefit of clustering the wind factors and reducing the size of the clusters from 50 to 6, is the time that is saved in obtaining the solutions. The difference in the CPU time for solving is large with the case of 50 scenarios, the model took over 99 minutes to solve while after clustering, the solution was arrived at in less than a minute at around 36 seconds.

4.4 Concluding Remarks

In this chapter, the power generation planning model from chapter 3 has been extended to include an energy storage system (ESS) block. The energy storage mechanism considered in this model is that of hydrogen that is produced by an electrolyser that converts excess wind power that is not used for meeting the load demand at any given hour. The hydrogen is stored in a tank and is converted back to power by a fuel cell during times of high load demand. The model was set up similar to the DCUC stochastic model that was used to model the power generation planning model in chapter 3.

With the inclusion of the ESS block, the total system cost of the power generation planning model with 6 probability scenarios was calculated to be USD 576.24 million per year which reflects the inclusion of the ESS block's capital and operating costs. The model was solved using the original 50 scenarios for the wind probability and the costs and design decisions were found to be comparable and slightly higher. However, the solution time of using 50 scenarios was much longer with the model taking over 99 minutes to arrive at the solution. One of the key benefits of using an ESS block with renewable energy integrated power system is the minimization of the amount of wind spilled. Wind spillage comes about due to the mismatch between the load demand and the

available wind profile and it was shown in this model how the ESS was able to bring down the average hourly amount of the wind spilled. The objective of showcasing the working of an ESS mechanism and the benefit to the overall energy system has been met in this chapter. In subsequent chapters of this work, the power generation planning model will be integrated with alternative storage mechanisms which include chemical production of value added products to form the basis of a renewable polygeneration energy system.

Chapter 5 Chemical Production Block

This chapter discusses the production pathway of methanol from syngas, in particular the development of a model that represents the production of methanol from coal that is not used directly to generate power from conventional generators. The model includes the gasification of coal to form syngas, following which the syngas reacts to form methanol via a conversion reaction and finally, a distillation step is involved in which the methanol is separated from the rest of the products mixture and the unreacted syngas is redirected back to the production system.

5.1 Methodology for the Methanol Production

In this study the methanol production model has been set up as a general framework so that any form of carbon intensive sources can be used as a potential feedstock, not just coal. The main underlying formulation of the model is comprised of mass and energy balances and other first principles models.

The first step in the model development will be a snapshot model. A snapshot model is deterministic in nature and captures the solution to all the variables at a particular time and does not consider their deviation in results over a time frame (for example 24 hours). Following the snapshot model, the model is then extended to represent the design and operation for a period of 24 hours, from which the annual cost of the methanol production system can be calculated.

The purpose of modelling at a process design level is to provide a mathematical way for the methanol production system to be designed and operated. The design decision variables will provide answers to the maximum capacity of each of the constituent units in the whole system.

The methanol production unit is comprised of 4 key unit components that will considered in this study, these include the gasifier, syngas clean-up unit, main methanol reactor and the distillation column.

The function of the gasifier and clean-up unit is to prepare clean synthesis gas for downstream utilization by the gasification of feedstock, typically coal, in a high temperature, high pressure and reductive atmosphere.

The methanol reaction is highly exothermic and therefore a large amount of steam can be produced for power generation, but in this study, this heat from steam is not considered as a power generation vector, instead the main purpose of the methanol is to serve as a commodity feed stock to be sold to the methanol economy as well as explore the option of using the methanol as a long duration storage mechanism. The products of the methanol synthesis reactor are separated into several streams in the methanol separation and processing unit: unreacted syngas, methanol with purity of 99.8% and higher alcohols that are by products of the methanol synthesis reaction. High purity methanol is one of the products of this RPES (renewable polygeneration energy system). The unreacted syngas is recycled to the methanol synthesis reactor.

Once the syngas leaves the clean-up unit, the clean syngas is split into two streams. One goes through an optional water gas shift reactor, and the other is bypassed, both mixing together again after the WGS. Through the water gas shift reaction, the mole composition of the syngas stream going through the reactor:

$$CO + H_2O \rightarrow CO_2 + H_2$$

While the bypassed stream remains unchanged. This is a means of adjusting the mole composition of the syngas according to the requirements of the methanol synthesis reactor. The degree of adjustment depends on the design variable called *splitpercent*.

The syngas then proceeds to a carbon dioxide removal unit, where the fraction of carbon dioxide in the syngas is adjusted to an appropriate level for the best performance of the catalysts in the methanol synthesis reaction.

After the carbon dioxide is removed, the syngas goes to the methanol synthesis reactor to produce methanol. Crude methanol produced in the synthesis reactor goes through a series of distillation columns to produce methanol as a final product. Mathematically, this process is formulated as splitting the crude product into two streams. One stream contains mainly methanol and a minor content of water, depending on the product degree whilst the other stream includes all the other components in the crude methanol. The mass flowrate of the final product methanol, or its production rate, must meet its market demand given by constraint equations (5.15) and (5.16).

5.2 Model Formulation

Objective Function:

$$cost_{Me}^{total} = \sum_{d} freq_d * \sum_{h} ma_{d,h}^{meoh_{st}} * Pr_{Me} + CRF * capcost + omcost + CFuel \qquad \forall d,h \tag{5.1}$$

The feed flow rates of the components are governed by the following equation:

$$ma_{d,h}^{inoxi} = rfuel^{inoxi} * ma_{d,h}^{feed} \qquad \forall d,h \tag{5.2}$$

The following is a component mass balance equation:

$$\sum_{sm \in inlet} ma_{d,h}^{sm} = \sum_{sm \in outlet} ma_{d,h}^{sm} \qquad \forall d,h$$

(5.3)

The following is an element balance equation:

$$\sum_{sm \in outlet} mo_{d,h}^{sm} * \sum_{rs} MWi_{ie} * STOIC_{rs}^{ie} * x_{rs}^{sm} = \sum_{sm \in inlet} z_{sm}^{ie} * ma_{d,h}^{sm} \quad \forall sm, rs, d, h$$

(5.4)

The following equations is a component-wise balance equation:

$$\sum_{sm \in outlet} mo_{d,h}^{sm} * x_{rs}^{sm} = \sum_{sm \in inlet} x_{rs}^{sm} * mo_{d,h}^{sm} \quad \forall d, h, rs, sm$$

(5.5)

Overall mol balance in the methanol production:

$$\sum_{sm \in outlet} mo_{d,h}^{sm} = \sum_{sm \in inlet} mo_{d,h}^{sm} \quad \forall d, h$$

(5.6)

Constraints to govern the separation of waste products in syngas stream

$$x_{rs\_waste}^{wastesg} * mo_{d,h}^{wastesg} \geq sfrac * x_{rs_{waste}}^{coolsg} * mo_{d,h}^{coolsg} \quad \forall d, h \qquad (5.7)$$

Calculation of mass flow rate from mol flow rate:

$$ma_{d,h}^{sm} = \sum_{rs} (mo_{dh}^{sm} * x_{rs}^{sm}) * MW_{rs} \quad \forall d, h, rs \tag{5.8}$$

The following equation calculates the enthalpy of the syngas stream

$$enthalpysg_{d,h}^{sm} = mo_{d,h}^{sm} * \sum_{rs} x_{rs}^{sm} * enthalpy_{rs}^{sm} \tag{5.9}$$

The following constraints represent the cleanup process of methanol following the methanol reaction in the reactor:

$$x_{Me}^{product} * mo_{d,h}^{product} \geq sfrac * x_{Me}^{meoh} * mo_{d,h}^{meoh} \quad \forall d, h \tag{5.10}$$

$$x_{otherproducts}^{otherprod} * mo_{d,h}^{otherprod} \geq sfrac * x_{otherproducts}^{meoh} * mo_{d,h}^{meoh} \quad \forall d, h \tag{5.11}$$

The equation below represents the mol balance around the methanol reactor:

$$mo_{d,h}^{meoh} * x_{rs}^{meoh} = \sum_{sm \in inlet} (x_{rs}^{sm} * mo_{d,h}^{sm}) + (STOIC_{rs} * conv_{co} * x_{co}^{sm} * mo_{d,h}^{sm}) + (STOIC_{rs} * conv_{co} * x_{co}^{sm} * mo_{d,h}^{sm}) \quad \forall d, h, rs \tag{5.12}$$

After the clean-up of methanol, the remaining unreacted components are split into two streams, one is purged as outlet, the other containing significant mol fractions of CO, CO_2, and H_2 are sent as a recycle stream to continue the reaction of methanol. The following two constraints describe this phenomenon:

$$mo_{d,h}^{purge} = splitpercent * mo_{d,h}^{otherprod} \quad \forall d, h \tag{5.13}$$

$$x_{d,h}^{purge} * mo_{d,h}^{purge} = splitpercent * mo_{d,h}^{otherprod} * x_{rs}^{otherprod} \quad \forall d, h, rs \tag{5.14}$$

The following constraints describe the upper and lower demands set as parameter for the methanol demanded by the market:

$$ma_{d,h}^{meoh\_out} \geq Mdem_{d,h}^{dn} \quad \forall d, h \tag{5.15}$$

$$ma_{d,h}^{meoh\_out} \leq Mdem_{d,h}^{up} \quad \forall d, h \tag{5.16}$$

The cost of fuel used for the production of methanol is described below:

$$CFuel = \sum_{d} freq_d * \sum_{h} ma_{d,h}^{feed} * Pr_{coal} - Pr_{Me} * ma_{d,h}^{meoh_{out}} \quad \forall d, h$$

(5.17)

For key units within the methanol production, the capacity variable is function of the highest mass flow rate of the component stream at hour h of day d over the course of the plant's operation. The constraint determining the capacity variables (in terms of both mass and mol) is described below:

$$capvar_{inletmass} \geq \sum_{sm \in inletmass} ma_{d,h}^{sm} \quad \forall d, h$$

(5.18)

$$capvar_{inletmol} \geq \sum_{sm \in inletmol} mo_{d,h}^{sm} \quad \forall d, h$$

(5.19)

The following equation describes the calculation of the capital cost of the plant:

$$mcapcost = \sum_{nd} capvar_{nd} * mslope_{nd} + BI_{nd} \quad \forall nd$$

(5.20)

The following equation describes the calculation of the operating and maintenance cost of the plant, assumed to be a fractional component of the total capital cost:

$$omcost = capcost * omfactor \tag{5.21}$$

The initial methanol level in the storage tank is assumed to be zero prior to the start-up of the plant:

$$Me_{d,h}^{level} = 0 \quad (h = 1, d = 1) \tag{5.22}$$

The level of the methanol present in the tank at any hour h of day d is governed by the following two equations:

$$Me_{d,h}^{level} = Me_{d,h-1}^{level} + ma_{d,h-1}^{meoh\_st} - ma_{d,h-1}^{meoh_{out}} - \sum_{gm} ma_{d,gm,h-1}^{meoh_p} \quad \forall d, h > 1, gm \tag{5.23}$$

$$ma_{d,h}^{meoh\_out} \leq Me_{d,h}^{level} + ma_{d,h}^{meoh_{st}} - \sum_{gm} ma_{d,gm,h}^{meoh_p} \quad \forall d, h, gm \tag{5.24}$$

$$Me_{d,h}^{level} = Me_{d-1,h=24}^{level} + ma_{d-1,h=24}^{meoh\_st} - ma_{d-1,h=24}^{meoh_{out}} - \sum_{gm} ma_{d-1,gm,h=24}^{meoh_p} \quad \forall d, h > 1, gm \tag{5.25}$$

The constraint below describes the mass flow of the methanol that is obtained from the production reactor and is directed towards the storage tank:

$$mo_{d,h}^{product} * x_{Me}^{product} * MW_{Me} \geq ma_{d,h}^{meoh_{st}} \quad \forall d, h \tag{5.26}$$

5.3 Results of Methanol Production Model

5.3.1 Results of Snapshot Model

The snapshot model was solved using the BARON solver version 15.9.22 in GAMS 24.5.6. In the snapshot model the capital cost equation is the non-linear version of the equation as was utilized in [15] and is shown below in equation (5.27):

$$mcapcost = \sum_{n} refcost_n * (\frac{capvar_n}{refflow_n})^{scale_n} \tag{5.27}$$

Additionally, the snapshot model has equations containing bi-linear terms which represent the mol fraction based calculation equations which include equations (5.12), (5.14) and (5.26).

The snapshot model characteristics include 274 single equations and 138 single variables. However, the model also indicates that it is highly nonlinear in nature and hence standard optimization solvers like CPLEX would not be applicable for this solution. The snapshot model solved in a total CPU time of 113.57 seconds.

The other key results of the snapshot model are summarized below:

Table 5.1 Mass and Flow Rates of Each Stream in the Snapshot Model

Stream	Mass Flow (kg/hr)
feed	197.61
air	296.415
water	296.415
rawsg	790.44
coolsg	790.44
cleangas1	770.034
wastesg	20.406
rxnoutput	5567.349
product	149.755
otherprod	5417.593
purge	620.279
recycle	4797.314

Table 5.2 Capacities of the Units Within the Snapshot Model

Chemical Production Unit Capacity(kg/hr)	Gasifier	197.61
	Cleanup	42.924
	Reactor	276.783
	Distillation	5567.349

The mass and mol flow rates of each of the streams in the methanol production model are shown in table 5.1 and table 5.2 lists the capacities (capvar) of the units within the production model. The mass flow rate of all the components emerging after the reaction (in stream labelled *rxnoutput*) takes place is found to be 5567.349 kg/hr. Following the distillation process the methanol (in stream labelled *product*) has a mass flow rate of 149.75 kg/hr which is an amount within the limits of methanol production set by the constraints (5.15) and (5.16). The remaining products (labelled *otherprod*) are sent to further downstream processing where a specific amount of it is purged as an outlet out of the production system and the non-purged amount (consisting mostly of unreacted syngas) is sent back to the reaction inlet stream in the form of a *recycle* stream. The model determined the percentage of the amount in the *otherprod* stream that is purged as the *splitpercent* variable which was found to be 11.4%.

The amounts listed as capacities of the units in table 5.2 are essentially the inlet mass flows for each of the units and are key design decision variables of the methanol production system.

Table 5.3 Main Costs of the Snapshot Model

Cost (USD Millions)	**Snapshot Model**
Annual Cost	385.690
Fuel Cost per year	78.352

As listed in table 5.3 the annual cost of the snapshot model was found to be 385.69 USD million while the total annual fuel costs (coal) was found to be 78.35 USD million. These costs are reflective of the amount of methanol that is produced based on the demand range provided in the

constraints and the corresponding capacity sizes that are designed for the units within the methanol production system.

In the next section, the model will be modified to operate for a period of 24-hours and compared with the snapshot model.

5.3.2 Methanol Production for 24-hour Period and Proposed Shortcut Approach

In order to model the methanol production model for 24 hours, the set of time, h for h1 to h24 needed to be introduced into the model as input. In order to shorten the solution time, the *splitpercent* variable (calculated to be 11.4%) from the snapshot model was instead input as a parameter. However, the nonlinear capital cost equation (5.27) along with the bilinear terms were included in the same manner as that from the snapshot model.

Solution to the 24-hour period Operation:

The model was solved using the same BARON solver in GAMS but this time the total number of single equations were 6,512 and the total number of single variables were 2,897. Once again, the model indicated high nonlinearity within it.

The annual cost, fuel cost per year, mass flowrate hourly and mol flowrate hourly was determined to be the same as the previous snapshot model. As expected, with the model being much larger in size, the arrival of the solution would take much longer and for this 24-hour period model, the total CPU time taken to solve was 5502 seconds (91.7 minutes) While the solutions are accurate and compare favourably with the snapshot model, it would be computationally tedious to have the model solve for 92 minutes, when the subsequent objective of this model is for it to be integrated with the power system planning model and form the basis of the polygeneration system.

Proposed Shortcut Method:

After observing the hourly results of the mol composition, mass flowrate of all the streams and production rates of methanol, an assumption can be made that some of the variable results at every hour can be kept constant as an inputs to the model. This would then reduce the computational size of the model with fewer equations and reduced bilinear terms, therefore also minimizing the level of nonlinearity of the overall model. The following variables from the earlier 24-hour period operation model was extracted into an excel data sheet: the mass flowrate (ma_h^{sm}), the mol flowrate (mo_h^{sm}), the mole compositions (x_h^{sm}), the capacity limits ($capvar_n$) of the units and the enthalpy of each stream. The model was then modified to switch the mol fractions x to a parameter and the remaining variable values extracted to act as upper limits in the model. Due to this modification, the total number of variables of the model will be reduced as well as the upper limit enforcement would provide bounds on the possible values that the variables may reach, hence tightening the area within which the optimal solution may be found.

The resultant shortcut model was set up to utilize the non-linear capital cost equations (equation 5.27), a split ratio of 11.4 % found from the snapshot model and time period of operation would be the same 24 hours. The model was solved using BARON solver in GAMS modelling system software.

The main results of the shortcut model are presented below:

Table 5.4 Main Costs of the Shortcut 24-hour Operation Model

Cost (USD Millions)	**Snapshot Model**
Annual Cost	385.690
Fuel Cost per year	78.352

Table 5.5 Capacity Limits on the Shortcut 24-hour Operation Model

Chemical Production Unit Capacity(kg/hr)	Gasifier	197.61
	Cleanup	42.924
	Reactor	276.783
	Distillation	5567.349

From Table 5.4 it can be seen that the annual cost of the methanol production system in the shortcut model is the same as the long-form original model at 385.69 USD million. The annual fuel cost for both the models is the same as well. Table 5.5 shows that the capacity limits of each of the units from the shortcut model identical to the limits determined by the original model. Therefore, these results validate that the shortcut model is a viable method as there is no deviation in the main results of the model. The key difference that is of interest is in the time taken to arrive at the optimal solution, which in the case of the shortcut model is a CPU time of 12.8 seconds. This difference in solution time, when compared to the original long form model's solution time of 5502 seconds, suggests that the shortcut model approach significantly reduces the computational effort needed without compromising on the accuracy and main results of the cost and design decision variables.

5.3.3 Linearization of the Methanol Production Model

While the shortcut model in the previous section drastically reduces the time needed to arrive at the solution, the model is still nonlinear on account of the capital cost equation being nonlinear. In this section, the equation 5.27 will be modified so that the capital cost is calculated using the following linear form:

$$mcapcost = \sum_{n} capvar_n * mslope_n \ + BI_n \quad \forall n \tag{5.28}$$

Where $mslope_n$, is the slope of the linearized cost curve of each of the capacity variable (capvar(n)) of the units and BI_n is the y-intercept. The figure 5.1 below shows the graphical representations of these linearized capital cost curves. These curves were generated by first using equation 5.27 and calculating numerically the numerical value of capital cost by using the capvar(n) variable obtained from the snapshot model. By varying the capvar(n) across many values less than and higher than the value obtained from the solution, corresponding values of the capital cost are obtained and then plotted as *capital cost vs capvar(n).*

Gasifier Unit

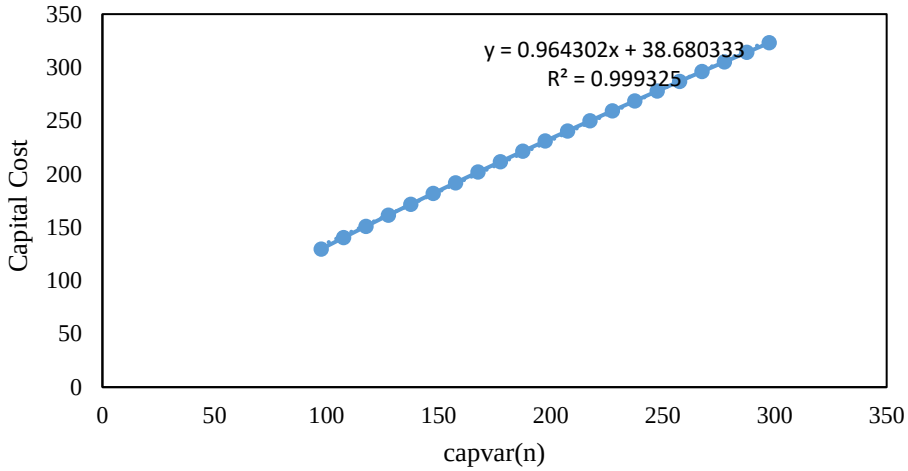

Clean-Up Unit

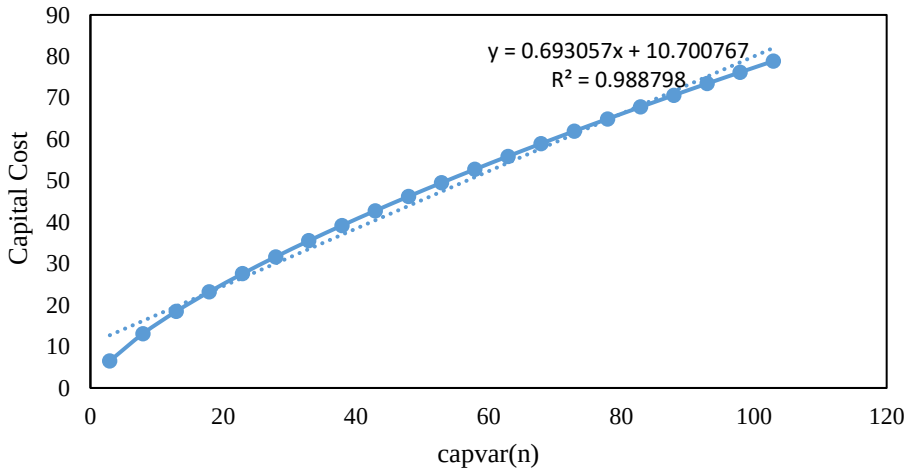

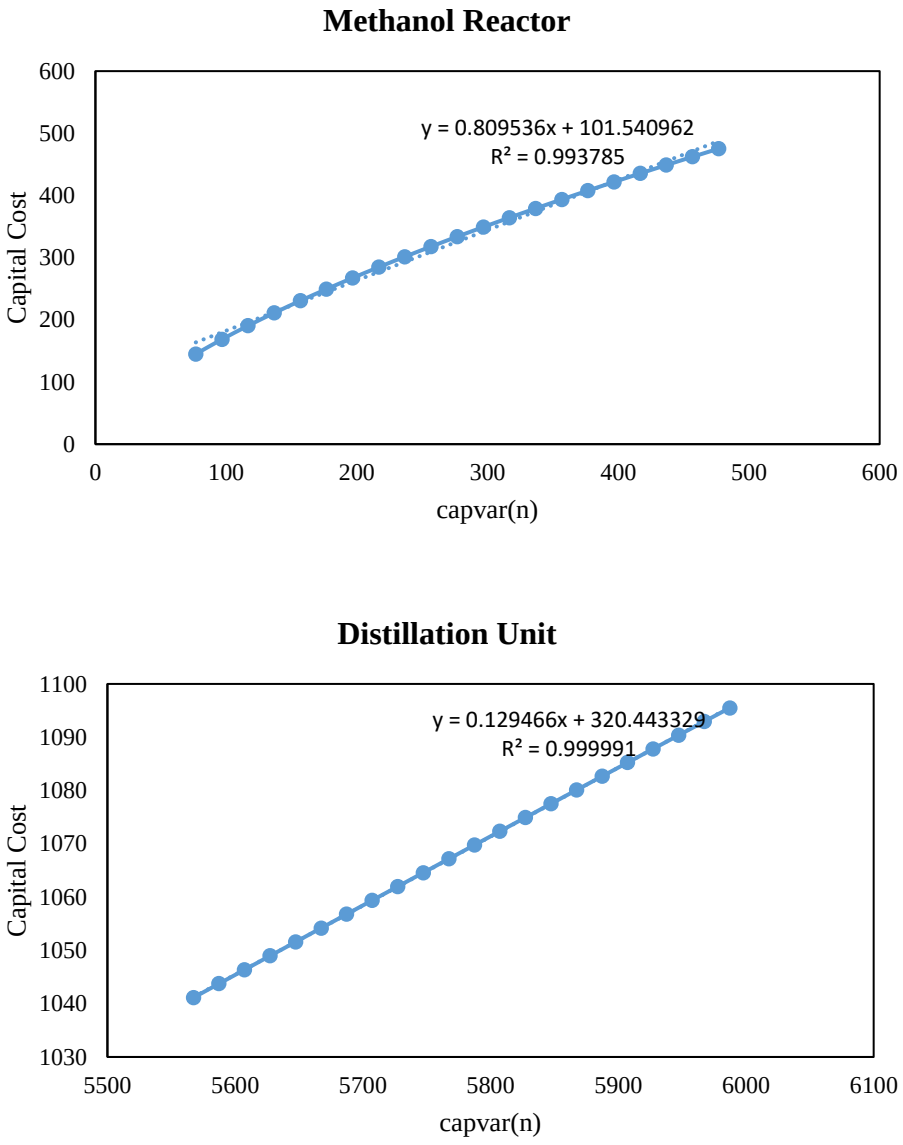

Figure 5.1 Capital Cost Curves for each unit in the Methanol Production System.

In figure 5.1 for each unit within the methanol production system, the plots for *capvar(n)* vs capital cost showcase a linear relationship between the two components. By performing basic linear regression, an linear approximation function linking the *capvar(n)* and capital cost terms can be obtained for each unit. The R^2 value in each of the linear approximation equations are very close

to 1 which underscore the linearity of the relationship. The respective slope and y-intercept values have been summarized in table 5.6 below:

Table 5.6 Slope and y-intercept Terms used as Inputs for the Linearized Methanol Production Model

Unit	mslope(n)	BI(n)
Gasifier	0.964302	38.68
Clean-Up Unit	0.693057	10.7
Methanol Reactor	0.809536	101.54
Distillation	0.129466	320.44

With equation (5.28) and the data above shown in table 5.6, the shortcut model presented in section 5.3.2 was updated and modified by replacing the original capital cost equation (5.27) which was nonlinear and table 5.6 above was input as a parameter table.

The linearized shortcut model was solved in GAMS using the standard CPLEX 11.1.1 solver as the model now is without any bilinear terms (due to the shortcut model) and now without a nonlinear capital cost equation. The model had 2500 single equations and 800 single variables and 0 nonlinear entries and the solution was arrived at in 1.28 seconds of CPU time, which is considerably faster than the shortcut model from the previous section. The annual cost which is the objective function and the fuel costs are displayed in table. 5.7 below:

Table 5.7 Main costs of the Linearized Shortcut Methanol Production Model

Cost (USD Millions)	Linearized Shortcut Model
Annual Cost	405.277
Fuel Cost per year	101.200

From table 5.7 above, it can be seen that the annual cost of the linearized shortcut methanol production is 405.277 Million USD which is higher than the cost reported by the nonlinear shortcut model in the previous section which was 385.693 Million USD, which is an increase in value by 5.08%. Similarly, the annual cost of fuel (coal) of the linearized model is 101.2 Million USD which

is higher than the shortcut model which was 78.35 Million USD. This is a 29.16% increase in fuel cost. The capacity limits on each of the units as well as the hourly production rate of methanol was found to be the same as the previous models for methanol production.

Table 5.8 Summary of Main Costs and Solution Times for Methanol Production Models

Cost (USD Millions)	**Snapshot Model**	**24-Hour Operation**	**24-Hour Shortcut**	**24-Hour Shortcut Linear**
Annual Cost	385.690	385.690	385.690	405.277
Fuel Cost	78.352	78.352	78.352	101.200
Solution CPU Time (seconds)	113.57	5502.54	12.8	1.2

From comparing the various key costs and solution times for each iteration of the methanol production model, the impact of both the proposed shortcut model as well as the linearization of the overall model can be seen clearly, as the solution time dropped significantly for the models that covered the operation over a 24-hour period. While the annual system cost and fuel cost are higher in the linearized model, the difference in the solution is not as significant and as such the error associated with the deviation in the cost values is low. The reason for the higher cost values could be attributed to the objective function being overestimated as a result of the linear approximation equations used to represent the capital cost calculations.

By considering the trade-off between the solution time and the deviation in the cost calculations, the shortcut linearized methanol production model is the one that is most suitable for the purpose of integrating with other model components to form the integrated polygeneration model. The integrated polygeneration model is expected to be larger in scale and having the chemical production model system that solves quickly without significant levels of error and very low inaccuracy is advantageous for the purposes of this study.

5.4 Concluding Remarks

This chapter discussed the production pathway of methanol from syngas, in particular the development of a model that represents the production of methanol from coal that is not used directly to generate power from conventional generators. The model includes the gasification of coal to form syngas, following which the syngas reacts to form methanol via a conversion reaction and finally, a distillation step is involved in which the methanol is separated from the rest of the products mixture and the unreacted syngas is redirected back to the production system.

In this study, the methanol production model was set up as a general framework so that any form of carbon intensive sources can be used as a potential feedstock. The main underlying formulation of the model is comprised of mass and energy balances and other first principles models.

From a computational perspective, the first model that was developed was a snapshot model, the purpose of this model was to see the mass flowrate, mol flowrate and mole composition of each stream within the production system while also determining the split percentage of the unreacted product streams to know how much of it needed to be redirected back into the reactor as syngas. The main design decision variables in this model comprised of the maximum capacity limits of each of the units within the production system, namely the gasifier, clean up unit, methanol reactor and the distillation column. The next step was extending the model to one that operates over a period of 24 hours. Both the 24-hour operation and the snapshot models were nonlinear and nonconvex and therefore computationally intensive and would take a long time to solve (5502 seconds). An attempt to address this was made by proposing an alternative shortcut model in which certain key variables were fixed with upper limits and as parameter inputs. To further simplify the model, modifications were made to remove bilinear terms and replace nonlinear constraints. This eventually led to a shortcut linearized version of the model that solved in 1.2 seconds while

maintaining a small level of inaccuracy in the model solutions. The shortcut linearized model will be the version used for subsequent model-building of the integrated renewable polygeneration energy system.

Chapter 6 Deterministic Renewable Polygeneration Energy System

This chapter discusses the integration of the power planning and methanol production models to form the renewable based polygeneration energy systems. The chapter showcases the deterministic approach taken towards this model with a focus on linking the chemical production and power systems models through the driving of compressors in the air separation unit prior to the gasification of coal

6.1 Motivation and Introduction

The polygeneration model, as defined earlier in the thesis, is an energy system that is capable of co-producing electric power and additional value added products. In previous chapters, the models for the main components in the polygeneration system have been developed with the aim of designing and operating them over a set period of time. The components include the power generation planning model and the chemical production block which designs the units that aid the production of methanol from coal and syngas.

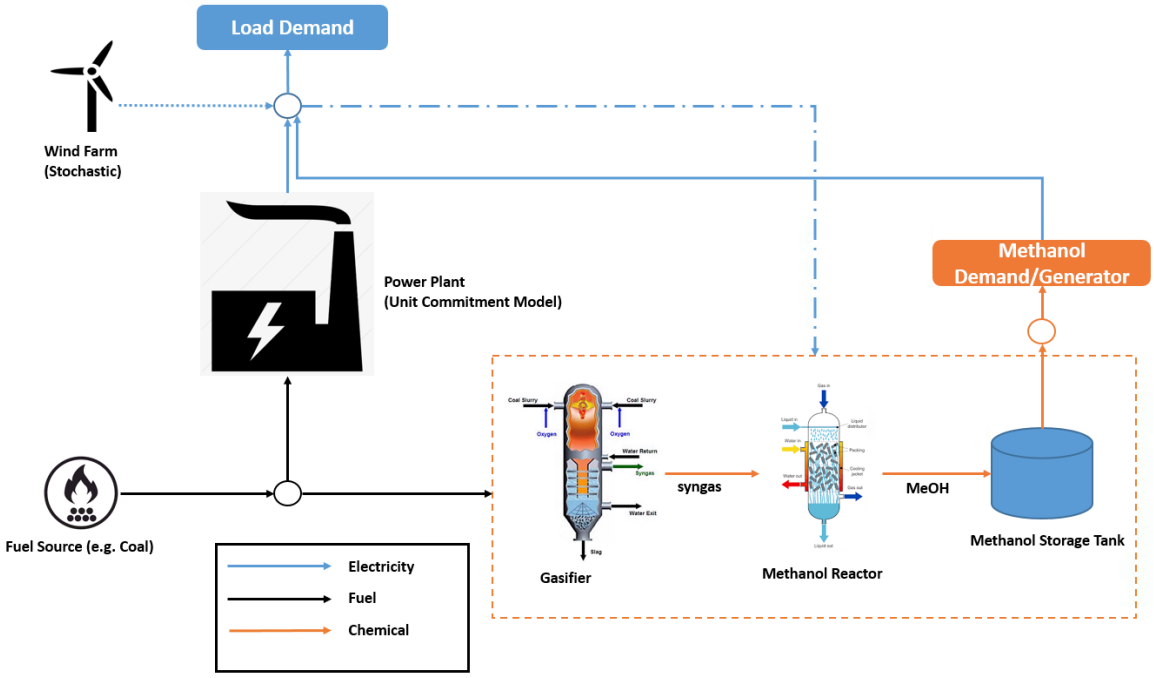

Figure 6.1 Process Flow Diagram of the Integrated Renewable Polygeneration Energy System.

One way of combining the two blocks is to focus on the electric power needs of the methanol production block. For instance, in chapter 5, a significant portion of the operating cost relied upon the purchasing of electricity from the grid in order to power the units that drive production. In this polygeneration model, the premise that is being explored, is the fulfilment of this electricity need from within the integrated system itself and not purchase the electricity. The expectation is that this electricity redirection to methanol will occur during times of very high wind power availability. This will be a productive use of the excess wind power, as opposed to selling it to alternative grids and/or dumping which is a practice undertaken today by electricity system operators to deal with excess power that cannot be stored or utilized for meeting the load demand. For the purposes of this model development, the emphasis will be on the compressors that are situated in front of the air separation unit of the chemical production block and after the main

distillation unit, to drive the recycle stream with unreacted syngas back towards the methanol synthesis unit.

6.2 Model Formulation

6.2.1 Clustering of Full Year's Data

For the integrated RPES model, it is essential to assess the system's behaviour across the full year of operation. On account of this, the power load demand and the wind power availability has to be input as parameters into the model. The data obtained for these parameters are values hourly for 8760 hours which represent the whole year. The challenge that arises from using the data in its raw form, is that with 8760 hourly values, the model can become computationally intractable and take an inordinate amount of time to solve. This was observed in chapter 3 where by reducing the number of scenarios from 50 to 6, the solution time was considerably shortened from 41.76 seconds to 15 seconds.

To address the issue, the full year data of power load demand and wind power availability has been clustered using k-means clustering. What this helped achieve, is the reduction of 8760 hourly data points to representative days, *d,* where the load and wind power is grouped in accordance to their most likely occurrence on a particular day and then the reduced number of days represents the whole year of operation. Which reduces the overall number of hours from 8760 sequential hours from 365 total days to 696 hours that are non-sequential from day 1 to day 29. Therefore, the whole year's data could be represented by 29 days, and thus considerably reducing the size of the model.

Clustering Methodology:

As introduced in chapter 2, the main clustering algorithm used is the k-means clustering algorithm. Wind power and load demand clustering was done together The following figure 6.2 shows the methodology undertaken for the clustering.

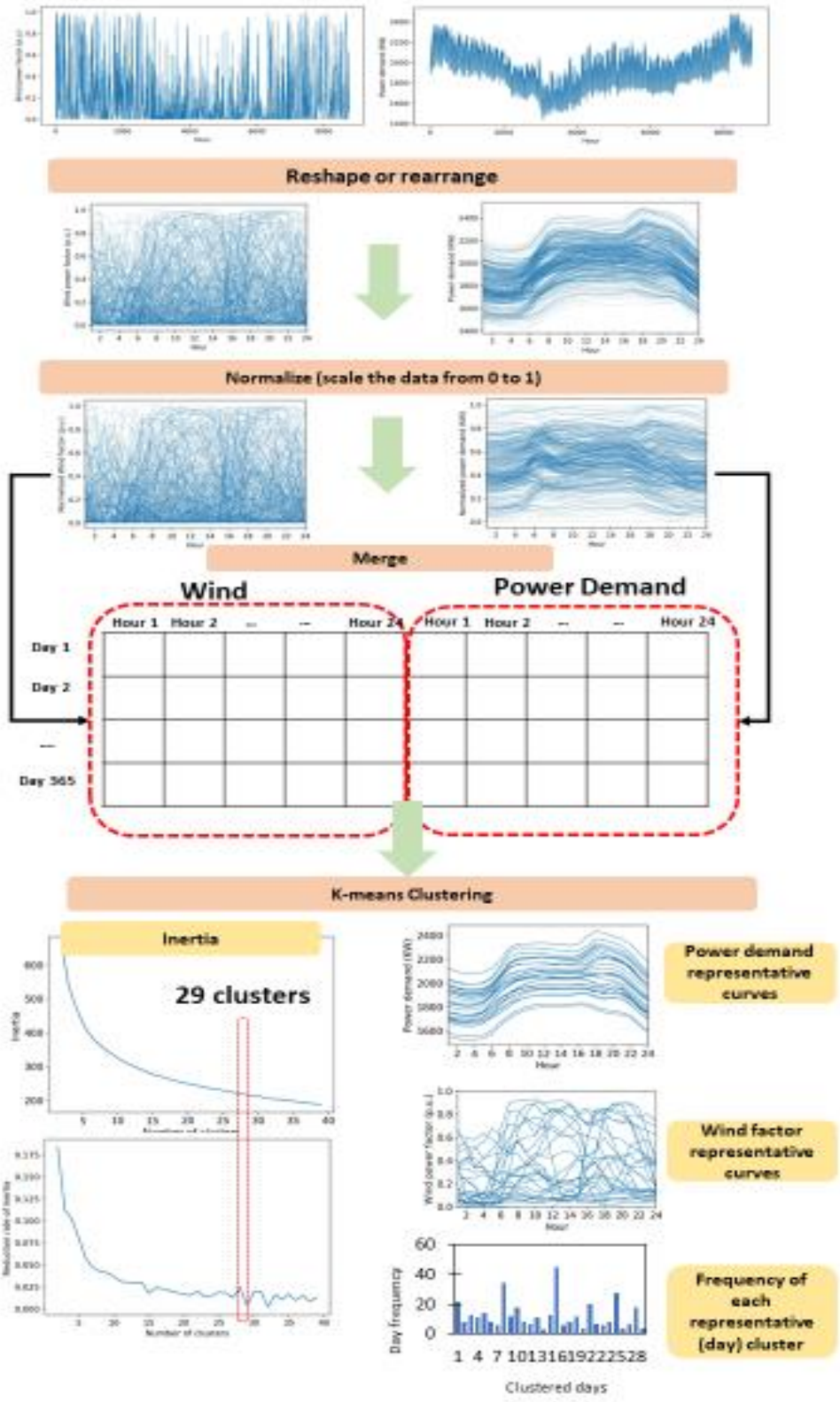

Figure 6.2 Methodology of K-means clustering for wind and load demand data.

According to figure 6.2 above, which shows the clustering methodology, the initial steps of the mechanism include uploading the original full year data at every hour for 365 days, representing the wind power and load demand into the python programming language editor. The data processing steps are then undertaken, which include reshaping and/or rearranging the data.

Each dataset is then normalized from a scale of 0 to 1. The K-means is a distance based machine learning algorithm having different scale for different attributes (in this case demand and wind). The computational effort will increase with varying distances between different attributes and features. And it might lead to inefficient clusters, if the normalizing step is ignored. The wind and load demand data sets also differ by order of 3 and 4 and hence it is a prudent step to bring them to the same scale.

The normalized data is then merged together and is based on the assumption that the occurrences of both wind and load demand is happening at the same time at the same hour and day, hence merging them together is a necessity so that the reduced order representative day will show both the wind and load clustered data accurately as inputs for the optimization model

Now that the data processing steps have been completed, the merged data is then input into the k-means clustering algorithm which is found in the sci-kit learn machine learning library in Python3. After the k-means clustering algorithm has converged, the clustered representative days indicating the total reduction inertia is obtained. Upon investigating it was found that 29 clustered days (representative days) was the ideal reduced order clustered day for the merged wind and load demand data. Any additional cluster has a negligible impact/improvement on the overall clustering metric (inertia) which is the key performance metric for the clustering method. The lower the inertia value, the better is the performance of the clustering algorithm. This would extend to the

fact that any further representative days in the clustered data would have no tangible impact on the overall solution of the optimization model either.

At the culmination of the clustering, the following table 6.1 shows the frequency of each of the 29 representative days:

Table 6.1 Frequency of Occurrence of Each Representative Day for the Full Year.

Representative Day	**Frequency of Occurrence**	**Representative Day**	**Frequency of Occurrence**
1	22	14	3
2	8	15	13
3	13	16	45
4	11	17	6
5	14	18	8
6	8	19	12
7	6	20	4
8	34	21	20
9	12	22	7
10	18	23	6
11	8	24	8
12	7	25	28
13	11	26	4
		27	7
		28	18
		29	4

This means that representative day 1 occurs 22 times over the whole year and day 29 occurs 4 times respectively.

6.2.2 Overall Optimization Model for the Integrated RPES

The presence of compressor units that drive the air separation unit and the recycle stream of unreacted syngas can allow for the existence of an additional node. Through this node, there can be connections made between the two main modelling blocks that have been set up in previous chapters.

In this chapter, the model is deterministic, which implies that the model will calculate key variable values for the system's design and operation for a full year's operation, but as a snapshot. It will not consider any stochastic behaviour of the wind power via probability scenarios, as was initially developed for the UC model in chapter 3.

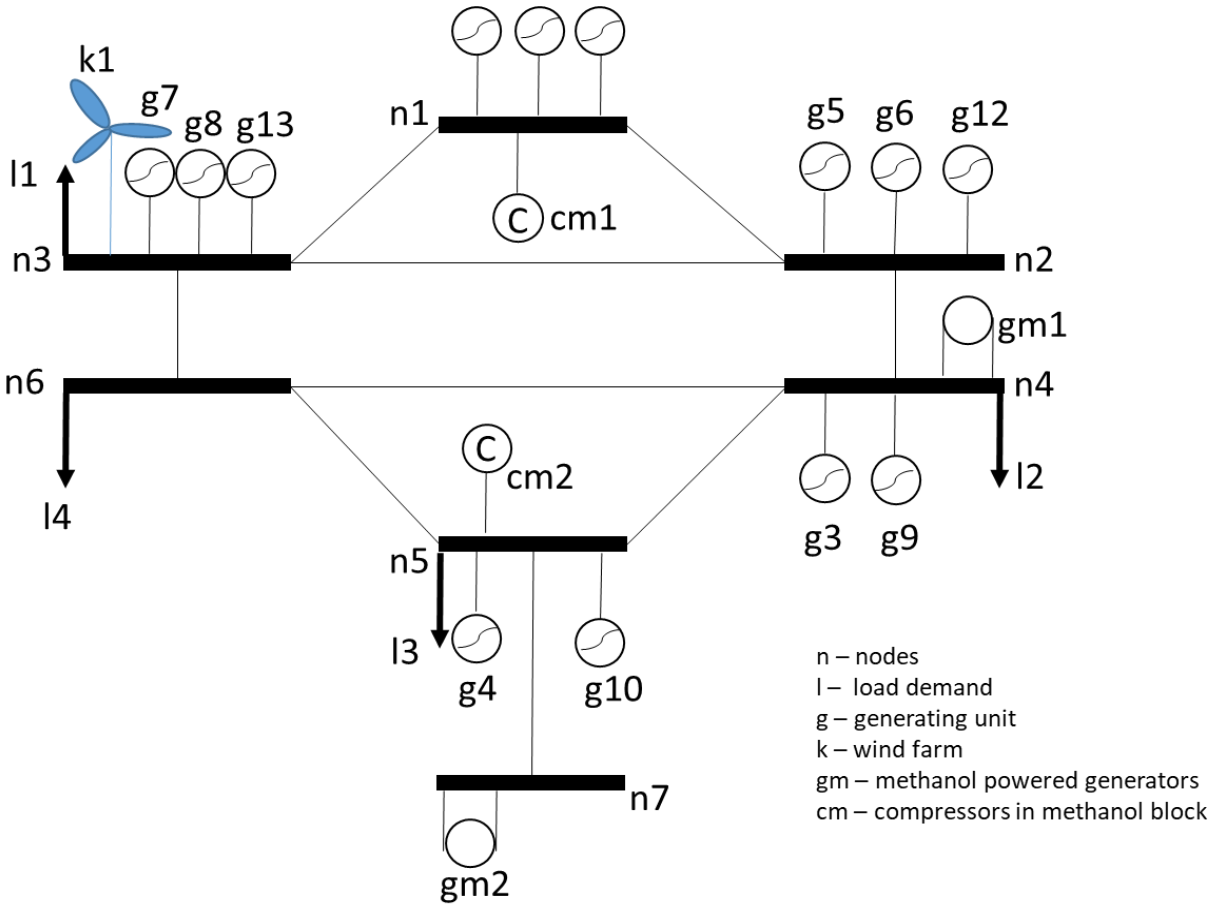

Figure 6.3 Topology representation of the Deterministic RPES model.

The figure 6.3 above is the topological representation of the deterministic RPES model. It has 7 nodes in total with the addition of compressors and the methanol-powered fuel cell generators labelled as *cm1, cm2* and *gm1, gm2* respectively. These additional units are linked to the chemical production block developed in chapter 5 and such show the link between power flow from the power generation planning block to the methanol production block. The number of conventional generators in this system is 13 as opposed to 15 in the previous chapters of the power generation planning model.

Objective Function:

The optimization criteria that is considered for this model is the total annual cost of the RPES system. The following equation represents the objective function of the integrated system which is set up for the minimization of the system's total annual cost denoted by $Intcost_{total}$:

$$Intcost_{total} = Anncost_{total} + PScost_{total} \tag{6.1}$$

The total annual cost of the RPES system is the summation of the individual blocks's annual cost, where $Anncost_{total}$ is the annualized cost for the methanol production block and $PScost_{total}$ is the annualized cost for the power generation planning block.

To further explain what the component costs are in equation (6.1), the following equations 6.2 and 6.3 list the components in the $Anncost_{total}$ and $PScost_{total}$ equations:

$$Anncost_{total} = CRF\ (Mcapcost + tankcap * tankcapcost) + omcost\ +\ Mcost_{fuel} \tag{6.2}$$

$$PScost_{total} = CRF(\sum_{g} PScapcost_g * xu_g + \sum_{k} Xcap_k * 1.3e6) + \sum_{gm} GMcapcost_{gm} * xm_{gm} + zf + PScostfuel + (ctax * CO2_{total}) \tag{6.3}$$

The individual term definitions within equations (6.2) and (6.3) are the same as the equations listed in previous chapters' respective model formulations. The *CRF* value is the same as calculated in previous sections with a lifetime operation of 25 years and a discount rate of 7%

Compressor Power Use Constraints:

The following equations within (6.4) represent the total power that is consumed by each of the compressors in the integrated model, as denoted by $cmpower_{cm,d,h}$:

$$cmpower_{cm,d,h} * refmolpower_{cm} \geq refpower_{cm} * mo_{sm,d,h}$$

$$cmpower_{cm,d,h} * refmolpower_{cm} * MW_{air} \geq refpower_{cm} * ma_{sm,d,h} \quad \forall sm, d, h \tag{6.4}$$

In equation (6.4), $refmolpower_{cm}$ represents the reference mol flow rate for the inlet of the compressors in Mmol per hour while $refpower_{cm}$ is the reference power ratings for compressors in MW. The numerical data used for these parameters is listed in table (6.2) which have been obtained from the following source [30].

Table 6.2 Reference Data to Assess the Performance of the Compressors

	$refmolpower_{cm}$ (Mmol/hr)	$refpower_{cm}$ (MW)
Compressor 1 (recycle stream)	5.8975	9.6435
Compressor 2 (air separation)	19.5507	11.8344

The *MWair* is the molecular weight of air (a value of 28.9647 kg/kmol is used in the model) and $mo_{sm,d,h}$ and $ma_{sm,d,h}$ is the molar and mass flowrate of syngas and methanol flow streams respectively.

Power Balance of Integrated Model Constraints:

Given that there is now power flowing between the power generation planning block and the methanol production block, it is crucial to make the necessary adjustments and updates to the overall power balance equation from chapters 3 and 4. Since the model is deterministic, only the initial day-ahead power balance equation (6.5) will be considered and included in the model.

$$\sum_{g,n} p_{g,d,h}^{DA} + \sum_{k,n} w_{k,d,h}^{DA} - \sum_{l,n} DL_{l,d,h} + \sum_{gm,n} powerm_{gm,d,h}^{DA} - \sum_{cm,n} cmpower_{cm,d,h} = \sum_{n,m} B_{(n.m)}\left(\theta_{n,d,h}^{DA} - \theta_{m,d,h}^{DA}\right) \quad (6.5)$$

Where $p_{g,d,h}^{DA}$ is the power scheduled by conventional power generators for every hour in each representative day for the whole year, $w_{k,d,h}^{DA}$ is the power scheduled from the wind farm for each hour in each representative day, $DL_{l,d,h}$ is the load demand for each hour in each representative day, $powerm_{gm,d,h}^{DA}$ is the power generated from methanol powered fuel cell generators for each hour in each representative day, $cmpower_{cm,d,h}$ is the power consumed hourly in each representative day by the compressor units in the chemical production block. The right hand side of the power balance equation is $B_{(n.m)}\left(\theta_{n,d,h}^{DA} - \theta_{m,d,h}^{DA}\right)$is the product of the imaginary part of the power admittance constant and the difference in the voltage angles which account for the flow of power between each node in the overall system.

6.3 Results and Discussion

6.3.1 Base Case Polygeneration Model

In order to assess the integrated RPES model, it is applied to the following base case which have the following key input data. The base case comprises of a system with 13 conventional generators, one wind farm, 2 methanol powered fuel cell generators and 2 compressors that have been mapped and updated using the node-based figure from chapters 3 and 4. The compressors are installed on nodes 1 and 5 while the methanol generators are mapped on node 4 and 7.

The components in the methanol production block are the same from chapter 5, and it is expected that the model will provide the necessary design decision values for the various units in that block.

Key Input Parameters:

Table 6.3 Conventional Generation Units Input Data.

Generator	λ_g^{SU} (USD)	λ_g^{SD} (USD)	C (USD/MWh)	p_g^{max} (MW)	p_g^{min} (MW)	R_g^{+} (MW/hr)	R_g^{-} (MW/hr)	p_g^{ini} (MWh)
g1	175	10	11	950	0	90	90	90
g2	175	10	11	350	0	90	90	90
g3	132	10	17	100	0	20	20	0
g4	175	10	11	76	0	20	20	0
g5	107	10	23	200	0	200	200	200
g6	132	10	17	350	0	70	70	130
g7	132	10	17	350	0	70	70	130
g8	223	10	19	197	0	70	70	150
g9	283	10	19	155	0	33	33	155
g10	215	10	14	100	0	65	65	100
g11	150	10	15	100	0	70	20	0
g12	150	10	15	100	0	70	20	0
g13	200	10	17	100	0	60	20	0

Table 6.3 includes the generator units' data that has been input into the model. Within the power planning block of the integrated RPES model, the following parameters are also defined as inputs. The price of coal is set at USD $61 per ton and the CRF is calculated for a 25-year operation at 7% discount rate, which equals to 0.0858105. The levelized cost of the wind power from the wind farm is set at $34 per MW. The capital cost of each conventional generator is set at $3.5 million and the capital cost of each methanol powered fuel cell generator is set at $7.5 million. For the base case, the default renewable portfolio adjustment (RPS) amount is set at 20% which implies that 20% of the power generated by the RPES needs to be sourced from wind power. The RPS constraint is defined as:

$$\sum_{k} Xcap_k \quad \geq \quad RPS * (\sum_{k} Xcap_k + Xgen) \quad \forall\, k \tag{6.6}$$

The upper and lower limits on the amount of methanol demand at each hour remained the same as in chapter 5 with 200 tons per hour and 100 tons per hour, respectively.

The wind power data used in this deterministic RPES model was obtained from one of the well-established wind farms, Summerhaven located in Ontario, Canada [90].

Base Case Results:

The model was solved in the GAMS environment with the use of the CPLEX 11.1.1 solver. The base case model has 161,835 equations, 9,063 discrete variables and 79,376 single variables. The following sections presents the results generated from the base case and discusses them in further detail.

Table 6.4 Base Case Results of Installed Power and Unit Capacity Sizes

Wind Power (MW)		594
Conventional Power (MW)		2376
Chemical Production Unit Capacity(ton)	Gasifier	271.71
	Cleanup	59.02
	Reactor	380.58
	Distillation	7655.1
Tank Capacity(ton)		5400

As can be seen from Table 6.4 above, the total wind power capacity installed is 594 MW and the total power capacity installed by the conventional generators is 2376 MW. The total capacities of each of the units within the chemical production unit are 271.71 tons for the gasification unit, 59.02 for the clean-up unit, 380.58 for the methanol reactor and 7655.1 tons for the distillation column. The main costs of the base case RPES system are presented in Table 6.5 below:

Table 6.5 Summary of Main Costs of the RPES

	Total Cost (USD Millions per Year)
Total RPES System	2317.930
Methanol Block	138.511
Power Planning Block	2179.416

As per the definition of the total annual cost of the RPES system described in equation 6.1 the individual costs of each block add up to the total system cost of the RPES. For the base case of the deterministic RPES integrated model, the total annual cost is USD $2317.93 million per year, the methanol block annual cost is $138.511 million per year and the power generation planning block is $2179.416 million per year.

The following figures in this section are graphical representations of the key operational behaviours of the overall RPES system for one year. Starting with the total power generated by the conventional power generators and the amount of wind power available hourly over the 29 representative days, which is shown in figure 6.4 below.

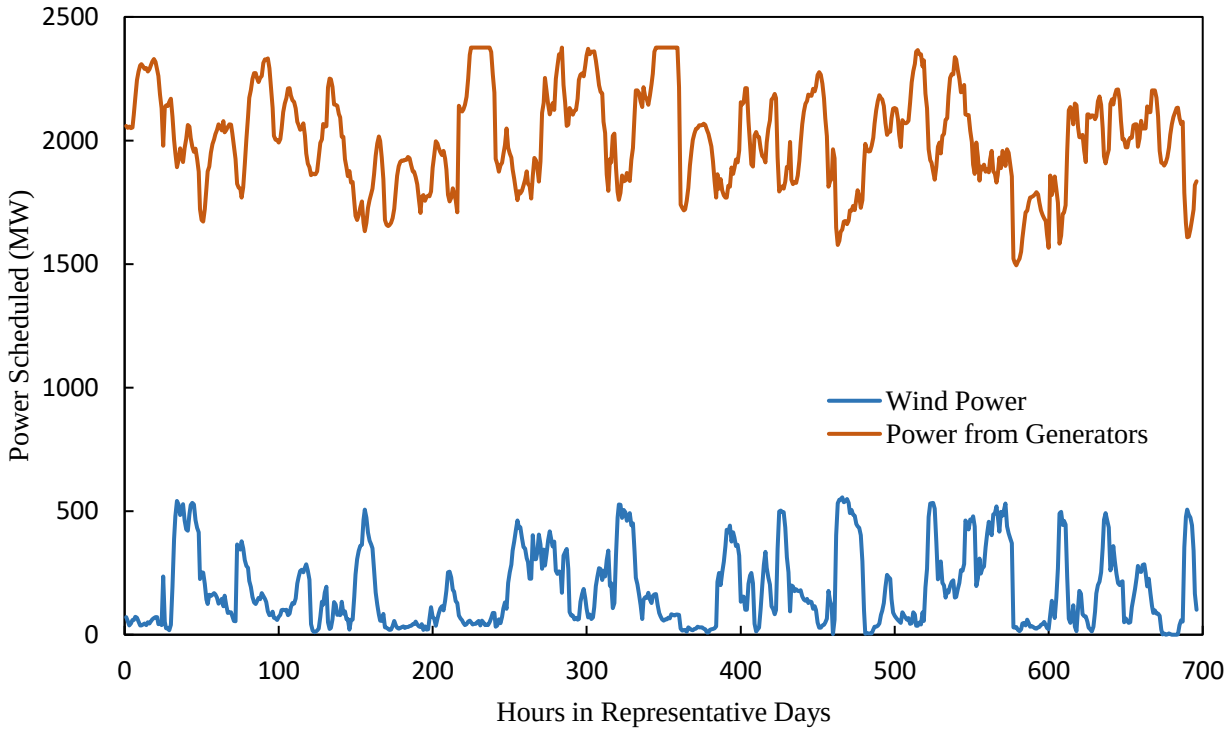

Figure 6.4 Hourly Power Scheduled for Conventional Generators and Wind Power Available in MW

In the above figure 6.4, the hourly variation in the power scheduled by the RPES deterministic model is shown. The maximum levels of hourly installed capacity for power generation from

conventional generators and the wind farm matches that of the *Xgen* and *Xcap* values reported in Table 6.4 (2376 MW and 594 MW) respectively. Additionally, as is expected from the model, to ensure that the base load demand is always met, the amount of power scheduled from conventional generators remains much higher on average than the wind power. On closer observation of the peaks and troughs in the figure, it can be seen that at times when the wind power harnessed is highest (peak), the corresponding hour's power scheduled from conventional generators is low, which asserts that the load is distributed by wind power providing the necessary majority power needed and at that time, the conventional generators do not need to produce electricity at higher levels and this lowers the cost of the overall RPES system.

The next aspect of the model that will be looked at, is the level of production of methanol per hour and how it varies with the amount of wind power available for harnessing. The graphical representation of this is presented below in figure 6.5:

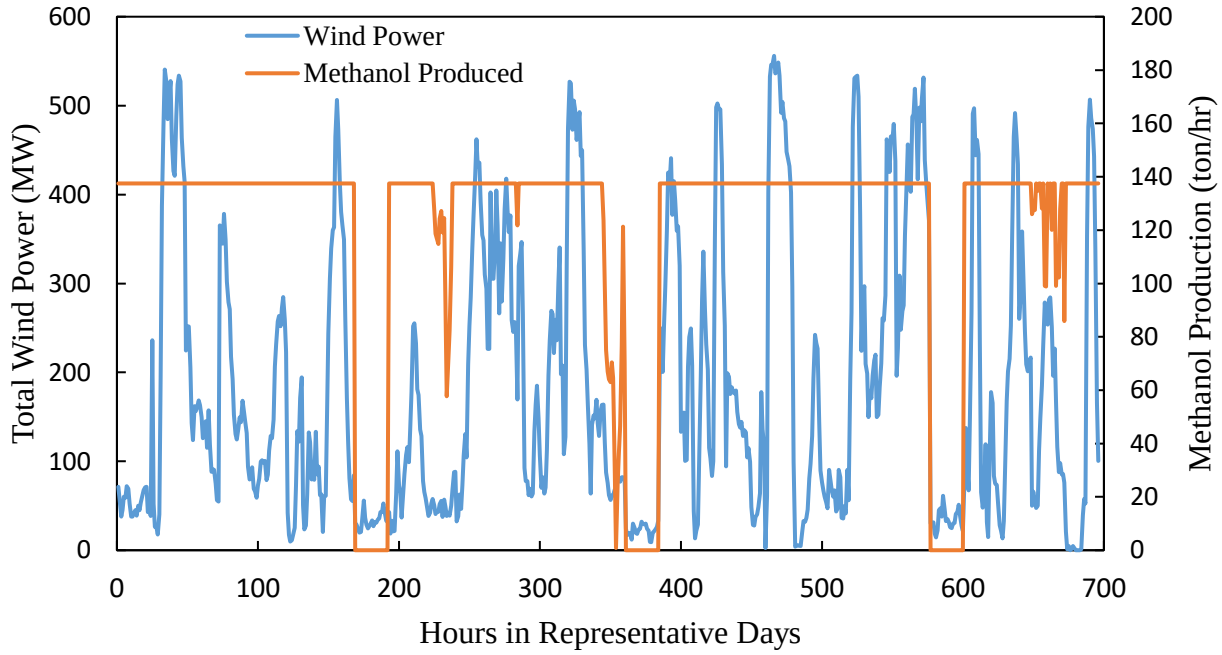

Figure 6.5 Hourly wind power available in MW versus the rate of methanol production in ton/hr.

One of the key operational modes that is characteristic of the RPES model is that both power and methanol production can take place simultaneously. In figure 6.4 above, a closer look is taken at how the methanol production rate hourly varies with the amount of wind power available. From the figure it is can been that at periods when the wind power that can be harnessed is at very low levels for instance between hour 174 and hour 192 of the representative days, the methanol production system block is off and the production rate is zero. The RPES system also shows a level of flexibility that responds to not just very low wind levels, but also marginal declines in wind power levels. For example, between hours 224 and 242, the methanol production rate declines in response to lower levels of wind, but does not switch off, implying that there was enough power redirection possible from the power system block to drive the compressors in the methanol production. This can also be verified by referencing figure 6.3 where during this same time period, the amount of power generated by the conventional generators is very high. Throughout the operation of the RPES, the methanol production rate varies between a low level of 57 tons/hr and a maximum of 137.5 tons/hr when the overall production block is on and operating. This is directly in response to the constraints that have been set up in the base case for ensuring the minimum and maximum levels of methanol production are always satisfied as long as the block is on.

Another useful aspect to visually explore is comparing the hourly load demand with the figure 6.4 represented above. The additional curve representing the power load demand is included below in figure 6.6.

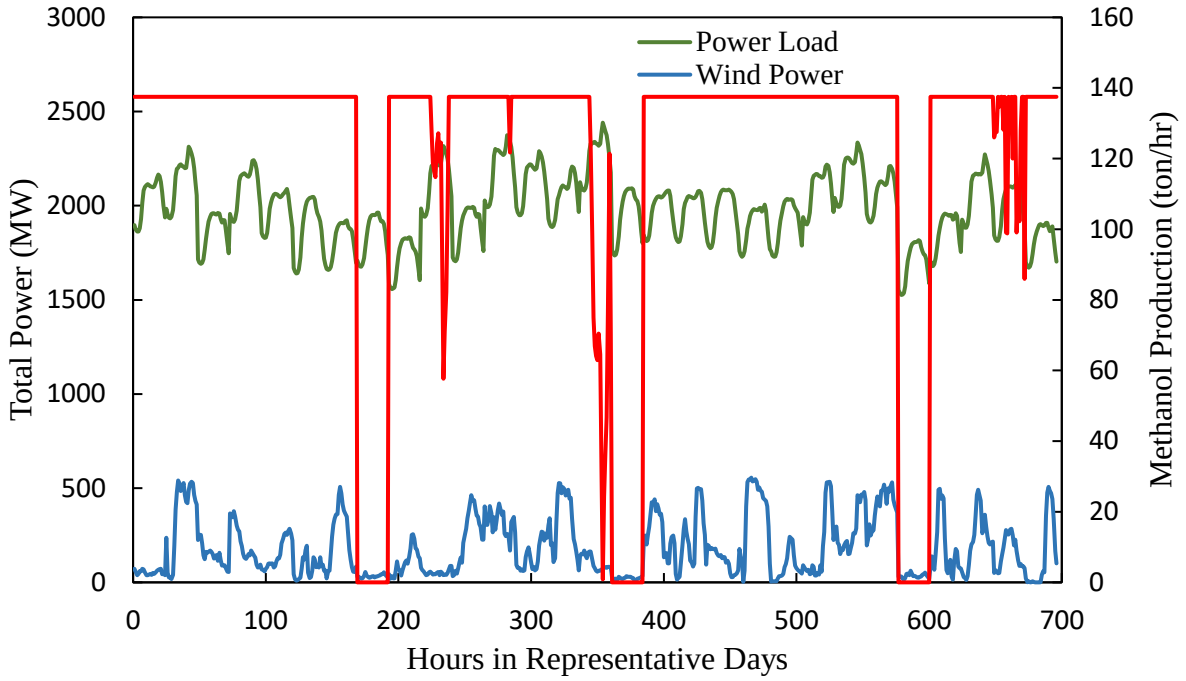

Figure 6.6 Load Demand Hourly and Available Hourly Wind Power in MW Versus the Rate of Methanol Production in ton/hr.

Since the amount of wind power that can be harnessed for satisfying load demand is not controllable due to its non-dispatchable nature, the need for conventional power generators is essential in this RPES system to always be ready to be switched on and generate power in response to the load demand. From figure 6.5 above, it can be seen that the load as such has no relationship with the wind power available since they are independent in their occurrence. But the interesting observation is in the response of the methanol production rate which has been shown to be linked to periods of high wind power availability in the previous section. The load demand over each 24-hour period of the 29 representative days considered has peak periods and low periods in response to the daily activities of the end use customers. Between the hours 383 and 575 on the figure, the wind power fluctuates as does the load demand according to the daily pattern, however the methanol production rate during this whole time period remains fixed at 137.5 tons/hr. What this means is that the conventional generators are able to meet the remaining load as needed whenever

the load reaches a peak but the wind power is able to be utilized for the purposes of chemical production and only switches off when the wind availability is significantly low and close to unavailable. Hence this accounts for a system that is always being able to utilize the power being generated/harnessed for dual purposes of meeting load demand and producing methanol. A reason for which the methanol production rates do not exceed the level of 137.5 tons/hr is that the model has decided on the optimal capacity for the units in the chemical production block which are reported in table 6.4 previously.

Since the main drivers of the chemical production block have been set up in this model to be the compressor units ahead of the air separation unit and the recycle stream of the unreacted syngas following distillation, it would be useful to notice the hourly power usage of the compressors and how that compares with the wind power available. This graphical representation is presented in figure 6.7 below.

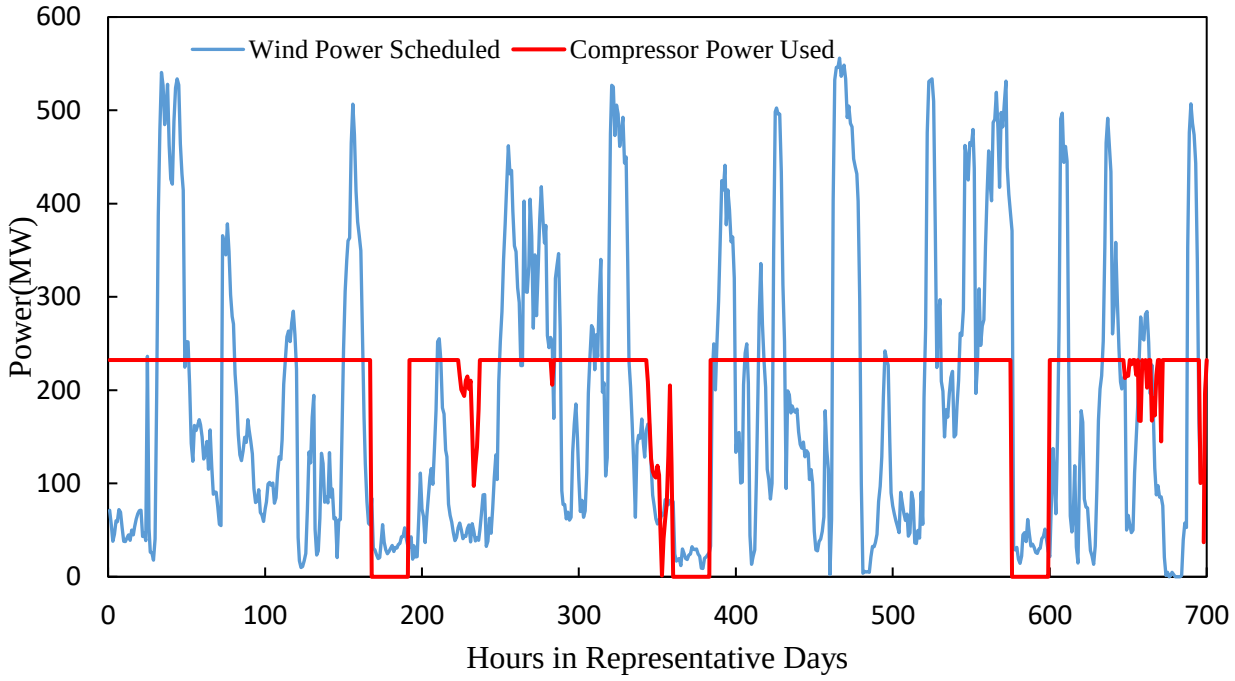

Figure 6.7 Wind Power Available Hourly in Representative Days and the Hourly Compressor Power Usage.

In figure 6.7 above, it can be seen that the compressor power (red curve) variation is in direct relationship with the amount of wind power available to be harnessed. So during periods of low wind availability, for instance between hours 168 and 192, the amount of power consumed by in total by the compressors is close to zero, implying that the methanol production is zero. This observed trend is in agreement with the methanol production rates observed in figures 6.4 and 6.5. The compressors' total power usage has an upper limit of about 232 MW/hr which also directly relates to how the methanol production rate does not exceed a level of 137.5 ton/hr as that is constrained by capacity limits that have been calculated by the model.

6.4 Case Study Investigations of the Deterministic RPES Model

With the base case model results obtained in the previous section, the following are case studies investigated to study the impact of varying input conditions on the overall deterministic polygeneration model.

6.4.1 Inclusion of Ramping and Minimum Up and Down Time on Methanol Production

In this study, the ramping constraints along with the minimum up and down time constraints have been included in the overall deterministic model. The purpose of these constraints is to allow for the methanol production block to behave under the similar commitment characteristics that were considered in chapters 3 and 4 of this thesis. In the real world behaviour of chemical process plants, the various reactor units are typically bound by minimum hour of operation once they are started up. Additionally, when the production units increase their production rates they are not permitted to increase their production rates by either extravagant or small amounts and have to step up by a fixed amount to maintain the proper operational conditions for the plant unit operations. These factors were not considered in the base case model set up in section 6.3. As such the minimum up

and down time constraints may be applied to any of the unit operations within the methanol production block.

The following equations represent the ramping constraints on the methanol production unit and the inclusion of the minimum up and down time on the compressor units.

Equations 6.6 and 6.7 ramping constraints:

$$ma_{sm=feed,d,h} \quad \leq \quad BigM * x_t^{cm} \quad \forall d, h, t \tag{6.6}$$

$BigM$ represents an assumed number, as is customary in the Big M method in operations research modeling. In this case a value of

$$ma_{sm=feed,d,h} \quad \geq \quad SmallM * x_t^{cm} \; \forall d, h, t \tag{6.7}$$

$SmallM$ represents an assumed number as is customary in the Big M method in operations research modelling.

In this case, to illustrate the need for a minimum up and down time on the overall methanol production unit the minimum up and down time has been set at 12 hours. Big M and Small M method was applied in this model.

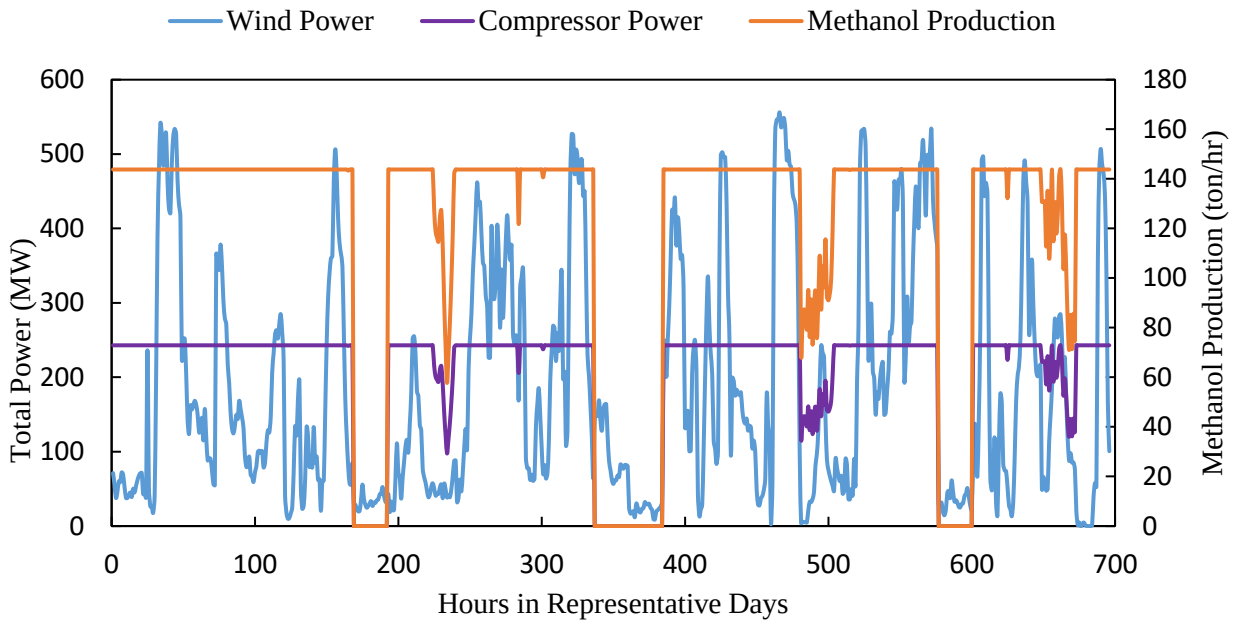

Figure 6.8 Methanol Production and Total Power from Wind Farm and Compressor Power used in the 29 Representative Days with Ramping and Min up and Down time Constraints.

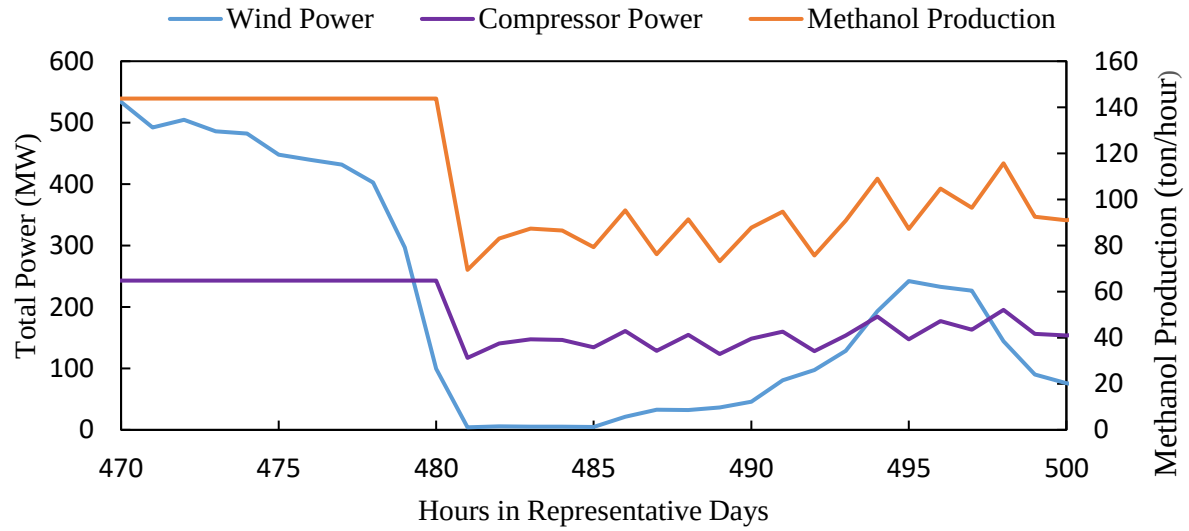

Figure 6.9 Sub Figure Showing Methanol Production and Total Power from Wind Farm and Compressor Power used in the 29 Representative Days with Ramping and min up and down time Constraints.

As can be seen from Fig. 6.8, the methanol production over the full year's representative days the maximum production rate is 143.78 ton per hour and once it is started up and producing methanol, it has to continue to stay on for minimum of 12 hours. Similarly, during periods of low wind power,

the methanol production is shut down, the overall production block remains shut down over a period of 12 hours before it can be started up again. In keeping with the overall flexibility of the system, it can be seen clearly from figures 6.8 and 6.9 that when there is a steep decline in the available wind power, the methanol production switches off and the compressors are turned off, which directly imply the chemical production block is turned off.

The commitment constraints like minimum up and down time and ramping for the methanol production block have a significant impact on the overall costs of the polygeneration system. The exact dynamic behaviour of the gasifier unit and the reactor unit within the methanol production block is beyond the scope of the present work, but the implementation of the constraints on the compressor min up and down time are sufficient in this study to illustrate that the inclusion of commitment like constraints is important to mimic the behaviour of real world process systems. Additionally, from a planning point of view, the model is able to integrate the key commitment features that have been demonstrated to have an effect on higher level planning of the polygeneration energy systems.

Going beyond the resolution presented in this case would require extensive computational effort and a more complex mathematical formulation with the use of partial derivative equations which would need to be solved simultaneously, an aspect that can be studied in the future work. Still, enough modelling considerations have been implemented to show the impact of dynamic behaviour on the costs of the overall system. And this further reinforces that the model developed is general enough to include the main dynamic characteristics of the methanol plant.

6.4.2 Effects of Wind Variation on the Deterministic RPES Model

In this case study, different levels of wind power have been input into the model to study the behaviour of the RPES. In addition to the wind power data used for the base case, two additional

data sets have been utilized, one with average wind power levels considerably lower than the base case data, and the other with average wind power levels much higher than the base case. The impact of these varying wind power levels on the methanol production rates have been graphically represented in figure 6.10 below.

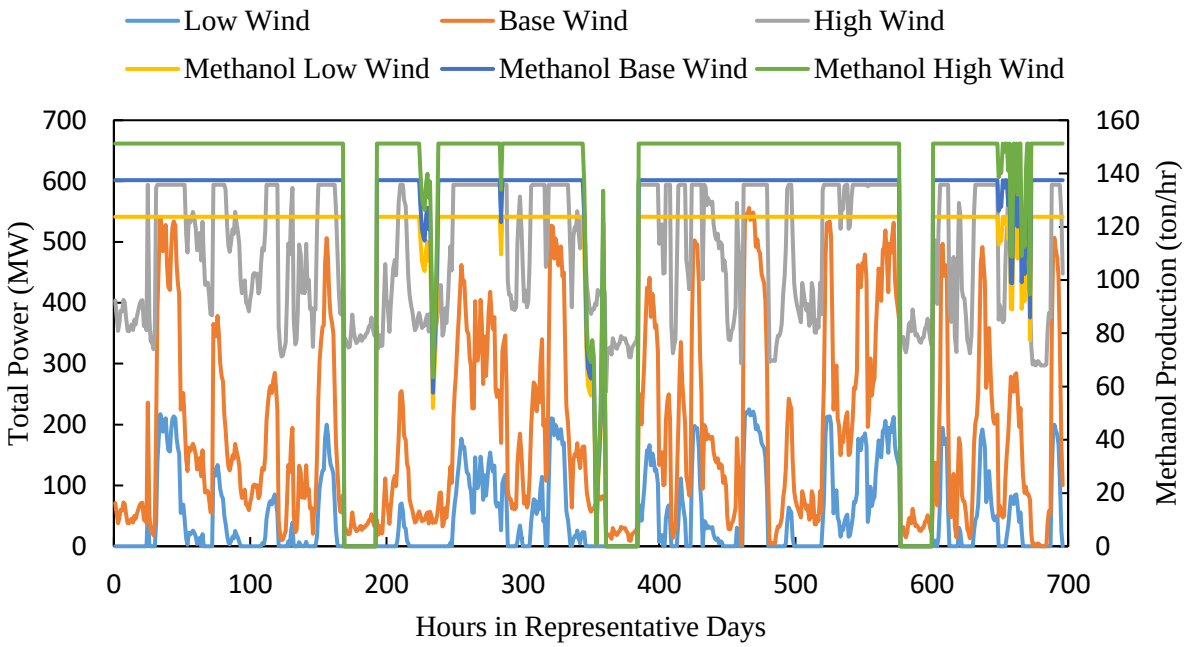

Figure 6.10 Methanol Production Levels with Varying Wind Power Levels Compared to the Base Case Data.

From figure 6.10, the methanol production rate can be seen to vary in level which is in accordance to the level of wind power that can be harnessed. Compared to the base case maximum production level of 137.5 ton/hr of methanol, when the wind levels are on average much higher than the base, the maximum production of the methanol rises to 151.25 ton/hr. While for the low average wind levels, the maximum methanol production level reduces to 123.75 ton/hr. These observations support the premise that when there is more wind available, the model, based on the size of the units and the wind farm capacity, will be inclined to produce more methanol as it can direct more excess wind to chemical production.

6.4.3 Effects of the Renewable Portfolio Standard on the Deterministic RPES Model.

In this case study, the renewable portfolio standard (RPS) as a percentage has been modified to observe the impact it has on the amount of methanol that is produced and the amount of wind power that can be harnessed by the RPES.

RPS portfolio is a portfolio constraint that forces the introduction of renewable energy into the system. The general definition of RPS is to set a minimum requirement for the share of electricity supply than comes from designated renewable energy resources with some future year target in mind. These resources typically include wind, solar and biomass.

As of September 2020, 38 states out of 50 in the US, have established an RPS, also known as a renewable goal. Out of the 38, 12 states have set the requirement to be 100% clean electricity by 2050 or earlier. The main driver behind why these RPS standards could be implemented in recent times, have been due to federal incentives as well as market conditions like the reduction in costs (levelized) of wind power and other technologies making use of renewable energy.

RPS or renewable energy standards are one of many initiatives that have been proposed by government entities and can be applied using different terminologies like carbon-neutral/carbon-free targets. An interesting observation from the RPS adoption in US, is that some states have been able to produce qualifying generation from renewables at levels much higher than the set RPS, some others have been producing enough to just meet the requirement set by the target while others may still need to import electricity from nearby regions to meet the target.

Objective of the case studies is to see how more wind can be penetrated into the power system

i) RPS of 20% will be the base level RPS for this system.

ii) A variation in the RPS will be implemented in the model to study its impact on wind power generation.

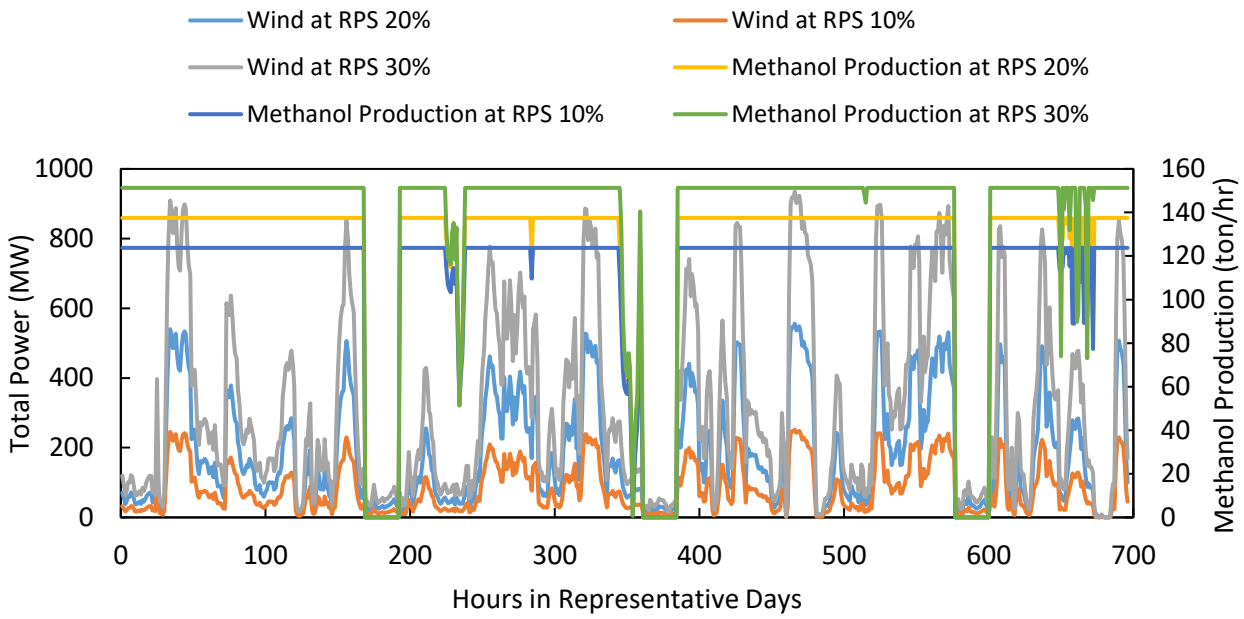

Figure 6.11 Methanol Production Levels and Wind Power Levels with Varying RPS Percentages Compared to the Base Case Data.

In the base case RPES model, the renewable portfolio standard (RPS) percentage was set at 20%. Two separate model solutions were generated for the RPES, one with a lower standard of 10% and one with a higher than base case standard at 30%. The resulting impact on the methanol production levels as well as the variation in the wind power availability at each hour is presented graphically in figure 6.10 above. At first glance, it is clear that levels of wind power that is available is a response to the percentage RPS set, with lower average wind power available with RPS of 10% and higher wind power available at RPS of 30%. Since the purpose of the RPS is to act as a policy to increase the use of renewable energy resources for electricity generation, the higher the RPS value the more the amount of electricity is generated by the system from wind.

6.5 Concluding Remarks

In this chapter, a deterministic model for the design and operation of the RPES was built and examined. The optimization models developed in chapters 3,4 and 5 were combined in a manner

that allowed for the power to flow from the generation planning model to the chemical production block via compressors that drive the start-up and production of methanol from coal via syngas gasification. The model was found to be effective in showcasing the flexible nature of the RPES energy system. The results of the base case model showed increased production levels of methanol during periods of high wind power generation availability, indicating that the model was able to redirect excess renewable power that was not required to satisfy the hourly load demand. Several graphical representations were generated to visually show that the variation in the wind power directly brought about a modification in the levels of methanol production via power transmission to the compressor units. A series of case studies were also investigated, by modifying the amount of wind power that is generated and harnessed by the RPES, first by using raw data that has a higher average expected value of wind power and a lower expected value of wind power. Following that, an external constraint was placed on the model by utilizing a RPS or renewable portfolio standard which enforces a minimum amount of power generation from renewable energy sources. For both these case studies, the impact the expected value of wind had on the production of methanol was studied. It was observed that the higher the amount of wind that can be harnessed, the greater is the maximum level of methanol that can be produced, which is attributed to the model choosing to design a greater capacity of methanol production units. Lastly, in one of the case study, the deterministic RPES model included ramping and minimum up and down time constraints on the overall chemical production block. This approach was undertaken to study the impact of having the methanol reactors and gasification units behave more like they do in the real world with commitment like constraints and therefore affected the times at which the methanol production units were switched on and off and impacted the system's annual cost by increasing it from the base case which did not include these constraints. The impact of ramping and other commitment

like constraints on the RPES model needs to be further studied with a deeper look into the exact dynamic behaviour of the methanol production system, which is out of the scope of this present work.

Chapter 7 Stochastic Renewable Polygeneration Energy System

This chapter discusses the implementation of the stochastic renewable polygeneration energy system model. This model is developed by introducing wind power realization scenarios to the deterministic model set up in the previous chapter. The purpose of this chapter is to show how allowing for uncertainties in wind to be realized, brings about a significant reduction in the total cost of the polygeneration system while also highlighting the importance of showing that the wind needs to be represented as high in intermittency.

7.1 Introduction to Stochastic RPES

A stochastic optimization formulation is relevant if the UC is affected by important uncertainty in the data. Handling stochastic behaviour is currently of great importance because of the uncertainty arising from the variability in generation from stochastic production facilities such as wind and solar based generating units. These types of generating units often benefit from priority in dispatch by virtue of their low marginal cost or regulatory policies. They are therefore not scheduled per se but rather their production is subtracted from the demand, and other units are then scheduled to meet the resulting net demand which is the actual demand minus the stochastic production.

When formulating a stochastic UC, we consider two stages:

- The first stage pertains to the optimal scheduling of the generation capacity which is the decisions about which units to commit in advance of the actual operation.
- The second stage constitutes a representation of a number of plausible operating conditions that may arise in the future as a result of the uncertainty realization. These possible operating conditions are called scenarios and for each scenario, and optimal dispatch can

be computed based on the commitment decisions made in the first stage.

Reserves are scheduled in the first stage so that the system will be able to accommodate any uncertainty realization/scenario.

The philosophy of this two-stage formulation is that in the first stage, scheduling decisions are made using only the information that is available hours or days in advance of real time operations. The uncertainty is then realized is the second stage, and the dispatch adjusts the amount scheduled in the first stage up or down, as required according to the scenario.

The scenarios take into account the possible wind realizations over the planning period. Each scenario is assigned a probability, and the optimization objective is to minimize the sum of the deterministic cost of the first stage decisions and the expected cost of the second stage decisions.

There are several limitations of the stochastic optimization approach, one of them is the quality of the solutions obtained critically depends on the choice of the scenarios, in the sense that having a broader range of scenarios usually leads to a more accurate model. However, increasing the number of scenarios increases the computational cost of the optimization. Another issue is that this approach assumes explicit knowledge of the probability distribution of the uncertain wind realization. In practice, this distribution is estimated empirically based on past data and experience and/or using simulation models and the limitations of the probability estimation may impact the quality of the results.

7.2 Approach and Methodology

The model considered is an extension of the deterministic model developed in chapter 6. The main changes to the model to make the model stochastic include the introduction of another set of s

number of scenarios. In this model, 6 different scenarios will be considered, each with their own probability of occurrence. Since the stochastic behaviour of the power planning block was already demonstrated in chapters 3 and 4 in response to wind power realizations, the main stochastic nature of the integrated model will be showcased based on the methanol production block. On account of this, the equations, variables and constraints that represent the methanol production will be bound by the set *s* representing the scenarios.

7.3 Model Formulation

Since the majority of the model is an extension of the deterministic model, the following selected equations and constraints have been shown to highlight the stochastic model:

Objective Function:

The objective function as such is the same as that defined in chapter 6 which is the sum of the annual costs from the chemical production block and the power generation planning block. The sum is of these costs which make up the objective function variable, $Stoch\_Intcost_{total}$, is shown in equation 7.1:

$$Stoch\_Intcost_{total} = Stoch\_Anncost_{total} + Stoch\_PScost_{total} \quad (7.1)$$

The annual cost (equation 7.2) of the methanol production block is the same as the one previously defined in past chapters, however the constituent terms within the equation have been updated to reflect the stochastic considerations and they are listed from equations (7.3) -(7.5):

$$Stoch\_Anncost_{total} = CRF\ (Mcapcost + tankcap * tankcapcost) + omcost\ +\ Mcost_{fuel} \quad (7.2)$$

$$Mcapcost = \sum_{nd} cap_{nd}^{var} * mslope_{nd} + bintercept_{nd}$$

(7.3)

Equation 7.3 is the linearized capital cost equation where cap_{nd}^{var} is the variable calculating the capacities of the constituent units within the chemical production block.

$$cap_{nd}^{var} = \sum_{sm} ma_{sm,d,h,s}$$

(7.4)

Where $ma_{sm,d,h,s}$ is the mass flowrate of components within the chemical production block for every stream, in each hour of each representative day in each scenario, s.

$$Mcost_{fuel} = \sum_{d} freq_d * \sum_{s} \rho_s (ma_{d,h,s}^{feed} * pr_{coal} - pr_{meoh} * meoh_{d,h,s}^{out})$$

(7.5)

Where $ma_{d,h,s}^{feed}$ is the flowrate of the feed stream entering the chemical production block, pr_{coal} and pr_{meoh} are the prices of coal feed and selling price of methanol, respectively and $meoh_{d,h,s}^{out}$ is the amount of methanol produced at the end of the distillation process of the chemical production block.

The power balance equation from chapter 6 has been updated to allow for the adjustments that come about with the inclusion of probability scenarios, s, that are central to the stochastic model. This equation 7.6 is shown below:

$$\sum_{g,n} p_{g,d,h}^{DA} + r_{g,d,h,s} + \sum_{k,n} w_{k,d,h}^{DA} - w_{k,d,h,s}^{SP} - \sum_{l,n} DL_{l,d,h} - p_{l,d,h,s}^{SH} + \sum_{gm,n} powerm_{gm,d,h,s}^{DA} - \sum_{cm,n} cmpower_{cm,d,h,s} = \sum_{n,m} B_{(n.m)}\left(\theta_{n,d,h,s}^{DA} - \theta_{m,d,h,s}^{DA}\right) \quad (7.6)$$

These adjustments include power adjustments to the conventional generators, $r_{g,d,h,s}$, the wind spillage associated with the wind turbine power $w_{k,d,h,s}^{SP}$, and the amount of power dissipated as load shedding $p_{l,d,h,s}^{SH}$. Additional terms in the power balance equation need to reflect that they are bound by the number of scenarios, s.

7.4 Results and Discussion

Stochastic programming based mixed-integer programming optimization was carried out using the CPLEX 11.1.1 solver in the GAMS 24.5.1 environment.

Table 7.1 Cost Comparisons Between the Base Case Deterministic and Stochastic RPES Models.

	Total Cost (USD Million per Year)	
	Stochastic RPES	**Deterministic RPES**
Integrated RPES System	1944.992	2317.928
Methanol Block	130.598	138.511
Power Planning Block	1814.394	2179.416

The total cost of the RPES is 1944.992 USD million per year which is less than the deterministic polygeneration model, with the methanol production block being 130.598 USD million per year and the power planning block being 1814.394 USD million per year. One possible reason for this decline in the overall costs, is that that scenario based wind realizations results in a design of methanol production units that are smaller on account of having variability in the wind. The same number of thermal generators have been designed.

Table 7.2 Comparison of Day-Ahead Capacities Between Stochastic and Deterministic RPES Models.

	Stochastic RPES	**Deterministic RPES**
Capacity of Wind Installed Day Ahead (MW)	536	594
Capacity of Conventional Power Installed Day Ahead (MW)	2370	2376

It appears from observing the Day-ahead capacity installed for the stochastic RPES model, the amount installed is less than that of the deterministic RPES. This accounts for the reduction in the overall annual cost of the stochastic RPES model.

The operation cost of the power planning block is less in stochastic as the model is utilizing more wind which has zero operational cost with it. As a result, the overall costs of the stochastic RPES is lower than the deterministic RPES.

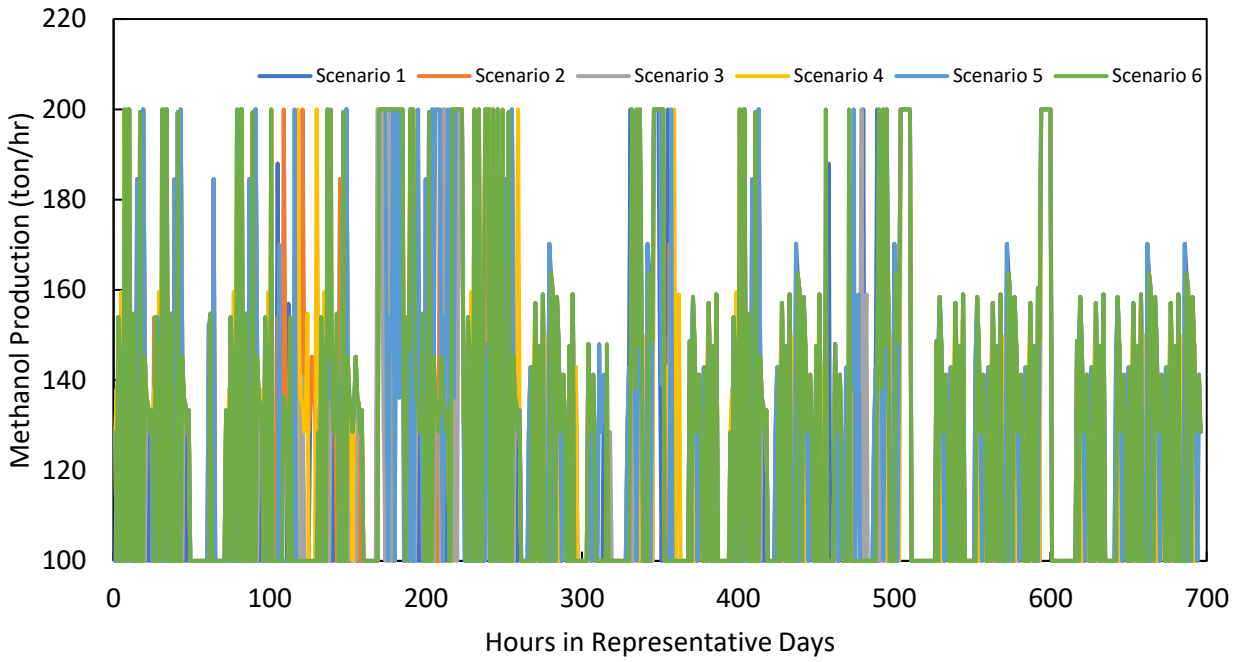

Figure 7.1 Methanol Production levels across 6 scenarios for 29 Representative Days' Hours.

As can be seen from the above figure 7.1, there is much variation in the hourly methanol production. The levels of production remain upper bound by 200 tons per hour and lower bound by 100 tons per hour as is the customary limits to maintain continuous operation of the methanol production units. The scenarios and their respective probabilities influence the amount of wind power realized in the real time stage of the model solution. Which is to say that after a design decision is made and the day-ahead wind power is scheduled in accordance to the data inputs, a scenario based actual wind power realization is either higher or lower than the day ahead levels predicted by the model. As is expected from methanol production variation observed in chapter 6, the amount of methanol produced depends on the amount of wind that is available as a surplus at every hour after it has contributed to fulfilling the load demand in tandem with the conventional generators. The higher the amount of excess wind realized, the larger is the hourly production of

methanol to drive as it is used to meet the power ratings of the compressor units among other unit operations of the methanol production unit.

7.5 Conclusion and Future Perspectives

From the development and execution of the stochastic RPES model, there are certain conclusions about the viability of this polygeneration energy system that can be gleaned from it. One stand-out feature is that the overall cost of the stochastic RPES model is less than the deterministic RPES. This indicates that there is a benefit to taking advantage of the uncertainty emerging from wind intermittency. The RPES system, regardless of what the hourly load demand might be, will always be in a position to take advantage of excess wind power to produce value added chemicals. If the system was designed in such a way that the wind power was only directed towards meeting the load or producing a greener pathway of a chemical, it would not prove to be profitable to have it behave in a stochastic manner taking the uncertainty into account. But, by having it operate in a flexible manner, it is useful in meeting load demand along with conventional power, while also using the excess wind for chemical production.

Hence, such an RPES system highlights that the variability and intermittency of renewable energy sources is not a source of higher costs and penalties when the system is design and operated together for meeting load and producing chemicals simultaneously.

Chapter 8 Conclusion and Future Work

All research objectives of the proposed work were successfully met. This thesis focused on the development of general models that represent the design and operation of a renewable energy based polygeneration energy system. The thesis addressed the objectives by first looking closely into the power generation design and operation model, by using a unit commitment based model to represent the power system comprising of conventional coal powered generators along with wind power scenarios. In chapter 3, a base case model is constructed as a DCUC network-constrained model with 6 nodes with one node connected to a wind farm and the remaining connected to various conventional generators. The objective function was designed to minimize the total capital and operating cost of the system while deciding how much wind power is to be harnessed from a wind farm and which generators to construct first as design decisions. Following the design step, the operation results provide results for how much power is to be scheduled in the day-ahead stage and then the necessary adjustments in the real-time stage once the actual wind power was realized. The model behaved in a stochastic manner to account for the wind power by introducing it as a probability based scenarios that respond to various levels of wind power realizations. This chapter also introduced the concept of clustering and applied it to the reduction of probability scenarios for wind, from 50 scenarios to 6 which captured the original frequencies but resulted in the model solving much faster. The clustered model solved in 15.83 CPU time seconds which is significantly lower than the base case model with 50 scenarios, which solved in 41.76 seconds.

In chapter 4, the power planning model was extended to include an energy storage system that comprised of an electrolyser and fuel cell. The purpose of the ESS was to show how the model

behaved when the wind power was at an excess in terms of the load, and redirected towards hydrogen production. Later scenarios were run on this model that further highlighted the ESS's flexibility by converting stored hydrogen back to power using the fuel cell. This was in response to a very high load demand that triggered the production of electricity back from hydrogen. With the inclusion of the ESS block, the total system cost of the power generation planning model with 6 probability scenarios was calculated to be USD 576.24 million per year which reflects the inclusion of the ESS block's capital and operating costs.

While chapter 4's ESS comprised of a black-box representation of an electrolyser and hydrogen system, the main value added chemical production this thesis focused on was that of coal to methanol production. In chapter 5, a first principles based model was developed for the process of converting coal to methanol, via gasification, methanol synthesis and finally a clean-up unit. This model was developed to be generic for all carbon based fuel feedstock as it was based on stoichiometric mass and energy balances for each of the unit operations. The chapter introduced the methanol production model first as a snapshot model, followed by making it multi-period to reflect the operation of the system for a period of 24 hours. The multi-period model proved to be time conducive for arriving at a solution, and therefore a shortcut model was proposed that significantly reduced the solution time. The methanol production block model was initially described as a mixed-integer nonlinear programming model due to the presence of bilinear terms in the stoichiometric balance equations as well as the capital cost calculation equations were non-linear in nature. A regression based linear approximation was performed on the capital cost equations to convert the model into a mixed integer linear programming model, a variation that was found to provide a faster solution time. Various comparisons between the non-linear and linear versions of the models were performed as individual case studies to show that the linearized

shortcut model was not only the version that solved the quickest but also provided solutions to key variables that did not vary significantly from the long-form nonlinear representation of the methanol block.

Chapter 6 introduced the renewable energy polygeneration model by combining the models developed in chapters 3,4 and 5 to form the integrated RPES model. In this chapter, the model was set up as deterministic to allow for investigating the viability of connecting the power production block and the methanol production block. The main manner in which they were integrated was by connecting the wind power from the wind farm to the compressors that drive two of the key unit operations in the methanol production system, which are the air separation unit and the unreacted syngas recycle streams. Several graphical representations were generated to visually show that the variation in the wind power directly brought about a modification in the levels of methanol production via power transmission to the compressor units. For the base case of the deterministic RPES integrated model, the total annual cost is USD $2317.93 million per year, the methanol block annual cost is $138.511 million per year and the power generation planning block is $2179.416 million per year. A series of case studies were also investigated, by modifying the amount of wind power that is generated and harnessed by the RPES, first by using raw data that has a higher average expected value of wind power and a lower expected value of wind power. Following that, an external constraint was placed on the model by utilizing a RPS or renewable portfolio standard which enforces a minimum amount of power generation from renewable energy sources. For both these case studies, the impact the expected value of wind had on the production of methanol was studied. It was observed that the higher the amount of wind that can be harnessed, the greater is the maximum level of methanol that can be produced, which is attributed to the model choosing to design a greater capacity of methanol production units. Lastly, in one of the case study,

the deterministic RPES model included ramping and minimum up and down time constraints on the overall chemical production block. This approach was undertaken to study the impact of having the methanol reactors and gasification units behave more like they do in the real world with commitment like constraints and therefore affected the times at which the methanol production units were switched on and off and impacted the system's annual cost by increasing it from the base case which did not include these constraints.

Chapter 7 showed how the integrated renewable polygeneration energy system can be made to design and operate in a stochastic manner. One interesting observation from the stochastic RPES model was that the overall cost of the stochastic RPES model was found to be less than the deterministic RPES. This indicated that there would be a benefit to taking advantage of the uncertainty emerging from wind intermittency. The results showed that if the system was designed so that the wind power was only directed towards meeting the load or producing a greener pathway of a chemical, it would not prove to be profitable to have it behave in a stochastic manner taking the uncertainty into account. But, since it was made to operate in a flexible manner, it was useful in meeting load demand along with conventional power, while also using the excess wind for chemical production.

All the models developed, helped to elucidate how the intermittency of renewable energy sources like wind, can facilitate the use of alternative chemical production pathways to act as energy carriers, either as storage for a longer duration or produce chemicals for sale that increase the profitability of the entire energy system as opposed to stand-alone plants.

Future Work:

As an extension to this work presented, other avenues may be explored when conducting future research on the topic of renewable polygeneration energy systems. One aspect that needs to be taken into consideration in future work is to investigate a wide array of renewable and fossil fuel inputs into the polygeneration energy system. For instance, in this work, the renewable energy source considered was wind, which is deemed the most intermittent to show how the energy system behaves in a flexible manner. However, future modelling studies using the above system could include solar power as a potential input to highlight that the system can handle multiple renewable energy sources within the portfolio requirements. Another manner to add complexity to the model would be to add additional energy storage mechanisms to the model, for instance, compressed air energy storage, alternative liquid fuels etc. It would then be the case that the model is too complicated and long to solve within a reasonable time, in particular for the stochastic model. In this case, it would be prudent to apply decomposition methods to shorten the solution time. The impact of ramping and other commitment like constraints on the RPES model needs to be further studied with a deeper look into the exact dynamic behaviour of the methanol production system, which is out of the scope of this present work.

References

[1] EPRI. Electric Power Resources Institute. Electric Power Systems Flexibility: Challenges and Opportunities. https://www.naseo.org/Data/Sites/1/flexibility-white-paper.pdf Published February 2016.

[2] IRENA. Renewable Energy Statistics 2017. http://www.irena.org/publications/2017/Jul/Renewable-Energy-Statistics-2017 Published July 2017

[3] Agora Energiewende. The Energiewende in a Nutshell. https://www.agora-energiewende.de/fileadmin/Projekte/2017/Energiewende_in_a_nutshell/Agora_The_Energiewende_in_a_nutshell_WEB.pdf Published March 2017

[4] European Commission - JRC Science and Policy Reports.https://ec.europa.eu/jrc/en/publication/eur-scientific-and-technical-research-reports/addressing-flexibility-energy-system-models Published 2015

[5] Jana, K., Ray, A., Majoumerd, M. M., Assadi, M., & De, S. (2017). Polygeneration as a future sustainable energy solution–A comprehensive review. *Applied Energy*, *202*, 88-111.

[6] Natural Resources Canada. Energy Factbook 2016-2017. https://www.nrcan.gc.ca/sites/www.nrcan.gc.ca/files/energy/pdf/EnergyFactBook_2016_17_En.pdf Published 2017.

[7] Zhang.Q., "*Enterprise-wide Optimization for Industrial Demand Side Management*" [Doctoral dissertation] Pittsburgh, PA, USA, Carnegie-Mellon University, 2016.

[8] Nikolakakis.T., "*A Mixed Integer Linear Unit Commitment and Economic Dispatch Model for Thermo-Electric and Variable Renewable Energy Generators with Compressed Air Energy Storage: Verification and Application Using Data From The Irish Grid.*"[Doctoral dissertation] New York City, NY, USA Columbia University, 2017

[9] REN21 - Renewable Energy Policy Networks for the 21st Century. REN21. 2017.

Renewables 2017 Global Status Report

(Paris: REN21 Secretariat).

[10] Liu, P., Pistikopoulos, E. N., & Li, Z. (2009). A mixed-integer optimization approach for polygeneration energy systems design. *Computers & Chemical Engineering*, *33*(3), 759-768.

[11] Liu, P., Pistikopoulos, E. N., & Li, Z. (2009). An energy systems engineering approach to polygeneration and hydrogen infrastructure systems analysis & design. *Chemical Engineering Transactions*, *18*, 373-378.

[12] Liu, P., "*Modelling and Optimization of Polygeneration Energy Systems.*"[Doctoral dissertation] London, UK, Imperial College London, 2009.

[13] Bose, A., Jana, K., Mitra, D., & De, S. (2015). Co-production of power and urea from coal with CO2 capture: performance assessment. *Clean Technologies and Environmental Policy*, *17*(5), 1271-1280.

[14] Bounamano A, Calise F, Ferruzi G, Vanoli L. A novel renewable polygeneration system for hospital buildings: design, simulation and thermo-economic optimization. Appl Therm Eng 2014;67:43–60.

[15] Chen Y, Adams II TA, Barton PI. Optimal design and operation of static energy polygeneration. Ind Eng Chem Res 2011;50:5099–113.

[16] De Kam MJ, Morey RV, Tiffany DG. Biomass integrated gasification combined cycle for heat and power at ethanol plants. Energy Convers Manage 2009;50:1682–90.
[17] Farhat K, Reichelstein S. Economic value of flexible hydrogen-based polygeneration energy systems. Appl Energy 2016;164:857–70.
[18] Gao L, Li H, Chen B, Jin H, Lin R, Hong H. Proposal of natural gas-based polygeneration system for power and methanol production. Energy 2008;33:206–12.
[19] Guo Z, Wang Q, Fang M, Luo Z, Cen K. Simulation of a lignite-based polygeneration system co producing electricity and tar with carbon capture. Chem Eng Technol 2015;38(3):463–72.
[20] Ilic DD, Dotzauer E, Trygg L, Broman G. Integration of biofuel production into district heating e part i: an evaluation of biofuel production costs using four types of biofuel production plants as case studies. J Clean Prod 2014;69:176–87.
[21] Jana K, De S. Environmental impact of biomass based polygeneration: a case study through life cycle assessment. Bioresour Technol 2017;227:256–65.
[22] Kyriakarakos G, Piromalis DD, Arvanitis KG, Dounis AI, Papadakis G. On battery-less autonomous polygeneration microgrids: investigation of the combined hybrid capacitors/hydrogen alternative. Energy Convers Manage 2015;91:405–15.
[23] Li Z, Liu P, He F, Wang M, Pistikopoulos EN. Simulation and exergoeconomic analysis of a dual-gas sourced polygeneration process with integrated methanol/DME/DMC catalytic synthesis. Comput Chem Eng 2011;35:1857–62.
[24] Lythcke-Jørgensen C, Haglind F, Clausen LR. Exergy analysis of a combined heat and power plant with integrated lignocellulosic ethanol production. Energy Convers Manage 2012;85:817–27.
[25] Narvaez A, Chadwick D, Kershenbaum L. Small-medium scale polygeneration systems: methanol and power production. Appl Energy 2014;113:1109–17.
[26] Pellegrini LF, De Oliveira Jr S. Combined production of sugar, ethanol and electricity: thermoeconomic and environmental analysis and optimization. Energy 2011;36:3704–15.
[27] Rubiyo-Maya C, Marcuello-Uche J, Martinez-Gracia A, Bayod-Rujula A. Design optimization of a polygeneration plant fuelled by natural gas and renewable energy sources. Appl Energy 2011;88(2):449–57.
[28] Salkuyeh YK, Adams II TA. A novel polygeneration process to co-produce ethylene and electricity from shale gas with zero CO2 emissions via methane oxidative coupling. Energy Convers Manage 2015;92:406–20.
[29] Song H, Starfelt F, Daianova L, Yan J. Influence of drying process on the biomass-based polygeneration system of bioethanol, power and heat. Appl Energy 2012;90:32–7.

[30] Yu B, Chien I. Design and economic evaluation of a coal-based polygeneration process to coproduce synthetic natural gas and ammonia. Ind Eng Chem Res 2015;54:10073–87.

[31] Zhu L, Zhang Z, Fan J, Jiang P. Polygeneration of hydrogen and power based on coal gasification integrated with a dual chemical looping process: thermodynamic investigation. Comput Chem Eng 2016;84:302–12.
[32] Adams II TA, Barton PI. Combining coal gasification and natural gas reforming for polygeneration. Fuel Process Technol 2011;92:639–55.
[33] Fan J, Zhu L. Performance analysis of a feasible technology for power and high-purity hydrogen production driven by methane fuel. Appl Therm Eng 2015;75:103–14.
[34] Hu L, Hongguang J, Lin G, Wei H. Techno-economic evaluation of coal-based polygeneration systems of synthetic fuel and power with CO2 recovery. Energy Convers Manage 2011;52:274–83.
[35] Jana K, De S. Sustainable polygeneration design and assessment through combined thermodynamic, economic and environmental analysis. Energy 2015;91:540–55.
[36] Li S, Jin H, Gao L, Zhang X. Exergy analysis and the energy saving mechanism for coal to synthetic/substitute natural gas and power cogeneration system without and with CO2 capture. Appl Energy 2014;130:552–61.
[37] Li S, Gao L, Jin H. Realizing low life cycle energy use and GHG emissions in coal based polygeneration with CO2 capture. Appl Energy 2017;194:161–71.
[38] Li Y, Zhang G, Yang Y, Zhai D, Zhang K, Xu G. Thermodynamic analysis of a coal-based polygeneration system with partial gasification. Energy 2014;72:201–14.
[39] Ng KS, Zhang N, Sadhukhanj J. Techno-economic analysis of polygeneration systems with carbon capture and storage and CO2 reuse. Chem Eng J 2013;219:96–108.
[40] Lund, P. D., Lindgren, J., Mikkola, J., & Salpakari, J. (2015). Review of energy system flexibility measures to enable high levels of variable renewable electricity. *Renewable and Sustainable Energy Reviews, 45*, 785-807.
[41] Tuohy A, O'Malley M. Wind power and storage. Wind power in power Systems.2nd ed. West Sussex, United Kingdom:Wiley;2012.p.465–87.
[42] Pimm, A. J., Garvey, S. D., & Drew, R. J. (2011). Shape and cost analysis of pressurized fabric structures for subsea compressed air energy storage. *Proceedings of the Institution of Mechanical Engineers, Part C: Journal of Mechanical Engineering Science*, *225*(5), 1027-1043.
[43] Breeze P. Power generation technologies. 1st ed. Elsevier Science; 2005.
[44] Denholm, P., & Margolis, R. M. (2007). Evaluating the limits of solar photovoltaics (PV) in electric power systems utilizing energy storage and other enabling technologies. *Energy Policy*, *35*(9), 4424-4433.
[45] Pistikopoulos, E. N., & Grossmann, I. E. (1989). Optimal retrofit design for improving process flexibility in nonlinear systems—I. Fixed degree of flexibility. *Computers & chemical engineering*, *13*(9), 1003-1016.
[46]Huber, M., Dimkova, D., & Hamacher, T. (2014). Integration of wind and solar power in Europe: Assessment of flexibility requirements. *Energy*, *69*, 236-246.
[47] Grossmann, I. E. (1983). Mixed-integer programming: is it a useful tool in process synthesis? *Paper presented at the AlChE Diamond Jubilee Meeting, Washington, D.C., November 1983.*
[48] Pistikopoulos, E. N. (1995). Uncertainty in process design and operations. *Computers & Chemical Engineering*, *19*, 553-563.

[49] Birge, J. R., & Wets, R. J. B. (1991). *Stochastic Programming*(Vol. 30). JC Baltzer AG.

[50] GAMS Development Corporation. General Algebraic Modeling System (GAMS) Release 24.2.1. Washington, DC, USA, 2013.

[51] Li, X., Chen, Y., & Barton, P. I. (2012). Nonconvex generalized benders decomposition with piecewise convex relaxations for global optimization of integrated process design and operation problems. *Industrial & Engineering Chemistry Research*, *51*(21), 7287-7299.

[52] Sahinidis, N. V. (1996). BARON: A general purpose global optimization software package. *Journal of global optimization*, *8*(2), 201-205.

[53] Serra, L. M., Lozano, M. A., Ramos, J., Ensinas, A. V., & Nebra, S. A. (2009). Polygeneration and efficient use of natural resources. *Energy*, *34*(5), 575-586.

[54] Murugan, S., & Horák, B. (2016). Tri and polygeneration systems-A review. *Renewable and Sustainable Energy Reviews*, *60*, 1032-1051.

[55] Calise, F., di Vastogirardi, G. D. N., d'Accadia, M. D., & Vicidomini, M. (2018). Simulation of polygeneration systems. *Energy*, *163*, 290-337.

[56] Rong, A., & Lahdelma, R. (2016). Role of polygeneration in sustainable energy system development challenges and opportunities from optimization viewpoints. *Renewable and Sustainable Energy Reviews*, *53*, 363-372.

[57] Pinto, E. S., Serra, L. M., & Lázaro, A. (2020). Evaluation of methods to select representative days for the optimization of polygeneration systems. *Renewable Energy*, *151*, 488-502.

[58] Adams II, T. A., & Ghouse, J. H. (2015). Polygeneration of fuels and chemicals. *Current Opinion in Chemical Engineering*, *10*, 87-93.

[59] Menon, R. P., Paolone, M., & Maréchal, F. (2013). Study of optimal design of polygeneration systems in optimal control strategies. *Energy*, *55*, 134-141.

[60] Adams II, T. A., & Barton, P. I. (2011). Combining coal gasification and natural gas reforming for efficient polygeneration. *Fuel Processing Technology*, *92*(3), 639-655.

[61] Lee, I., Tester, J. W., & You, F. (2019). Systems analysis, design, and optimization of geothermal energy systems for power production and polygeneration: State-of-the-art and future challenges. *Renewable and Sustainable Energy Reviews*, *109*, 551-577.

[62] Ahmadi, P., Rosen, M. A., & Dincer, I. (2012). Multi-objective exergy-based optimization of a polygeneration energy system using an evolutionary algorithm. *Energy*, *46*(1), 21-31.[63] Uçkun, C., Botterud, A., & Birge, J. R. (2015). An improved stochastic unit commitment formulation to accommodate wind uncertainty. *IEEE Transactions on Power Systems*, *31*(4), 2507-2517.

[64] Cheung, K., Gade, D., Silva-Monroy, C., Ryan, S. M., Watson, J. P., Wets, R. J. B., & Woodruff, D. L. (2015). Toward scalable stochastic unit commitment. *Energy Systems*, *6*(3), 417-438.

[65] Shiina, T., & Birge, J. R. (2004). Stochastic unit commitment problem. *International Transactions in Operational Research*, *11*(1), 19-32.

[66] Zheng, Q. P., Wang, J., Pardalos, P. M., & Guan, Y. (2013). A decomposition approach to the two-stage stochastic unit commitment problem. *Annals of Operations Research*, *210*(1), 387-410.

[67] Blanco, I., & Morales, J. M. (2017). An efficient robust solution to the two-stage stochastic unit commitment problem. *IEEE Transactions on Power Systems*, *32*(6), 4477-4488.

[69] Håberg, M. (2019). Fundamentals and recent developments in stochastic unit commitment. *International Journal of Electrical Power & Energy Systems*, *109*, 38-48.

[70] Tumuluru, V. K., & Tsang, D. H. (2016). A two-stage approach for network constrained unit commitment problem with demand response. *IEEE Transactions on Smart Grid*, *9*(2), 1175-1183.

[71] Anjos, M. F., & Conejo, A. J. (2017). Unit commitment in electric energy systems. *Foundations and Trends® in Electric Energy Systems*, *1*(4), 220-310.

[72] Schwele, A., Kazempour, J. & Pinson, P. Do unit commitment constraints affect generation expansion planning? A scalable stochastic model. *Energy Syst* **11,** 247–282 (2020). https://doi.org/10.1007/s12667-018-00321-z

[73] Albertus, P., Manser, J. S., & Litzelman, S. (2020). Long-duration electricity storage applications, economics, and technologies. *Joule*, *4*(1), 21-32.

[74] Dowling, J. A., Rinaldi, K. Z., Ruggles, T. H., Davis, S. J., Yuan, M., Tong, F., ... & Caldeira, K. (2020). Role of long-duration energy storage in variable renewable electricity systems. *Joule*, *4*(9), 1907-1928.

[75] Hunter, C. A., Penev, M. M., Reznicek, E. P., Eichman, J., Rustagi, N., & Baldwin, S. F. (2021). Techno-economic analysis of long-duration energy storage and flexible power generation technologies to support high-variable renewable energy grids. *Joule*, *5*(8), 2077-2101.

[76] Rehman, S., Al-Hadhrami, L. M., & Alam, M. M. (2015). Pumped hydro energy storage system: A technological review. *Renewable and Sustainable Energy Reviews*, *44*, 586-598.

[77] Deane, J. P., Gallachóir, B. Ó., & McKeogh, E. J. (2010). Techno-economic review of existing and new pumped hydro energy storage plant. *Renewable and Sustainable Energy Reviews*, *14*(4), 1293-1302.

[78] Lund, H., & Salgi, G. (2009). The role of compressed air energy storage (CAES) in future sustainable energy systems. *Energy conversion and management*, *50*(5), 1172-1179.

[79] Zhou, Q., Du, D., Lu, C., He, Q., & Liu, W. (2019). A review of thermal energy storage in compressed air energy storage system. *Energy*, *188*, 115993.

[80] Zhao, H., Wu, Q., Hu, S., Xu, H., & Rasmussen, C. N. (2015). Review of energy storage system for wind power integration support. *Applied energy*, *137*, 545-553.

[81] Wade, N. S., Taylor, P. C., Lang, P. D., & Jones, P. R. (2010). Evaluating the benefits of an electrical energy storage system in a future smart grid. *Energy policy*, *38*(11), 7180-7188.

[82] Jiang, Z., & Yu, X. (2009, July). Modeling and control of an integrated wind power generation and energy storage system. In *2009 IEEE Power & Energy Society General Meeting* (pp. 1-8). IEEE.

[83] Yuan, Y., Zhang, X., Ju, P., Qian, K., & Fu, Z. (2012). Applications of battery energy storage system for wind power dispatchability purpose. *Electric Power Systems Research*, *93*, 54-60.

[84] Li, X., Hui, D., & Lai, X. (2013). Battery energy storage station (BESS)-based smoothing control of photovoltaic (PV) and wind power generation fluctuations. *IEEE transactions on sustainable energy*, *4*(2), 464-473.

[85] Dalena, F., Senatore, A., Marino, A., Gordano, A., Basile, M., & Basile, A. (2018). Methanol production and applications: An overview. *Methanol*, 3-28.

[86] Marjani, A., Rezakazemi, M., & Shirazian, S. (2012). Simulation of methanol production process and determination of optimum conditions. *Oriental Journal of Chemistry*, *28*(1), 145.

[87] Zhang, Y., Cruz, J., Zhang, S., Lou, H. H., & Benson, T. J. (2013). Process simulation and optimization of methanol production coupled to tri-reforming process. *International journal of hydrogen energy*, *38*(31), 13617-13630.

[88] Bansal, A., Sharma, M., & Goel, S. (2017). Improved k-mean clustering algorithm for prediction analysis using classification technique in data mining. *International Journal of Computer Applications*, *157*(6), 0975-8887.

[89] Yesilbudak, M. (2016, November). Clustering analysis of multidimensional wind speed data using k-means approach. In *2016 IEEE International Conference on Renewable Energy Research and Applications (ICRERA)* (pp. 961-965). IEEE.

[90] The Wind Power – Wind Energy Market Intelligence. https://www.thewindpower.net/windfarm_en_21039_summerhaven-wind-energy-centre.php Published 2020. Accessed June 2020.

[91] ELIA. Elia Group Wind Power Generation Data and Forecasts. https://www.elia.be/en/grid-data/power-generation/wind-power-generation Published February 2019. Accessed January 2020.

[92] PJM.PJM Transmission Peak Load data https://www.pjm.com/-/media/library/reports-notices/load-forecast/2019-load-report.ashx Published June 2019.Accessed January 2020.

Appendix –Python Code for Clustering

```
#wind speed kmean clustering using ontario data
import pandas as pd
import matplotlib.pyplot as plt
import numpy as np
import sys
from sklearn import datasets, cluster
import numpy as np
import matplotlib.pyplot as plt
from mpl_toolkits.mplot3d import Axes3D
%matplotlib inline
import datetime as dt

data = pd.read_excel('summerhaven.xlsx' )
#data = data.dropna(axis=0).copy()
demand_data = pd.read_excel('cluster results.xlsx',sheet_name='demand',index_
col=[0])
date = pd.DataFrame({'date': pd.date_range(start='2018-01-01 00:00:00', perio
ds=len(data), freq='H')})
data.index = date.date

#data.SUMMERHAVEN.fillna(data.SUMMERHAVEN.rolling(72,min_periods=48).mean())
#wind  = data.SUMMERHAVEN.rolling(72,min_periods=48).mean()

#wind_data = data.SUMMERHAVEN.interpolate(method='from_derivatives')
wind_data  =  data.SUMMERHAVEN.fillna(data.SUMMERHAVEN.rolling(72,min_periods
=48).mean())
data.plot(y=['SUMMERHAVEN'])
wind_data.plot()

<matplotlib.axes._subplots.AxesSubplot at 0x1f8715e7160>

png

png
pp = np.argwhere(np.isnan(data.SUMMERHAVEN.values))

wind_data.values[pp]

array([[23.09859155],
       [23.42857143],
       [23.76811594],
       [24.11764706],
       [24.47761194],
       [24.84848485],
       [25.23076923],
       [25.625     ],
       [25.74603175],
       [26.12903226],
       [25.39344262],
```

```
        [25.7       ],
        [26.13559322],
        [26.5862069 ],
        [26.40350877],
        [25.82142857],
        [25.05454545],
        [24.46296296],
        [24.09433962],
        [23.82692308],
        [23.50980392],
        [23.44      ],
        [23.91836735],
        [24.41666667],
        [ 1.3943662 ],
        [ 1.41428571],
        [ 1.43478261],
        [ 1.45588235],
        [ 1.47761194],
        [ 1.5       ],
        [ 1.52307692],
        [ 1.546875  ],
        [ 1.57142857],
        [ 1.59677419],
        [ 1.62295082],
        [ 1.65      ],
        [ 1.6440678 ],
        [ 1.65517241],
        [ 1.68421053],
        [ 1.71428571],
        [ 1.74545455],
        [ 1.77777778],
        [ 1.81132075],
        [ 1.84615385],
        [ 1.88235294],
        [ 1.92      ],
        [ 1.95918367],
        [ 2.        ]])

wind_data_np = wind_data.values.reshape((int(len(wind_data)/24),24))
demand_data_np = demand_data.values[:,:-1]
maxw = wind_data_np.max()

plt.figure(2,figsize=(5,3.5),dpi=100)
#centroid_min= dic_results['centriod_20']
#centroid_min = hourly_daily.inverse_transform(centroid_min)
#day_clu = []
for i in range(0,len(wind_data_np)):
        plt.plot(nphour, wind_data_np[i,:]/maxw,c='tab:blue',linewidth=0.2)
        day_clu = day_clu+['Cluster'+str(i+1)]
```

```
#plt.legend(day_clu)
plt.ylabel('Wind power factor (p.u.)')
plt.xlabel('Hour')
plt.xlim(1,24)

plt.tight_layout()
plt.xticks([2,4,6,8,10,12,14,16,18,20,22,24])
plt.savefig('wind_data.jpeg',dpi=200,tight_layout = True)

plt.show()
```

png

png

```
plt.figure(2,figsize=(5,3.5),dpi=100)
#centroid_min= dic_results['centriod_20']
#centroid_min = hourly_daily.inverse_transform(centroid_min)
#day_clu = []
for i in range(0,len(demand_data_np)):
        plt.plot(nphour, 0.217010664*demand_data_np[i,:],c='tab:blue',linewid
th=0.2)
        day_clu = day_clu+['Cluster'+str(i+1)]

#plt.legend(day_clu)
plt.ylabel('Power demand (KW)')
plt.xlabel('Hour')
plt.xlim(1,24)

plt.tight_layout()
plt.xticks([2,4,6,8,10,12,14,16,18,20,22,24])
plt.savefig('demand_data.jpeg',dpi=200,tight_layout = True)

plt.show()
```

png

png

```
demand_data_np
```

```
array([[ 9232.,  9082.,  8919., ...,  9573.,  9398.,  9150.],
       [ 8956.,  8794.,  8665., ...,  9889.,  9658.,  9380.],
       [ 9157.,  8988.,  8877., ...,  9982.,  9599.,  9263.],
       ...,
       [ 9307.,  9167.,  9075., ..., 10240.,  9935.,  9626.],
       [ 9386.,  9247.,  9149., ..., 10192.,  9876.,  9575.],
       [ 9324.,  9195.,  9125., ..., 10059.,  9799.,  9533.]])
```

```
demand_yr = 0.217010664*demand_data_np.reshape((len(demand_data_np)*len(deman
d_data_np.T)),)
```

```
plt.figure(2,figsize=(7.5,3.5),dpi=100)
plt.plot(range(1,len(demand_yr)+1), demand_yr,c='tab:blue',linewidth=0.5)
plt.ylabel('Power demand (KW)')
plt.xlabel('Hour')
plt.tight_layout()
plt.savefig('demand_yr.jpeg',dpi=200,tight_layout = True)
plt.show()
```

png

png

```
demand_yr = 0.217010664*demand_data_np.reshape((len(demand_data_np)*len(deman
d_data_np.T)),)
plt.figure(2,figsize=(7.5,3.5),dpi=100)
plt.plot(range(1,len(wind_data)+1), wind_data/wind_data.max(),c='tab:blue',li
newidth=0.5)
plt.ylabel('Wind power factor (p.u.)')
plt.xlabel('Hour')
plt.tight_layout()
plt.savefig('wind_yr.jpeg',dpi=200,tight_layout = True)
plt.show()
```

png

png

```
from sklearn.preprocessing import MinMaxScaler
wind_scale = MinMaxScaler()
demand_scale = MinMaxScaler()
wind_scale.fit(wind_data_np)
demand_scale.fit(demand_data_np)
wind_s = wind_scale.transform(wind_data_np)
demand_s= demand_scale.fit_transform(demand_data_np)

plt.figure(2,figsize=(5,3.5),dpi=100)
#centroid_min= dic_results['centriod_20']
#centroid_min = hourly_daily.inverse_transform(centroid_min)
#day_clu = []
for i in range(0,len(demand_s)):
        plt.plot(nphour, demand_s[i,:],c='tab:blue',linewidth=0.2)
        day_clu = day_clu+['Cluster'+str(i+1)]

#plt.legend(day_clu)
plt.ylabel('Normalized power demand (KW)')
plt.xlabel('Hour')
plt.xlim(1,24)
plt.tight_layout()
plt.xticks([2,4,6,8,10,12,14,16,18,20,22,24])
plt.savefig('demand_scaled.jpeg',dpi=200,tight_layout = True)
```

```
plt.show()
```

png

png

```
plt.figure(2,figsize=(5,3.5),dpi=100)
#centroid_min= dic_results['centriod_20']
#centroid_min = hourly_daily.inverse_transform(centroid_min)
#day_clu = []
for i in range(0,len(wind_s)):
        plt.plot(nphour, wind_s[i,:],c='tab:blue',linewidth=0.2)
        day_clu = day_clu+['Cluster'+str(i+1)]

#plt.legend(day_clu)
plt.ylabel('Normalized Wind factor (p.u.)')
plt.xlabel('Hour')
plt.xlim(1,24)
plt.tight_layout()
plt.xticks([2,4,6,8,10,12,14,16,18,20,22,24])
plt.savefig('Wind_scaled.jpeg',dpi=200,tight_layout = True)

plt.show()
```

png

png

```
x_train = np.concatenate((wind_s,demand_s),axis = 1)
x_train.shape
```

```
(365, 48)
```

```
step = 1
start = 2
end = 50
range_n_clusters = np.array(range(start,end,step))
ineria= np.empty_like((range_n_clusters),dtype=float)
ineria.shape
for i in range_n_clusters:
    ineria[int(i/step)-start] = 5
ineria
```

```
array([5., 5., 5., 5., 5., 5., 5., 5., 5., 5., 5., 5., 5., 5., 5., 5.,
       5., 5., 5., 5., 5., 5., 5., 5., 5., 5., 5., 5., 5., 5., 5., 5.,
       5., 5., 5., 5., 5., 5., 5., 5., 5., 5., 5., 5., 5., 5., 5.])
```

```
from sklearn import metrics
from sklearn.metrics import pairwise_distances
n_clusters = 0
```

```
start = 2
end = 50
step = 1
range_n_clusters = np.array(range(start,end,step))
print(range_n_clusters)
score = np.empty_like((range_n_clusters),dtype=float)
final_error = np.empty_like((range_n_clusters),dtype=float)
final_std= np.empty_like((range_n_clusters),dtype=float)
ineria= np.empty_like((range_n_clusters),dtype=float)
i = 0
dic_results = {}
for n_clusters in range_n_clusters:
        np.random.seed(24)
        print('Processing cluster'+str(n_clusters))
        k_means = cluster.KMeans(n_clusters, precompute_distances=True ,n_ini
t=1000, max_iter = 10000)
        k_means.fit(x_train)
        labels_1= k_means.labels_
        label = labels_1.astype(np.float)
        centroid =  k_means.cluster_centers_
        ineria[int(n_clusters/step)-start] = k_means.inertia_
        ss = metrics.silhouette_score(x_train, label)
        score[int(n_clusters/step)-start] = ss
        error= {}
        error_per_clus = {}
        single_clus={}
        np_single_clus = {}
        error_std_clus = 0.0
        error_mean_clus =0.0
        nn = label.reshape((len(label),1))
        print(np_data.shape)
        np_result = np.concatenate((x_train, nn), axis=1)
        df_result_f= pd.DataFrame(data = np_result)
        dic_results['results_%d'%n_clusters] = df_result_f
        j = 0
        for j in range(n_clusters):
                single_clus[j] = df_result_f.loc[df_result_f.iloc[:,-1]==i]
                np_single_clus[j] = np.array(single_clus[j] )
                error[j] = abs(centroid[j,:] - np_single_clus[j][:,:-1])/np_s
ingle_clus[j][:,:-1]
                input_val = error[i][:,:-1]
                error_mean_clus = error_mean_clus + float(np.mean(error[i],dt
ype=np.float64))
                error_std_clus = error_std_clus + float(np.std(error[i],dtype
=np.float64))
        dic_results['centriod_%d'%n_clusters] = centroid
        dic_results['error_%d'%n_clusters] = error
        dic_results['mean_error_%d'%n_clusters] = error_mean_clus/n_clusters
        dic_results['std_%d'%n_clusters] = error_std_clus/n_clusters
        final_error[int(n_clusters/step)-start] =   error_mean_clus/n_cluster
```

```
s
        final_std[int(n_clusters/step)-start]   =   error_std_clus/n_clusters
plt.scatter(range_n_clusters,score)
plt.rcParams.update({'font.size':12})
plt.ylabel("silhouette_score")
plt.xlabel('Number of clusters')
#plt.savefig('plot2_kmean_ontario_score.png')
plt.show()
```

```
[ 2  3  4  5  6  7  8  9 10 11 12 13 14 15 16 17 18 19 20 21 22 23 24 25
 26 27 28 29 30 31 32 33 34 35 36 37 38 39 40 41 42 43 44 45 46 47 48 49]
```